Metabolic Pathways of Carotenoid Metabolism: Insights into the Biochemical and Regulatory Pathways of Carotenoid Cleavage

A dissertation submitted by

Jonathan R. Mein, M.S.

In partial fulfillment of the requirements for the degree of

Doctor of Philosophy

Biochemical and Molecular Nutrition

TUFTS UNIVERSITY

October 2010

Advisor

Dr. Xiang-Dong Wang

Gerald J. and Dorothy R. Friedman School of Nutrition Science and Policy, Tufts University, Nutrition and Cancer Biology Laboratory, Jean Mayer U.D.S.A Human Nutrition Research Center on Aging at Tufts University, Boston, MA

ABSTRACT

Consumption of a diet high in carotenoid-rich fruits and vegetables is strongly associated with a decreased risk of many chronic and degenerative diseases. Carotenoids are a class of lipophilic compounds found in many fruits and vegetables and have often been targeted as imparting some of the beneficial effects associated with fruit and vegetable consumption. However, our understanding of the biochemical and molecular framework of carotenoid metabolism is incomplete. Investigating the biochemical and molecular pathways of carotenoid metabolism are important to understanding their biological functions.

Carotene-15,15'-monooxygenase (CMO1) is involved in vitamin A formation, while recent studies suggest that carotene-9',10'-monooxygenase (CMO2) may have a broader substrate specificity than previously recognized. The first part of this research investigated the *in vitro* cleavage activity of recombinant ferret CMO2 towards the xanthophylls lutein, zeaxanthin and β-cryptoxanthin. Utilizing HPLC, LC-MS and GC-MS, we identified both volatile and non-volatile apocarotenoid products including 3-OH-β-ionone, 3-OH-α-ionone, β-ionone, 3-OH-α-apo-10'-carotenal, 3-OH-β-apo-10'-carotenal, and β-apo-10'-carotenal, indicating cleavage at both the 9,10 and 9',10' carbon-carbon double bond. Kinetic analysis indicated the xanthophylls zeaxanthin and lutein are preferentially cleaved over β-cryptoxanthin, indicating a key role of CMO2 in non-provitamin A carotenoid metabolism. Furthermore, incubation of 3-OH-β-apo-10'-carotenal with CMO2 lysate resulted in the formation of 3-OH-β-ionone. In the presence of NAD^+, *in vitro* incubation of 3-OH-β-apo-10'-carotenal with ferret hepatic homogenates resulted in the formation of 3-OH-β-apo-10'-carotenoic acid. Since apo-carotenoids serve as important signaling molecules in a variety of biological processes, enzymatic cleavage of xanthophylls by mammalian CMO2 represents a potential new avenue of investigation regarding vertebrate carotenoid metabolism and biological function.

Several well-implemented cohort studies have shown blood levels and dietary intake of β-cryptoxanthin to be strongly associated with a decreased risk of lung cancer independent of vitamin A. The objective of this study was to assess the regulation of CMO1 and CMO2 expression in selected ferret tissues in response to varying doses of β-cryptoxanthin supplementation. We first partially cloned the ferret CMO1 gene and compared the relative abundance of CMO1 and CMO2 expression in various tissues. Tissue-specific comparisons revealed significant differences in expression levels of CMO1 and CMO2. CMO1 expression was significantly higher in the intestinal mucosa while CMO2 expression was significantly higher in the lungs, visceral adipose and kidneys compared to CMO1. Low-dose (7.5 μg/kg body weight per day) and high-dose (37.5 μg/kg body weight per day) β-cryptoxanthin supplementation for 9 weeks resulted in a dose-dependent increase in β-cryptoxanthin concentrations with no changes in retinyl palmitate selected tissues. There was a significant decrease in lung CMO2 expression in both low- and high-dose supplementation groups with little changes in CMO1 or CMO2 expression in other tissues. The relative abundance of CMO2 expression in the lungs and down-regulation by β-cryptoxanthin supplementation indicates a potential role of CMO2 in the biological activity of β-cryptoxanthin in human health.

ACKNOWLEDGEMENTS

A special debt of gratitude and thanks is reserved for my thesis advisor and mentor, Dr. Xiang-Dong Wang. Xiang possess tremendous optimism and enthusiasm that is infectious. He always makes himself available to all his students and possesses many of the attributes that one could hope for in a mentor.

I am also grateful to the contributions of my thesis committee members, Dr. Gregory G. Dolnikowski and Dr. Robert M. Russell, whose advice, technical expertise and mentorship has made great contributions to my research and professional development.

I also owe an immeasurable amount of thanks and gratitude to the current and former members of the Nutrition and Cancer Biology Laboratory, whose discussions helped improve and strength my dissertation project. I am especially indebted to Connie Hu, who laid much of the foundation for my research and was always willing to take the time to teach me new techniques.

Last but not least, I want to thank my wife, Debra, and my entire family for their continued support throughout my academic career. Without their support, I would not have been able to persevere.

TABLE OF CONTENTS

LIST OF TABLES

Chapter 5.

LIST OF FIGURES

Chapter 2.

Chapter 3.

Chapter 4.

Chapter 5.

Chapter 7.

LIST OF ABBREVIATIONS

CMO1	β,β-Carotene-15,15'-Monooxygenase
CMO2	Carotene-9',10'-Monooxygenase
HPLC	High Pressure Liquid Chromatography
LC-MS	Liquid Chromatography – Mass Spectrometry
GC-MS	Gas Chromatography – Mass Spectrometry
THF	Tetrahydrofuran
AMD	Age-Related Macular Degeneration
RALDH	Retinaldehyde Dehydrogenase
RA	Retinoic acid
RAR	Retinoic acid receptor
CDA	Carotenoid-derived Aldehyde
HCS	High Content Screening
RPE	Retinal Pigment Epithelia
ISX	Intestine-specific homeobox transcription factor

Chapter 1

Introduction, Hypotheses, Specific Aims

1.1 BACKGROUND

Carotenoid metabolism has a long storied history as a research discipline. Beginning in the 1930's, researchers demonstrated that vitamin A could be synthesized from β-carotene, followed by the discovery in the 1960's of a vertebrate enzymatic pathway of β-carotene cleavage to vitamin A via a central cleavage pathway. In addition to the central cleavage pathway, an alternative pathway of carotenoid metabolism, termed the excentric cleavage pathway, was proposed as an alternative pathway in β-carotene metabolism. However, the existence of such a pathway remained a question of debate for several decades. With the cloning and characterization of both the β-carotene-15,15'-monooxygenase (CMO1) and carotene-9',10'-monooxygenase (CMO2), the existence of both the central and excentric cleavage pathways were confirmed. While the central cleavage pathway has been extensively investigated for its role in production of vitamin A from provitamin A carotenoids, the relevance of the excentric cleavage pathway and its role in carotenoid metabolism remains a question of debate.

Evidence from *in vitro* and *in vivo* studies have demonstrated a potential role of CMO2 in non-provitamin A metabolism. Initial reports suggested in addition to β-carotene that CMO2 enzymatically cleaved lycopene. It was further demonstrated that recombinant CMO2 displayed a higher affinity towards lycopene than β-carotene. While evidence from plants suggests additional CMO2 substrates may exist, no additional biochemical evidence is available investigating CMO2 cleavage of additional carotenoid substrates. More recently, single nucleotide polymorphisms within the CMO2 gene have been associated with the accumulation of xanthophylls carotenoids in the adipose tissue and skin of sheep and chickens, respectively. These findings suggest that CMO2 possess

substrate specificity beyond what is currently known. Non-provitamin A carotenoids, such as lycopene, lutein and zeaxanthin have been associated with a decreased risk of chronic and degenerative diseases. Additionally, the pro-vitamin A carotenoid β-cryptoxanthin has been associated with a decreased risk of lung cancer independent of β-carotene, suggesting that conversion to vitamin A is independent of potential anti-carcinogenic properties. These reports suggest that the effects of carotenoids, especially non-provitamin A carotenoids, may be mediated by their conversion to apo-carotenoid metabolites formed via the excentric cleavage pathway. To our knowledge, there is no biochemical evidence to support metabolism of additional non-provitamin A carotenoids by CMO2.

1.2 SIGNIFICANCE

Chronic and degenerative diseases are some of the most common, costly and preventable health problems and, thus, remain a considerable public health concern. Modifiable risk behaviors, such as lack of physical activity, poor nutrition, tobacco use and excessive alcohol consumption, are responsible for much of the illness, suffering and early death related to chronic diseases. Nutrition represents an effective strategy to reduce the risk of chronic and degenerative disease. Consumption of a diet rich in carotenoid-containing fruits and vegetables is strongly associated with a decreased risk of many chronic and degenerative diseases, including certain cancers, cardiovascular disease and AMD. While fruits and vegetables contain many essential nutrients, minerals, and fiber, particular research interest has focused on the presence of potential bioactive compounds, such as carotenoids. However, the metabolic pathways of

carotenoid metabolism are not fully understood. Results from two β-carotene supplementation trials demonstrating the deleterious effects of high-dose supplementation with a single carotenoid underscores our need to fully understand the metabolic pathways involved in carotenoid metabolism. Our understanding of the biochemical and molecular basis of carotenoid metabolism is incomplete. Furthering our understanding of carotenoid metabolism will significantly impact how recommendations are made regarding carotenoid intakes for health and disease.

1.3 HYPOTHESIS

The purpose of the dissertation described herein is to investigate the *in vitro* and *in vivo* biochemical and regulatory pathways of carotenoid metabolism by the carotenoid cleavage oxygenases, COM1 and CMO2. The central hypothesis for this research is that vertebrate carotenoid cleavage oxygenases possess broad substrate specificity, cleaving a broad range of carotenoid substrates into potentially biologically important carotenoid cleavage metabolites. More specifically, I hypothesize that 1) ferret CMO2 cleaves the xanthophyll carotenoids lutein, zeaxanthin and β-cryptoxanthin at the 9',10' double bond forming 3-OH-apo-carotenoid metabolites; and 2) supplementation of the xanthophyll carotenoid β-cryptoxanthin differentially effects the *in vivo* expression of the carotenoid cleaving enzymes, CMO1 and CMO2.

1.4 SPECIFIC AIMS

1.4.1 Specific Aim 1: *To determine the in vitro cleavage activity of recombinant ferret CMO2 towards β-cryptoxanthin, lutein and zeaxanthin and to characterize the in vitro production and identification of apo-carotenoid metabolites.*

A baculovirus system will be utilized to produce recombinant ferret CMO2 protein. HPLC, LC-MS and GC-MS methods will be developed and used for the detection and quantification of resultant apo-carotenoid metabolites. Enzymatic cleavage activity will be determined using the xanthophylls lutein, zeaxanthin and β-cryptoxanthin as substrates. Initial velocity parameters (protein- and time-dependent activity) will be determined to estimate *in vitro* kinetic parameters (K_M and V_{max}) of CMO2 cleavage.

1.4.2 Specific Aim 2: To examine the relative abundance and tissue-specific expression of CMO1 and CMO2 and to determine effect of β-cryptoxanthin supplementation on the *in vivo* regulation of CMO1 and CMO2 expression in the ferret animal model.

The ferret CMO1 gene will be cloned and the sequence analyzed. CMO1 and CMO2-specific real time PCR primers will be designed and used to determine the relative abundance and tissue specific expression of CMO1 and CMO2 in the ferret model. The effect of two doses (low and high) of β-cryptoxanthin supplementation on CMO1 and CMO2 expression will be examined in selected ferret tissues after 9 weeks of supplementation. The tissue accumulation of β-cryptoxanthin and retinoids after supplementation will be assessed using HPLC.

Chapter 2

Literature Review

2.1 BACKGROUND

Chronic and degenerative diseases are the most common, costly and preventable human health problems. Among Americans, 7 out of 10 deaths each year can be attributed to chronic disease. It is estimated that 45% of Americans 20 or older have at least one diagnosed or undiagnosed chronic disease conditions, such as hypertension, hypercholesterolemia or diabetes (1). Among the major contributors, heart disease, cancer and stroke account for more than 50% of all deaths (2). Modifiable risk behaviors, such as tobacco use, excessive alcohol consumption, poor nutrition, and lack of physical activity, are responsible for much of the illness, suffering and early death related to chronic diseases (3, 4). Poor nutrition is associated with nearly a fifth of all deaths, and its impact continues to increase (5, 6). Thus, nutrition represents an attractive approach to lowering the chronic disease burden in the U.S.

Consumption of a diet rich in fruits and vegetables is strongly associated with a decreased risk of many chronic and degenerative diseases, including certain cancers, cardiovascular disease and age-related macular degeneration (AMD) (7-9). Thus, worldwide dietary guidelines have been formulated to reflect this relationship. Many potential mechanisms have been suggested to account for the beneficial effects of fruit and vegetable consumption on disease reduction. While fruits and vegetables contain many essential nutrients, minerals, and fiber, particular interest has focused on the presence of potential bioactive compounds. One class of bioactive compounds found in fruits and vegetables that have garnered considerable research inquiry are carotenoids.

Carotenoids represent a class of lipophilic compounds, consisting of a polyisoprenoid structure, found in various fruits and vegetables. Carotenoids represent a

diverse group of >730 compounds and responsible for much of the yellow to red colors of our natural world, owing there presence to the bright colors to many flowers, fruits and vegetables. Among the diverse array of carotenoids found in nature, around 50 are found within the human diet with six major carotenoids accounting for approximately 90% of all carotenoids identified in human plasma and tissues (10-12). Carotenoids are typically divided into two structural groups. Carotenoids consisting of pure hydrocarbons, such as β-carotene and lycopene, are referred to as carotenes, while oxygenated derivatives, such as lutein, zeaxanthin and β-cryptoxanthin, are referred to as xanthophylls.

Carotenoids, especially those found in human plasma and serum, are typically classified according to vitamin A activity. The major provitamin A carotenoids are β-carotene, α-carotene and β-cryptoxanthin, while the major non-provitamin A carotenoids include lutein, zeaxanthin and lycopene (Figure 1). Besides provitamin A activity, the physiological functions most often attributed to these carotenoids are related to their ability to function as antioxidants, e.g., functioning as free radical scavengers, and, in the case of lutein and zeaxanthin, functioning as blue light filters, possibly preventing photodamage of the retina (13). However, recent research has moved beyond the function of intact carotenoids and focused on enzymatic formation of apo-carotenoid metabolites other than retinoids, which may impart some of the biological effects associated with carotenoids. Our understanding of the biochemical and molecular framework of carotenoid metabolism is incomplete. Lack of such knowledge has significantly hindered recommendations for carotenoid intake in health and disease.

2.2 CAROTENOID METABOLISM

2.2.1 Absorption and Transport

Due to their hydrophobic nature, carotenoids follow the same absorptive path as dietary lipids. Thus, release from the food matrix and dissolution in the lipid phase are critical steps for absorption. In the small intestine, carotenoids are incorporated into mixed micelles and absorbed by the mucosa (mainly the duodenum) via passive diffusion and packaged into triacylglycerol-rich chylomicrons. Carotenoids are also actively transported in the intestinal mucosa via the scavenger receptor class B type 1 (SR-B1) transporter (14). In addition, the surface glycoprotein cluster determinant 36 (CD36), which is located in the duodenum and jejunum, is involved in uptake of long chain fatty acids and oxidized low density lipoproteins. Because CD36 and SR-B1 share similar functions in lipid absorption, it has been suggested that CD36 also has a role in carotenoid uptake into cells (15, 16). Provitamin A carotenoids, such as β-carotene and β-cryptoxanthin, are partly converted into vitamin A, primarily retinyl esters, in the enterocytes of the intestinal mucosa (17, 18). Both retinyl esters and intact carotenoids are incorporated into chylomicrons and secreted into the lymph for transport to the liver (19). In fasting blood, up to 75% of hydrocarbon carotenoids, such as β-carotene and lycopene, are found in low-density lipoprotein (LDL) while xanthophylls are more evenly distributed between LDL and high-density lipoprotein (HDL) (20). Delivery of carotenoids to extrahepatic tissues occurs mainly thru the interaction of lipoproteins with receptors and the degradation of lipoprotein particles by lipoprotein lipase.

2.2.2 Carotenoid Cleavage Oxygenases (CCO)

Vitamin A synthesis from β-carotene was first demonstrated as far back as 1930 (21). Then, in 1965, Olson and Hayaishi (22) and Goodman and Huang (23) independently demonstrated enzymatic cleavage of β-carotene using crude enzyme fractions isolated from rat livers and intestines. Another 30 years would pass before a plant enzyme with specific carotenoid cleavage activity would be characterized (24, 25). Since then, a myriad of enzymes possessing carotenoid cleavage activity, which are responsible for synthesis of biologically significant apo-carotenoids, have been characterized.

The carotenoid cleavage enzymes represent an ancient family of enzymes with family members present in plant, bacteria, and animal families. Regardless of taxa, carotenoid cleavage oxygenases (CCOs) share a number of common characteristics; they require Fe^{2+} for catalytic activity (24, 26-28), contain four conserved histidine residues responsible for iron coordination (29), and possess a conserved peptide sequence in carboxyl terminus constituting a family signature sequence (27, 28). Searching sequence databases yields approximately 200 putative CCOs yet fewer than 30 have been characterized in the laboratory (30, 31). In animals, three CCO's have been isolated, cloned, and characterized: β-carotene-15, 15'-oxygenase (CMO1) (18, 28), carotene-9', 10'-oxygenase (CMO2) (26, 27), and Retinal Pigment Epithelium 65 (RPE65) (32). Evidence from previous reports suggests that CMO1 and CMO2 are not only involved in retinoid biosynthesis but also in synthesis of biological active apo-carotenoid compounds. RPE65, on the other hand, while lacking cleavage activity, has been recently shown to be function as a retinoid isomerase (33). While CMO1 and CMO2 have been exhaustively

studied in regard to their cleavage activity towards β-carotene, scant evidence is available identifying cleavage activity towards carotenoids other than β-carotene and lycopene, such as β-cryptoxanthin, lutein, or zeaxanthin. Evidence from bacterial, mammalian, and plant carotene cleavage oxygenases suggests that CMO1 and CMO2 may cleave carotenoids other than β-carotene into potentially biologically important apo-carotenoids.

2.2.2.1 Carotenoid cleavage by vertebrate carotene-15, 15'-oxygenase (CMO1)

For provitamin A carotenoids, such as β-carotene, α-carotene, and β-cryptoxanthin, central cleavage is a major pathway leading to vitamin A formation (Figure 2) (22, 23, 34). The carotene 15,15'-oxygenase (CMO1) gene, which is responsible for central cleavage at the 15, 15' double bond (18, 35), has been cloned and characterized in a number of species including the human and mouse (28, 36-39). With the molecular characterization of CMO1, it has been definitively shown that CMO1 catalyzes the central cleavage of β-carotene to yield two molecules of retinal, thus, contributing to vitamin A stores (40).

Using the murine CMO1 Redmond and colleagues demonstrated cleavage activity towards lycopene (28). Using lycopene accumulating *Escherichia coli* expressing mouse CMO1, they observed a distinct bleaching of color when induced with L-arabinose suggesting cleavage of lycopene. Additionally, purified recombinant mouse CMO1 displayed *in vitro* cleavage activity towards lycopene, yet *acyclo*-retinal, which is the central 15, 15'-double bond cleavage product of lycopene, was only detected when the lycopene concentrations used were 2.5-3 times higher than the observed K_m for β-carotene (K_m=6 μM). In contrast, Yan and colleagues observed no detectable activity of

human retinal pigment epithelium CMO1 towards lycopene or lutein (39), which supported previous reports of the *Drosohpila* homologue of CMO1 (18) and crude preparations of rat liver and intestine (41). Additionally, Lindqvist and Andersson, using a purified recombinant CMO1 isolated from a human liver cDNA library, demonstrated cleavage activity towards both β-carotene and β-cryptoxanthin but no activity towards lycopene or zeaxanthin (36). Although CMO1 was shown to cleave β-cryptoxanthin, analysis of the apparent K_m revealed an approximate 4-fold lower affinity towards β-cryptoxanthin (K_m=30.0±3.8 μM) than towards β-carotene (K_m=7.1±1.8 μM) (36), which lies in contrast to recent *in vivo* reports suggesting β-cryptoxanthin may be a more effective source of retinal compared to β-carotene (42, 43). More recently, it was reported that chicken CMO1 showed substrate specificity towards a broad array of carotenoid substrates displaying activity towards α-carotene, β-carotene, γ-carotene, β-carotene, β-cryptoxanthin, apo-4'-carotenal, and apo-8'-carotenal (44). No cleavage activity was demonstrated towards lycopene. In light of the combined evidence, authors have concluded that the presence of at least one unsubstituted β-ionone ring appears to be sufficient for catalytic cleavage of the central carbon 15,15' double bond.

2.2.2.2 Carotenoid cleavage by vertebrate carotene-9', 10'-oxygenase (CMO2)

An alternative pathway for carotenoid metabolism in mammals, termed the excentric cleavage pathway, remained a controversial issue for several decades. The controversy centered on whether there was a dedicated enzyme responsible for excentric carotenoid metabolism (45, 46). Demonstration of random cleavage of β-carotene and identification of a series of homologous carbonyl cleavage products, including β-apo-14'-

, 12'-, 10'-, and 8'-carotenals, β-apo-13-carotenone and retinoic acid, had been previously accomplished in tissue homogenates of humans, ferrets, and rats (47-49). This controversy was put to rest with the cloning and characterization of the murine carotene-9', 10'-oxygenase by Kiefer and colleagues, thus, confirming the existence of the asymmetric cleavage pathway of carotenoids (27). Keifer *et al.* isolated the murine CMO2 and demonstrated enzymatic cleavage of both β-carotene and lycopene. Cleavage of β-carotene was demonstrated using the isolated murine CMO2 *in vitro* and by using beta-carotene synthesizing and accumulating *Escherichia coli* strains expressing the mouse CMO2. A similar *E. coli* model, which synthesizes and accumulates lycopene, was used to demonstrate cleavage of lycopene by CMO2. When CMO2 was induced, a distinct color shift from red to white occurred, indicating cleavage. Although the author's state that significant amounts of apo-lycopenals were detected and tentative identifications were made based upon UV-visible spectra, no data were shown to accompany these observations (27). No other carotenoids were investigated in this study.

Because ferrets (*Mustela putorius furo*) and humans are similar in terms of carotenoid absorption, tissue distribution and concentrations, and metabolism (50, 51), the ferret CMO2 gene was cloned and characterized (26). Using the recombinant ferret CMO2 expressed in *Spodoptera frugiperda* (Sf9) insect cells for kinetic analysis, it was found that the cleavage of carotenoids by the ferret CMO2 occurs in a pH, incubation time, protein dose, and substrate dose-dependant manner (26). Of particular note is the difference in optimum pH; the optimum pH for CMO2 is 8.5, which differs from the reported optimum pH (7.7) of CMO1 (36). Similar to CMO1, it was found that the cleavage activity of ferret CMO2 for both β-carotene and lycopene was iron-dependent,

which is supported by the existence of four conserved histidines residues in the ferret CMO2 (26). These data are in agreement with previous observations demonstrating the conserved histidines act as putative iron-binding residues for iron coordination in apocarotenoid 15,15'-oxygenase (52) and CMO1 (29), supporting the notion that the entire superfamily of oxygenases shares a common structure (29).

It was further demonstrated that the recombinant ferret CMO2 catalyzes the excentric cleavage of *all-trans* β-carotene and *cis*-lycopene isomers effectively but not *all-trans* lycopene at the 9', 10' double bond (26). While an estimated K_m of 3.5 μM for *all-trans* β-carotene was calculated, kinetic constants of CMO2 cleavage of lycopene could not be calculated due to difficulty in controlling auto-isomerization, thus, necessitating the use of mixed isomers of lycopene as the substrate for kinetic analysis. Since the lycopene substrate mixture contains only ~20% as *cis* isomers and considering the ferret CMO2 would not cleave *all-trans* lycopene, it is speculated that the K_m for *cis*-lycopene is actually much lower than that of the lycopene isomer mixture. This indicates that *cis*-lycopene may act as a better substrate than *all-trans* β-carotene for the ferret CMO2. While demonstration of β-carotene and lycopene cleavage by CMO2 is clear, whether CMO2 cleaves additional substrates is unclear. However, recent genetic evidence combined with substrate specificity of plant CMO2 homologues suggests that CMO2 may, in fact, cleave additional carotenoid substrates.

2.2.2.3 Carotenoid Cleavage by Plant and Cyanobacterial CCO

While CMO2 has been shown to cleave both β-carotene and *cis*-lycopene (26, 27), it is unclear if other carotenoids can serve as potential substrates. Characterization of

carotenoid cleavage oxygenases from plants and cyanobacteria, however, provides evidence suggesting broad substrate specificity. A number of plant carotenoid cleavage dioxygenase (CCD) enzymes show a broad substrate specificity at the 9,10 as well as the 9',10' position (31). These enzymes constitute the CCD subfamily, named after the CCD1 from *Arabidopsis* (53). CCD1 possesses cleavage activity towards a wide range of all-*trans* and 9-*cis*-carotenoids as well as epoxycarotenoids, among them the C_{30} apo-carotenoid all-*trans*-8'-apo-β-carotenal (53, 54). When 9-*cis*- substrates are present, CCD1 generally cleaves at the 9',10' initially, yielding C_{27} apo-carotenoids. The melon CCD1 has been demonstrated to cleave all-*trans* phytoene and lycopene in addition to β- and δ-carotene at the 9,10 (9',10') double bond producing C_{13} products (55). CCD1 from crocus (56) and grapevine (*Vitis vinifera*) (57) displayed cleavage activity towards zeaxanthin, producing 3-OH-β-ionone. CCD1 from petunia cleaves β-carotene yielding β-ionone (58). The maize CCD1 (ZmCCD1) was shown to cleave lycopene, β-carotene, zeaxanthin, ζ-carotene, and δ-carotene at the 9', 10' double bond (59). Strawberry CCD1 (FaCCD1) was also shown to have a broad substrate affinity cleaving β-apo-8-carotenal, β-carotene, lutein, and zeaxanthin (60). All CCD1s are expected to accept a wide range of substrates similar to those found in the *Arabidopsis* and tomato (61).

Cyanobacteria CCDs also possess broad substrate specificity. A CCD orthologue found in cyanobacteria, *Nostoc* carotenoid cleavage dioxygenase (NosCCD), was shown to cleave a broad array of carotenoid substrates similar to plant CCDs. In addition to excentric cleavage of zeaxanthin, echinenone, canthaxin, and astaxanthin, several monocyclic carotenoids, such as γ-carotene, myxol, and myxoxanthophylls were cleaved excentrically at the 9', 10' and 8', 7' double bond (62). A CCD orthologue from the

cyanobacteria *Nostoc* sp PCC 7120 was shown to cleave β-carotene and β-apo-8'-carotenal at the 9,10 double bond (63). Whether human CMO2 can cleave a broad range of substrates similar to those found in plants and cyanobacteria is unclear.

2.2.3 Genetic Alterations in Human and Animal Carotenoid Metabolism

Variability in β-carotene metabolism has been well documented (64, 65)}, leading to the description of low-responder and low-converter phenotypes. While regulation of CMO1 (66) and regulation of carotenoid absorption (14) may partially explain these phenotypes, several genetic alterations have been recently identified in humans that also affect β-carotene metabolism. An elevation in plasma β-carotene and decreased plasma retinol was recently demonstrated in an individual possessing a heterozygous mutation in the human CMO1 gene (67). Biochemical analysis of the mutant CMO1 protein identified the replacement of a highly conserved threonine residue by a methionine residue. Kinetic characterization demonstrated an ~90% decrease in activity compared to wild type CMO1, suggesting functional mutations in CMO1 can cause impairments in β-carotene metabolism.

A number of SNPs have also been identified in the protein-coding region human CMO1 gene resulting in several different protein variants (67-69). Two SNPs in the CMO1 gene, A379V and R267S variant T allele, were shown to occur in 24% and 42%, respectively, of a U.K. cohort (69). Biochemical analysis again determined varying degrees of activity, which were corroborated through a human intervention study. Women carrying either the 267S+379S or 379V variants displayed decreased intestinal β-carotene conversion efficiency. In a separate study, a SNP located upstream of the

CMO1 gene was associated with increased β-carotene and α-carotene blood levels (68). Interestingly, lycopene, lutein and zeaxanthin levels were lower in SNP carriers. Nonetheless, the presence of SNPs within the CMO1 gene may partially explain low-converter phenotypes.

While there are no reports of genetic alterations in the human CMO2 gene, SNPs within carotenoid-associated genes may have an influence on metabolism by CMO2. Indeed, SNPs within components of lipoprotein metabolism, such as ApoB, lipoprotein lipase (LPL) and SR-B1, are associated with altered plasma carotenoid profiles in humans (70-72). These genes have a profound effect not only on absorption of carotenoids but also on the tissue distribution of carotenoids. Interestingly, a SNP within the SR-B1 gene has been identified as a risk factor for age-related macular degeneration (73).

Recent animal genetic reports have provided evidence of the role of CMO2 in carotenoid metabolism and provided evidence of broad substrate specificity. Bovine CMO2 was shown to contain a single nucleotide polymorphism resulting in a truncated, and presumably non-functional, CMO2 protein (79 amino acids versus 530 amino acids) (74, 75). The resulting CMO2 SNP was significantly associated with a yellow adipose and milk fat color and adipose β-carotene concentration (75). The same CMO2 SNP was significantly associated with increased β-carotene milk content (78% and 55% compared with +/+ and +/-, respectively). Hepatic CMO2 expression was four fold lower in homozygous carriers. Additionally, serum β-carotene was significantly increased while hepatic retinol stores were decreased (74).

A SNP in the sheep CMO2 gene was also associated with increased carotenoid accumulation. In Norwegian white sheep (*Ovis aries*), a nonsense mutation in the CMO2 gene was significantly associated with a yellow adipose phenotype (76). Interesting, sheep predominating accumulate lutein and flavoxanthin in their adipose (77). In chickens, a yellow skin phenotype was shown to be associated with a SNP in the CMO2 gene (78). Interestingly, the CMO2 SNP resulted in a tissue-specific decrease in skin but not hepatic CMO2 expression. In heterozygotes (possessing both white and yellow skin alleles) pyrosequencing revealed that skin CMO2 expression was due to the white skin allele, but hepatic CMO2 expression was due to both the yellow and white skin alleles. The CMO2 SNP may affect a cis-regulatory element thereby decreasing skin CMO2 expression. Interestingly, chickens predominately accumulate the xanthophylls lutein and zeaxanthin in their skin (79).

The accumulation of xanthophylls in both sheep in chickens and association with mutations in the CMO2 gene suggests that CMO2 may cleave a broader subset of carotenoids than previously known. More specifically, CMO2 may cleave xanthophyll carotenoids, such as lutein, zeaxanthin and β-cryptoxanthin. Cleavage of lutein (Figure 3), zeaxanthin (Figure 4) or β-cryptoxanthin (Figure 5) by CMO2 is expected to occur at the 9',10' or 9,10 double bond, producing 3-OH-apo-carotenoids, β-apo-carotenoids, β-ionone or 3-OH-β-ionone. Providing biochemical evidence regarding CMO2 cleavage will further our current understanding of carotenoid metabolism, especially of non-provitamin A carotenoids.

2.2.4 Apo-carotenoid Activity

While genetic evidence suggests a broader role for CMO2 in carotenoid metabolism, especially in non-provitamin A metabolism, there is currently no biochemical evidence to support cleavage of additional substrates by CMO2. While it is unclear if excentric cleavage products of carotenoids other than β-carotene or lycopene are formed, several putative metabolites have already been shown to have biological activity *in vitro* and *in vivo* (80, 81). Apo-carotenoids and apo-lycopenoids have been demonstrated a diverse array of biological activities including differentiation, cell proliferation, apoptosis, activation of nuclear receptors, induction of phase I and II enzymes and interactions with growth factors (Figure 6).

Recent studies have implicated that lutein and zeaxanthin apo-carotenoids may possess biological activity. Using HeLa cervical cancer cells, lutein and lutein oxidation products were shown to possess antioxidant properties and effect cell viability (82). Lutein oxidation products were prepared by photooxidation of lutein liposomes (exposure to direct sunlight) and were tentatively identified by LC-MS as a mixture of dehydration products and apo-carotenoids. However, the mixture did not contain 3-OH-β-apo-10'-carotenoids. Oxidized lutein products decreased cell proliferation and increased apoptosis compared to lutein alone (20 μM). Interestingly, lutein oxidation products exhibited greater antioxidant capabilities than lutein, demonstrated by increased radical scavenging activity, decreased glutathione and decreased malondialdehyde (MDA) levels. While lutein oxidation products were shown to have a significant effect on antioxidant status and cell viability, the use of a mixture of oxidation products does not allow the isolation of any particular lutein oxidation compound. Whether the effects

observed are due to one compound or the presence of many oxidation products is unknown.

In human retinal pigment epithelial ARPE-19 cells carotenoid-derived aldehyde (CDA) breakdown products were shown to induce oxidative stress leading to apoptotic cell death (83). β-carotene, lutein and zeaxanthin were oxidized with NaOCl to obtain CDA oxidation products, which dose-dependently decreased cell viability (0 -100 uM). There was an increase in apoptosis when cells were incubated with β-carotene, lutein and zeaxanthin oxidation products as measured by DNA-fragmentation. Increases in apoptosis were paralleled by a decrease in mitochondrial potential. Additionally, β-carotene CDA products time-dependently decreased cell proliferation and dose-dependently increased reactive oxygen species (ROS). Oxidation products also increased protein expression of AP-1 and NF-κB. Many of the oxidative effects of carotenoid oxidation products were inhibited by the addition of the antioxidant *n*-acetylcysteine (NAC). These results indicate a potential role of apo-carotenoid products in oxidative stress and regulation of cell death. While the products used in this study were not determined, the first products formed from enzymatic cleavage contain aldehyde function groups. Thus, potential 3-OH-apo-carotenals could play an important role in cellular toxicity and apoptosis.

2.3 Regulation of Carotene Cleavage Oxygenases:

2.3.1 Background

While increasing our understanding of the biochemical basis of carotenoid metabolism is needed, critical details regarding the regulation of carotenoid metabolism

are also lacking. Without such knowledge, it remains difficult to understand the true physiologic impact of carotenoids on human health and disease. Interestingly, very little is known regarding the regulatory mechanisms of carotenoid cleavage oxygenases (CCO), especially CMO2. Supplementation with non-provitamin A carotenoids has shown to influence CMO2 expression, while CMO1 tends to be influenced primarily by provitamin A carotenoids. Thus, a potential model of investigating the effect of both provitamin A and non-provitamin A carotenoids on CCO expression would be the use of β-cryptoxanthin.

2.3.2 β-cryptoxanthin and Lung Cancer Prevention

β-Cryptoxanthin (3-hydroxy-β-carotene) is unique among the commonly identified carotenoids in humans; It is the only xanthophyll carotenoid to possess pro-vitamin A activity. Oranges and orange juices are rich dietary sources of β-cryptoxanthin (84). Average U.S. dietary intakes are approximately 100 μg/day (85, 86). Recent studies have suggested that β-cryptoxanthin may play an important role in chemoprevention, especially against lung cancer. Importantly, these studies have suggested that the biological effects of β-cryptoxanthin may be mediated by specific metabolites. Thus, investigating the effect of β-cryptoxanthin on carotenoid cleavage oxygenase expression may provide insight into its potential mechanisms of chemoprevention.

2.3.2.1 Epidemiological Evidence

Individual carotenoids like β-cryptoxanthin have been linked in particular to a reduced risk of lung cancer in a number of studies. The strongest evidence to support a link between reduced risk of lung cancer and β-cryptoxanthin intake are data from the pooled analysis of seven cohort studies. These studies investigated 3,155 incident lung cancer cases among 399,765 participants after 7 – 16 years of follow-up. Subjects consuming the highest intake of β-cryptoxanthin had a 24% reduction (RR=0.76; CI 0.67 – 0.86) in lung cancer risk when compared to the lowest consumption levels (87). Interestingly, the protective effect of β-cryptoxanthin was independent of vitamin A formation, suggesting other potential mechanisms of risk reduction. A more recent systematic review demonstrated a protective effect of both β-cryptoxanthin and lycopene against lung cancer (88). A significant protective effect against lung cancer due to dietary intake of β-cryptoxanthin (RR=0.80, 0.72 – 0.89) was seen when highest versus lowest intake were compared. These studies support earlier conclusions from the World Cancer Research Fund (WCRF) stating a "probable" association between carotenoid intake and a decreased risk of several cancers especially those of the lung and bronchus (7).

Whilst the association between carotenoid intakes and chronic and degenerative disease exists, questions remain as to whether the associations are due to the intact carotenoid molecule or is due to carotenoid metabolites. This is a pertinent question in light of the results of the ATBC and CARET studies. In the Finnish ATBC Study (89), there was a significant 18% increase (RR= 1.18; 95% CI: 1.03 – 1.30) in lung cancer incidence in participants receiving 20 mg β-carotene per day for 5 to 8 years compared to

no β-carotene supplement. There was also an 8% increase in mortality (RR= 1.08; 95% CI: 1.01 – 1.16) for those receiving β-carotene supplements compared to no β-carotene supplement. In the CARET study, participants who were either heavy smokers or had been occupationally exposed to asbestos received 30 mg β-carotene and 25,000 IU vitamin A daily for 4 years (90). The supplemental arm of the study experienced a significant 28% increase in lung cancer incidence (RR= 1.28; 95% CI: 1.04 – 1.57) and a significant 17% increase in all-cause mortality (RR= 1.17; 95% CI: 1.03 – 1.33). There was also a significant increase in death from lung cancer associated with β-carotene (RR=1.46; 95% CI: 1.07 – 2.00). The results of these studies were subsequently shown to be related to increased oxidized β-carotene metabolite formation with high-dose but not low-dose β-carotene supplementation (91-96). These results underlie the need to understand basic metabolism of carotenoids, especially the regulatory mechanisms of carotene cleavage oxygenases.

2.3.3 Dietary and Molecular Regulation of CMO1 Expression

2.3.3.1 Dietary Regulation

Various dietary components have been shown to influence the bioconversion of provitamin A carotenoids (97). Several studies have indicated that quantity (98) and quality (99) of dietary fat affects CMO1 activity. Protein quality and quantity have also been demonstrated to affect CMO1 activity (98, 100). While many dietary components have been associated with CMO1 activity, they may be more relevant to carotenoid absorption and bioavailability than actual cleavage activity.

Unlike vitamin A, high-dose β-carotene supplementation does not result in hypervitaminosis A, indicating that cleavage of β-carotene to vitamin A is tightly regulated. Indeed, a number of studies have indicated that CMO1 activity is regulated by vitamin A status (100, 101). Significant differences in intestinal CMO1 expression were observed in rats fed a vitamin A-deficient diet compared to vitamin A-sufficient rats (102). Intestinal CMO1 activity was also associated with hepatic vitamin A stores (101, 103). The relationship of CMO1 and vitamin A status has been recently clarified, identifying concerted molecular mechanisms governing CMO1 expression.

2.3.3.2 Molecular Regulation

Considering the role of CMO1 in β-carotene metabolism, it is not surprising then, many studies have indicated an intimate relationship between vitamin A homeostasis and transcriptional regulation of CMO1. Studies have indicated that expression of CMO1 may be regulated through feedback regulatory mechanisms via interactions between retinoic acid and its nuclear receptors (66, 104, 105) (Figure 7). This relationship has been recently clarified, indicating an intricate network affecting not only CMO1 expression but also carotenoid absorption. An intestine-specific homeobox (ISX) transcription factor was shown to repress intestinal expression of SR-B1 (106), which facilitates the absorption of dietary lipids and carotenoids (107, 108). ISX was also found to repress expression of intestinal CMO1 (109). Using CMO1-KO mice, it was further demonstrated that ISX is under the control of RA/RAR-dependent mechanisms (14). During vitamin A insufficiency, both CMO1 and SR-B1 expression is induced to increase absorption and conversion of β-carotene. Cleavage of β-carotene by CMO1 produces

retinoic acid, which induces expression of the ISX transcription factor via RAR. ISX represses expression of both CMO1 and SR-B1, thus, completing the dietary feedback mechanism (Figure 7).

The regulatory network between lipid absorption and CMO1 expression further implicate an intimate link between carotenoid and lipid metabolism. Molecular studies of the mouse and human CMO1 promoter demonstrated the presence of a peroxisome proliferator response element (PPRE) (110, 111). PPARγ and RXRα agonists were shown to transactivate the CMO1 promoter-reporter when co-transfected with the corresponding nuclear receptor (110). Analysis of the human CMO1 promoter identified an additional enhancer element; a myocyte enhancer factor-2 (MEF2) binding site was identified and when mutated reduced luciferase activity by ~30% (111).

The regulation of CMO1 by PPAR and RXR indicates a regulatory link between carotenoid and lipid metabolism, and several recent reports have shed light on this relationship. In F344 rats supplemented with lycopene, CMO1 expression was significantly decreased in the adrenal gland and kidney (112). Interestingly, fatty acid binding protein-3 (FABP-3), a PPARγ target gene, was downregulated in parallel with CMO1. In CMO1-KO mice, a gross impairment in lipid metabolism was observed (40). There was a significant increase in several fatty acid metabolism genes, including CD36 and fatty acid binding protein-4 (FABP4) expression, both PPARγ target genes, in visceral adipose tissue. There also were significant increases in serum free fatty acids and total lipids resulting in hepatic steatosis. It has been suggested that cleavage products of β-carotene may fine-tune the crosstalk between the nuclear receptors that regulate lipid

metabolism (113-115). The relationship between carotenoid and lipid metabolism deserves further inquiry.

2.3.4 Dietary and Molecular Regulation of CMO2 Expression

2.3.4.1 Dietary Regulation

Unlike CMO1, little evidence is available regarding CMO2 regulation. However, much of the evidence produced thus far have indicated that supplementation with various carotenoids, especially non-provitamin A carotenoids, may impact CMO2 expression (Figure 7). Using male adult ferrets, a significant 4-fold increase in lung CMO2 expression was observed after 9 weeks of lycopene supplementation (26). The ferrets in this study received a lycopene dose of 4.3 mg/kg body weight per day, which is equivalent to 60 mg per day in a 70-kg human (26, 116). This dose is approximately 7 times the average intake of lycopene in the American diet (117). In a separate studying utilizing F344 rats, lycopene supplementation for various time periods resulted in a subtle yet significant down-regulation of CMO2 expression in several tissues (112). F344 rat were fed AIN-93G control diets or AIN-93G diets supplemented with 0.25 g/kg lycopene for various time points: 3 days, 7 days, 30 days, 37 days, and 30 days followed by 7 days of control diet. Kidney CMO2 expression was significantly decreased regardless of supplementation length. The reasons for this are unknown. In the lung, there was a significant decrease in CMO2 expression after 37 days of lycopene supplementation compared to all other time points. There was also a significant decrease in expression in the intestinal mucosa after 37 days compared to 7 days of lycopene supplementation. There were no changes in CMO2 expression in the liver, testes, adrenal gland, or prostate (ventral, dorsolateral, and anterior prostate) gland.

In a previous study, we demonstrated that β-carotene supplementation had no significant effect on lung and liver CMO2 expression. Ferrets were supplemented with low- or high-dose β-carotene (equivalent to 6.7 and 33.6 mg/day in humans), with or without ascorbic acid and α-tocopherol, and/or exposed to cigarette smoke for six weeks. After 6 weeks, we observed no significant changes in liver or lung CMO2 mRNA expression (118). A recent report recently identified a possible link between CMO2 expression and alcohol consumption (119). Chronic alcohol consumption resulted in a significant increase in CMO1 mRNA expression as well as a significant increase in both PPARγ and PPARα protein and mRNA expression. Alcohol consumption was also association with a decrease in hepatic retinoid concentrations. Interestingly, there was also a small, yet significant, increase in CMO2 protein and mRNA expression. As expected CMO1 expression was highly positively correlated with PPARγ expression (110, 111). Interestingly, hepatic CMO2 expression was positively correlated with both PPARγ and PPARα expression. No recognized response elements within the CMO2 promoter have been identified to date (112). Thus, the potential relationship between CMO2 and PPAR definitely deserves further inquiry. Taken together, these results indicate that dietary factors may influence CMO2 expression, especially carotenoid supplementation. Additionally, CMO2 expression may be regulated in a tissue- and model-specific manner.

2.3.4.2 Molecular Regulation

The molecular mechanisms regulating CMO2 expression remain largely unknown. Unlike CMO1, a recent molecular analysis failed to identify a peroxisome

proliferator response element (PPRE) within the mouse CMO2 promoter (112). Work in our own laboratory has also failed to identify any potential nuclear receptor response elements, such retinoic acid response elements (RARE) or any other enhancer sequences (MEF2) within the ferret CMO2 promoter (unpublished data). This lack of molecular knowledge has proven to be a significant barrier regarding regulation of CMO2 expression.

Some insight into CMO2 regulation has been gained from the use of the CMO1-KO mouse model. Compared to wild type mice, CMO1-KO mice have significantly elevated expression of hepatic CMO2 expression (40, 120). CMO2 expression was significantly increased in intact livers and isolated hepatocytes and hepatic stellate cells of CMO1-KO mice compared to wild type mice (120). This suggests the presence of concerted mechanisms governing the expression of CMO1 and CMO2. It is possible that elevated levels of expression are due to increased tissue concentrations of β-carotene and/or increased concentrations of apo-carotenoids. Interestingly, while both apo-10'- and apo-12'- were detected in the plasma and liver samples, only apo-12'-carotenal was significantly increased in CMO1-KO mice. β-Carotene concentrations, however, were increased 40-times and 20-times in the plasma and livers of CMO1-KO compared to wild type mice. This suggests that increases in tissue concentrations of intact carotenoids may have a direct effect on CMO2 expression. While the lack of molecular regulatory mechanisms has provided little insight into the regulation of CMO2, feeding studies of carotenoids have provided some evidence of tissue-specific regulation in response to carotenoid feeding. Information regarding the effect of other carotenoids (ex. β-

cryptoxanthin) on CMO2 expression will add to the knowledge of CMO2 regulation and help provide evidence of its physiologic function.

2.4 Summary

The molecular and regulatory framework of carotenoid metabolism is far from complete. This is ever apparent regarding excentric metabolism by CMO2. While evidence from plants and animal genetic reports support wide substrate specificity for CMO2, biochemical evidence to support these observations remains absent. Providing biochemical evidence regarding CMO2 substrate specificity, especially of non-provitamin A carotenoids, will greatly improve our current understanding of carotenoid metabolism and biological activity. While biochemical evidence regarding CMO2 is lacking, there is also a lack of knowledge regarding CMO2 regulation. Questions remain as to whether dietary factors, such as carotenoid supplementation, influence CMO2 expression in a tissue- and model-specific manner. New research towards these above questions will further broaden our understanding of carotenoid metabolism and potentially identify new compounds and pathways that may exert many of the beneficial effects of carotenoids on human health and disease.

Figure 1.

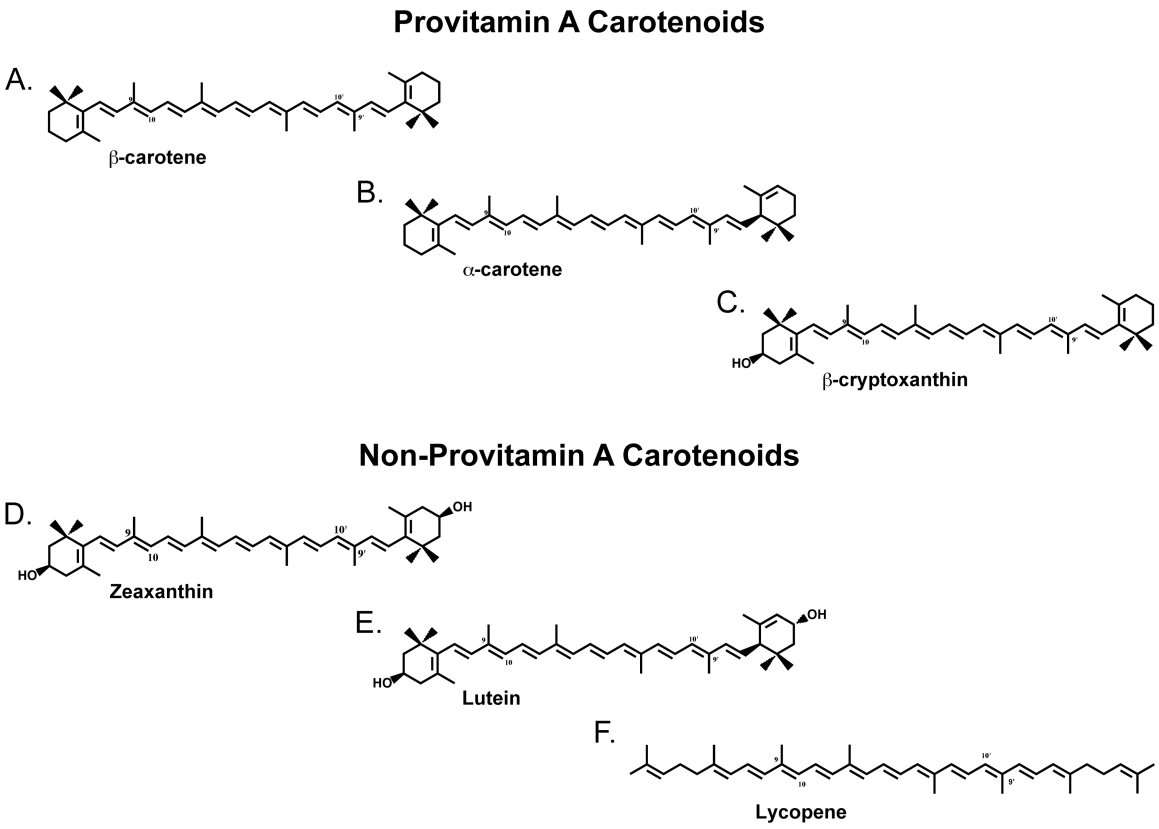

Figure 1. Chemical structures of the major carotenoids found in human plasma and tissues. The major provitamin A carotenoids found in human plasma and tissues include β-carotene (*A*), α-carotene (*B*) and β-cryptoxanthin (*C*). The major non-provitamin A carotenoids found in human plasma and tissues include zeaxanthin (*D*), lutein (*E*) and lycopene (*F*).

Figure 2.

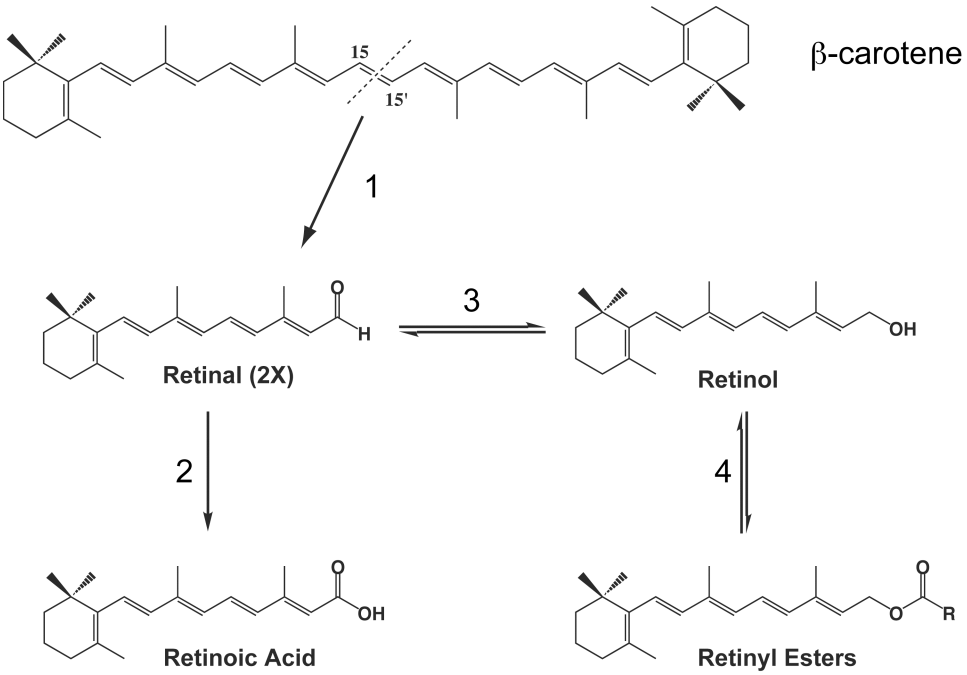

Figure 2. Metabolic pathway of β-carotene cleavage by carotene-15,15'-monooxygenase (CMO1) and subsequent retinoid bioconversion. (*1*) β-carotene is symmetrically cleaved at the 15,15' double bond by CMO1 producing two molecules of all-*trans* retinal. (2) Retinal can be oxidized to retinoic acid and/or (3) reduced to retinol. (4) Retinol can also be converted to retinyl esters for storage.

Figure 3.

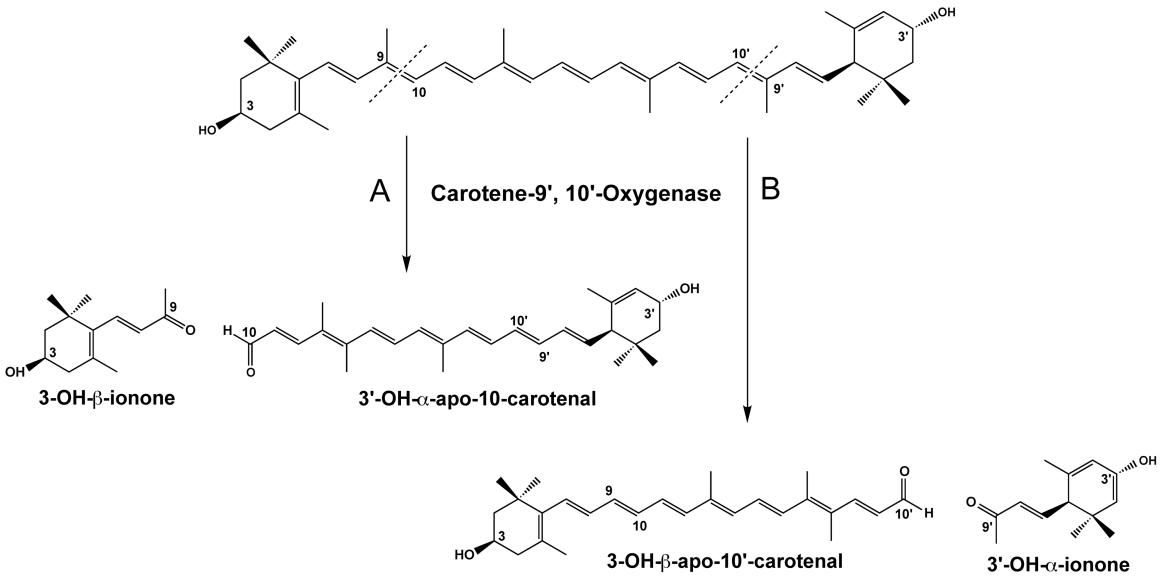

Figure 3. Proposed metabolic pathway of lutein cleavage by CMO2. Cleavage of lutein by CMO2 may occur at either the 9,10 or 9',10' double bond. (*A*) Cleavage at the 9,10 double bond would produce 3-OH-β-ionone and 3'-OH-α-apo-10'-carotenal. (*B*) Cleavage at the 9',10' double bond would produce 3-OH-β-apo-10'-carotenal and 3'-OH-α-ionone.

Figure 4.

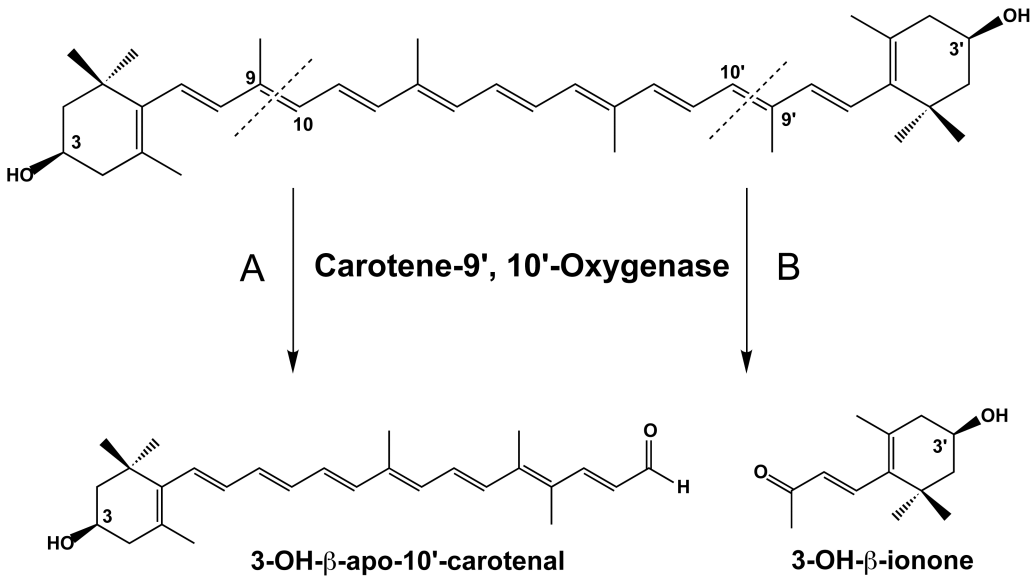

Figure 4. Proposed metabolic pathway of zeaxanthin cleavage by CMO2. Cleavage of zeaxanthin by CMO2 may occur at either the 9,10 (*A*) or 9',10' (*B*) double bond producing both 3-OH-β-ionone and 3-OH-β-apo-10(10')-carotenal.

Figure 5.

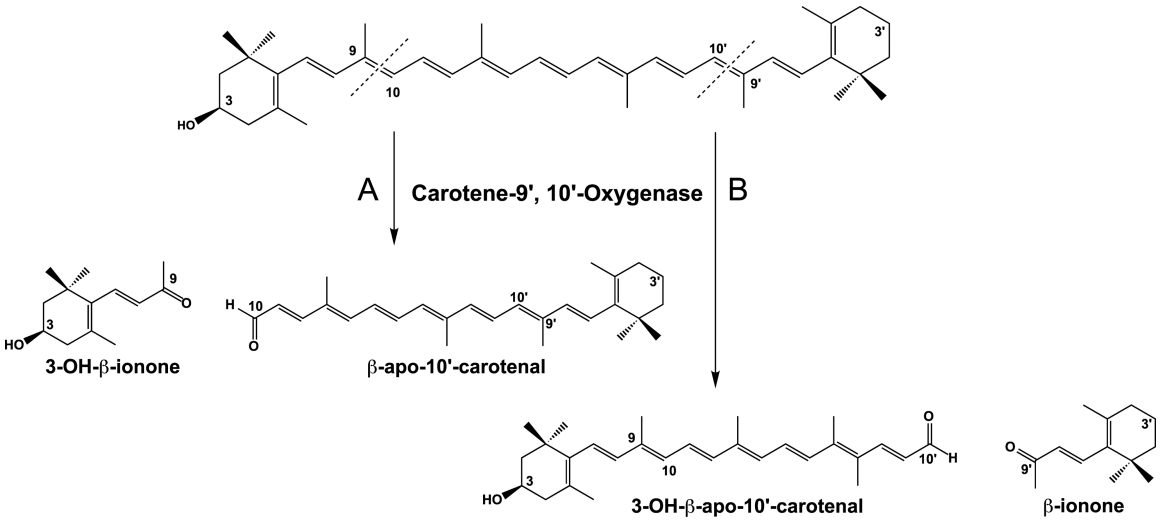

Figure 5. Proposed metabolic pathway of β-cryptoxanthin cleavage by CMO2. Cleavage of β-cryptoxanthin by CMO2 may occur at either the 9,10 or 9',10' double bond. (*A*) Cleavage at the 9,10 double bond would produce 3-OH-β-ionone and β-apo-10'-carotenal. (*B*) Cleavage at the 9',10' double bond would produce 3-OH-β-apo-10'-carotenal and β-ionone.

Figure 6.

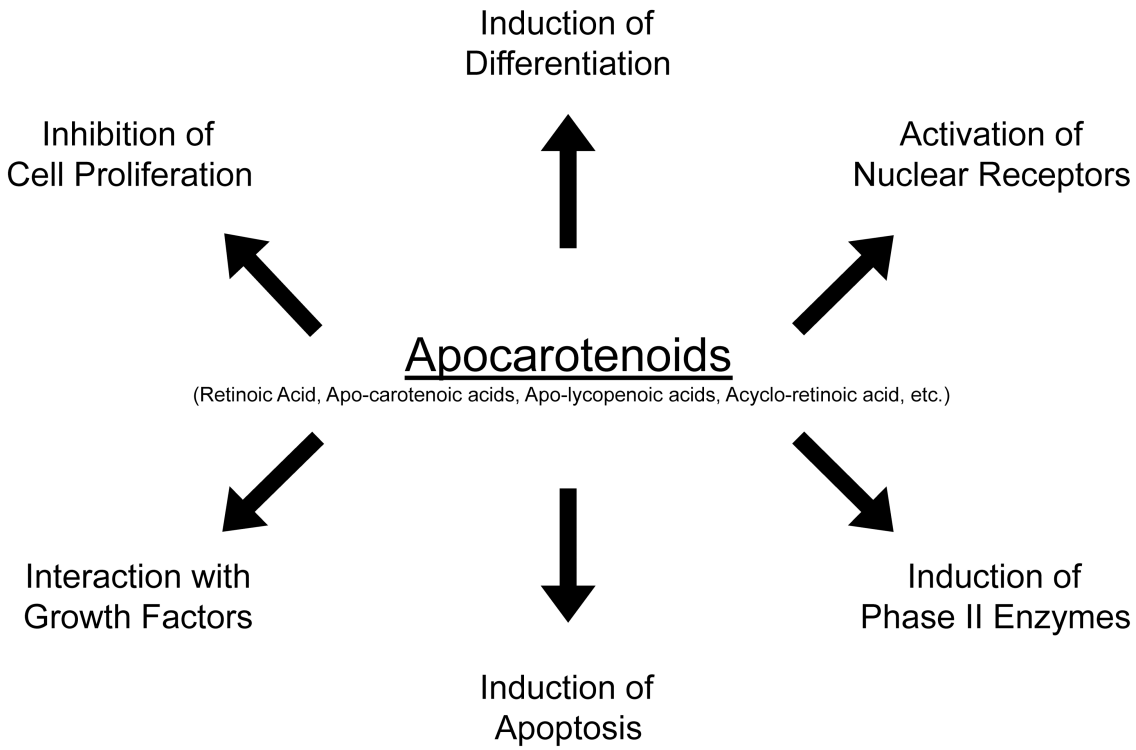

Figure 6. Proposed mechanisms of apo-carotenoid biological activities.

Figure 7.

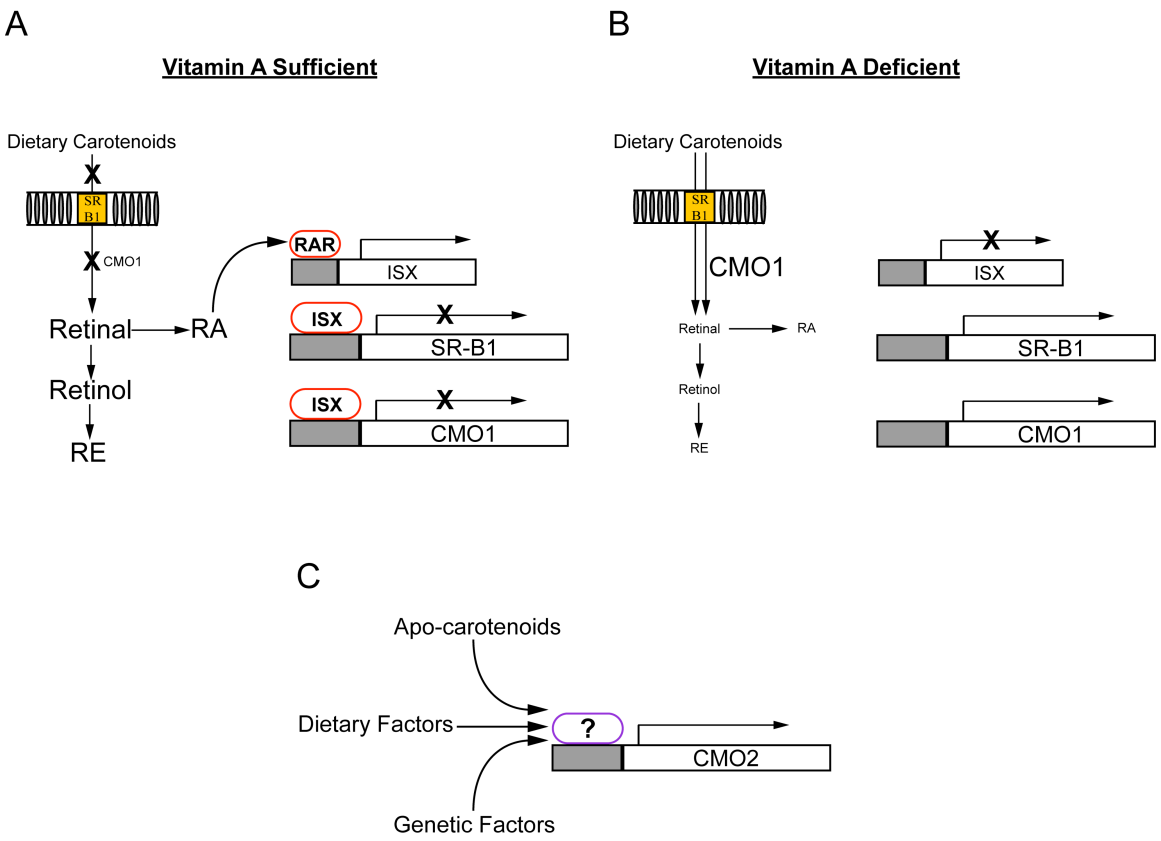

Figure 7. Proposed regulatory mechanisms of CMO1 and CMO2 expression. Regulation of CMO1, especially intestinal regulation, is dependent upon vitamin A status. In vitamin A sufficiency (*A*), increased RA, via RAR, stimulates expression of the intestine specific homeobox (ISX) transcription factor, which represses expression of both SR-B1 and CMO1. During vitamin A deficiency (*B*), decreased RA levels result in decreased ISX expression, which stimulates expression of SR-B1 and CMO1. Very little is known regarding regulatory mechanisms of CMO2 expression (*C*). Possible contributors in CMO2 regulation include dietary factors, such as carotenoid supplementation, genetic factors and/or formation of apo-carotenoid metabolites.

2.5 References

1. Fryar CD, Hirsch R, Eberhardt MS, Yoon SS, Wright JD. Hypertension, high serum total cholesterol, and diabetes: racial and ethnic prevalence differences in U.S. adults, 1999-2006. NCHS Data Brief. 2010 Apr:1-8.

2. Kung HC, Hoyert DL, Xu J, Murphy SL. Deaths: final data for 2005. Natl Vital Stat Rep. 2008 Apr 24;56:1-120.

3. Prevalence of self-reported physically active adults--United States, 2007. MMWR Morb Mortal Wkly Rep. 2008 Dec 5;57:1297-300.

4. Eaton DK, Kann L, Kinchen S, Shanklin S, Ross J, Hawkins J, Harris WA, Lowry R, McManus T, et al. Youth risk behavior surveillance--United States, 2007. MMWR Surveill Summ. 2008 Jun 6;57:1-131.

5. McGinnis JM, Foege WH. Actual causes of death in the United States. JAMA. 1993 Nov 10;270:2207-12.

6. Mokdad AH, Marks JS, Stroup DF, Gerberding JL. Actual causes of death in the United States, 2000. JAMA. 2004 Mar 10;291:1238-45.

7. (WCRF/AICR) WCRFAIfCR. Food, nutrition, physical activity, and the prevention of cancer: a global perspective. 2007; Washington DC; 2007.

8. Van Duyn MA, Pivonka E. Overview of the health benefits of fruit and vegetable consumption for the dietetics professional: selected literature. J Am Diet Assoc. 2000 Dec;100:1511-21.

9. Liu S, Manson JE, Lee IM, Cole SR, Hennekens CH, Willett WC, Buring JE. Fruit and vegetable intake and risk of cardiovascular disease: the Women's Health Study. Am J Clin Nutr. 2000 Oct;72:922-8.

10. Bendich A. Symposium conclusions: biological actions of carotenoids. J Nutr. 1989 Jan;119:135-6.

11. Khachik F, Spangler CJ, Smith JC, Jr., Canfield LM, Steck A, Pfander H. Identification, quantification, and relative concentrations of carotenoids and their metabolites in human milk and serum. Analytical chemistry. 1997 May 15;69:1873-81.

12. Gerster H. The potential role of lycopene for human health. Journal of the American College of Nutrition. 1997 Apr;16:109-26.

13. Krinsky NI, Johnson EJ. Carotenoid actions and their relation to health and disease. Molecular aspects of medicine. 2005 Dec;26:459-516.

14. Lobo GP, Hessel S, Eichinger A, Noy N, Moise AR, Wyss A, Palczewski K, von Lintig J. ISX is a retinoic acid-sensitive gatekeeper that controls intestinal {beta},{beta}-carotene absorption and vitamin A production. Faseb J. 2010 Jan 8.

15. During A, Dawson HD, Harrison EH. Carotenoid transport is decreased and expression of the lipid transporters SR-BI, NPC1L1, and ABCA1 is downregulated in Caco-2 cells treated with ezetimibe. J Nutr. 2005 Oct;135:2305-12.

16. During A, Doraiswamy S, Harrison EH. Xanthophylls are preferentially taken up compared with beta-carotene by retinal cells via a SRBI-dependent mechanism. Journal of lipid research. 2008 Aug;49:1715-24.

17. von Lintig J, Hessel S, Isken A, Kiefer C, Lampert JM, Voolstra O, Vogt K. Towards a better understanding of carotenoid metabolism in animals. Biochim Biophys Acta. 2005 May 30;1740:122-31.

18. von Lintig J, Vogt K. Filling the gap in vitamin A research. Molecular identification of an enzyme cleaving beta-carotene to retinal. The Journal of biological chemistry. 2000 Apr 21;275:11915-20.

19. Parker RS. Absorption, metabolism, and transport of carotenoids. FASEB J. 1996 Apr;10:542-51.

20. Clevidence BA, Bieri JG. Association of carotenoids with human plasma lipoproteins. Methods in enzymology. 1993;214:33-46.

21. Moore T. Vitamin A and carotene: The absence of the liver oil vitamin A from carotene. VI. The conversion of carotene to vitamin A in vivo. The Biochemical journal. 1930;24:692-702.

22. Olson JA, Hayaishi O. The enzymatic cleavage of beta-carotene into vitamin A by soluble enzymes of rat liver and intestine. Proc Natl Acad Sci U S A. 1965 Nov;54:1364-70.

23. Goodman DS, Huang HS. Biosynthesis of Vitamin a with Rat Intestinal Enzymes. Science (New York, NY. 1965 Aug 20;149:879-80.

24. Schwartz SH, Tan BC, Gage DA, Zeevaart JA, McCarty DR. Specific oxidative cleavage of carotenoids by VP14 of maize. Science (New York, NY. 1997 Jun 20;276:1872-4.

25. Tan BC, Schwartz SH, Zeevaart JA, McCarty DR. Genetic control of abscisic acid biosynthesis in maize. Proc Natl Acad Sci U S A. 1997 Oct 28;94:12235-40.

26. Hu KQ, Liu C, Ernst H, Krinsky NI, Russell RM, Wang XD. The biochemical characterization of ferret carotene-9',10'-monooxygenase catalyzing cleavage of

carotenoids in vitro and in vivo. The Journal of biological chemistry. 2006 Jul 14;281:19327-38.

27. Kiefer C, Hessel S, Lampert JM, Vogt K, Lederer MO, Breithaupt DE, von Lintig J. Identification and characterization of a mammalian enzyme catalyzing the asymmetric oxidative cleavage of provitamin A. The Journal of biological chemistry. 2001 Apr 27;276:14110-6.

28. Redmond TM, Gentleman S, Duncan T, Yu S, Wiggert B, Gantt E, Cunningham FX, Jr. Identification, expression, and substrate specificity of a mammalian beta-carotene 15,15'-dioxygenase. The Journal of biological chemistry. 2001 Mar 2;276:6560-5.

29. Poliakov E, Gentleman S, Cunningham FX, Jr., Miller-Ihli NJ, Redmond TM. Key role of conserved histidines in recombinant mouse beta-carotene 15,15'-monooxygenase-1 activity. The Journal of biological chemistry. 2005 Aug 12;280:29217-23.

30. Auldridge ME, McCarty DR, Klee HJ. Plant carotenoid cleavage oxygenases and their apocarotenoid products. Current opinion in plant biology. 2006 Jun;9:315-21.

31. Kloer DP, Schulz GE. Structural and biological aspects of carotenoid cleavage. Cell Mol Life Sci. 2006 Oct;63:2291-303.

32. Hamel CP, Tsilou E, Pfeffer BA, Hooks JJ, Detrick B, Redmond TM. Molecular cloning and expression of RPE65, a novel retinal pigment epithelium-specific microsomal protein that is post-transcriptionally regulated in vitro. The Journal of biological chemistry. 1993 Jul 25;268:15751-7.

33. Jin M, Li S, Moghrabi WN, Sun H, Travis GH. Rpe65 is the retinoid isomerase in bovine retinal pigment epithelium. Cell. 2005 Aug 12;122:449-59.

34. Mernitz H, Wang XD. The Bioconversion of Carotenoids into Vitamin A: Implications for Cancer Prevention. In: Loessing IT, editor. Vitamin A: New Research: Nova Science Publishers, Inc.; 2007. p. 39-57.

35. Wyss A, Wirtz G, Woggon W, Brugger R, Wyss M, Friedlein A, Bachmann H, Hunziker W. Cloning and expression of beta,beta-carotene 15,15'-dioxygenase. Biochem Biophys Res Commun. 2000 May 10;271:334-6.

36. Lindqvist A, Andersson S. Biochemical properties of purified recombinant human beta-carotene 15,15'-monooxygenase. The Journal of biological chemistry. 2002 Jun 28;277:23942-8.

37. Paik J, During A, Harrison EH, Mendelsohn CL, Lai K, Blaner WS. Expression and characterization of a murine enzyme able to cleave beta-carotene. The formation of retinoids. The Journal of biological chemistry. 2001 Aug 24;276:32160-8.

38. Wyss A, Wirtz GM, Woggon WD, Brugger R, Wyss M, Friedlein A, Riss G, Bachmann H, Hunziker W. Expression pattern and localization of beta,beta-carotene 15,15'-dioxygenase in different tissues. The Biochemical journal. 2001 Mar 15;354:521-9.

39. Yan W, Jang GF, Haeseleer F, Esumi N, Chang J, Kerrigan M, Campochiaro M, Campochiaro P, Palczewski K, Zack DJ. Cloning and characterization of a human beta,beta-carotene-15,15'-dioxygenase that is highly expressed in the retinal pigment epithelium. Genomics. 2001 Mar 1;72:193-202.

40. Hessel S, Eichinger A, Isken A, Amengual J, Hunzelmann S, Hoeller U, Elste V, Hunziker W, Goralczyk R, et al. CMO1 deficiency abolishes vitamin A production from

beta-carotene and alters lipid metabolism in mice. The Journal of biological chemistry. 2007 Nov 16;282:33553-61.

41. Nagao A, Olson JA. Enzymatic formation of 9-cis, 13-cis, and all-trans retinals from isomers of beta-carotene. Faseb J. 1994 Sep;8:968-73.

42. Davis C, Jing H, Howe JA, Rocheford T, Tanumihardjo SA. beta-Cryptoxanthin from supplements or carotenoid-enhanced maize maintains liver vitamin A in Mongolian gerbils (Meriones unguiculatus) better than or equal to beta-carotene supplements. Br J Nutr. 2008 Oct;100:786-93.

43. Davis CR, Howe JA, Rocheford TR, Tanumihardjo SA. The xanthophyll composition of biofortified maize (Zea mays Sp.) does not influence the bioefficacy of provitamin a carotenoids in Mongolian gerbils (Meriones unguiculatus). J Agric Food Chem. 2008 Aug 13;56:6745-50.

44. Kim YS, Oh DK. Substrate specificity of a recombinant chicken beta-carotene 15,15'-monooxygenase that converts beta-carotene into retinal. Biotechnology letters. 2009 Mar;31:403-8.

45. Glover J. The conversion of beta-carotene into vitamin A. Vitamins and hormones. 1960;18:371-86.

46. Glover J, Redfearn ER. The mechanism of the transformation of beta-carotene into vitamin A in vivo. The Biochemical journal. 1954 Jul 16;58:xv-xvi.

47. Wang XD, Tang GW, Fox JG, Krinsky NI, Russell RM. Enzymatic conversion of beta-carotene into beta-apo-carotenals and retinoids by human, monkey, ferret, and rat tissues. Arch Biochem Biophys. 1991 Feb 15;285:8-16.

48. Tang GW, Wang XD, Russell RM, Krinsky NI. Characterization of beta-apo-13-carotenone and beta-apo-14'-carotenal as enzymatic products of the excentric cleavage of beta-carotene. Biochemistry. 1991 Oct 15;30:9829-34.

49. Wang XD, Russell RM, Liu C, Stickel F, Smith DE, Krinsky NI. Beta-oxidation in rabbit liver in vitro and in the perfused ferret liver contributes to retinoic acid biosynthesis from beta-apocarotenoic acids. The Journal of biological chemistry. 1996 Oct 25;271:26490-8.

50. Wang XD, Krinsky NI, Marini RP, Tang G, Yu J, Hurley R, Fox JG, Russell RM. Intestinal uptake and lymphatic absorption of beta-carotene in ferrets: a model for human beta-carotene metabolism. The American journal of physiology. 1992 Oct;263:G480-6.

51. Wang XD. Can smoke-exposed ferrets be utilized to unravel the mechanisms of action of lycopene? The Journal of nutrition. 2005 Aug;135:2053S-6S.

52. Kloer DP, Ruch S, Al-Babili S, Beyer P, Schulz GE. The structure of a retinal-forming carotenoid oxygenase. Science (New York, NY. 2005 Apr 8;308:267-9.

53. Schwartz SH, Qin X, Zeevaart JA. Characterization of a novel carotenoid cleavage dioxygenase from plants. The Journal of biological chemistry. 2001 Jul 6;276:25208-11.

54. Schmidt H, Kurtzer R, Eisenreich W, Schwab W. The carotenase AtCCD1 from Arabidopsis thaliana is a dioxygenase. The Journal of biological chemistry. 2006 Apr 14;281:9845-51.

55. Ibdah M, Azulay Y, Portnoy V, Wasserman B, Bar E, Meir A, Burger Y, Hirschberg J, Schaffer AA, et al. Functional characterization of CmCCD1, a carotenoid cleavage dioxygenase from melon. Phytochemistry. 2006 Aug;67:1579-89.

56. Bouvier F, Suire C, Mutterer J, Camara B. Oxidative remodeling of chromoplast carotenoids: identification of the carotenoid dioxygenase CsCCD and CsZCD genes involved in Crocus secondary metabolite biogenesis. Plant Cell. 2003 Jan;15:47-62.

57. Mathieu S, Terrier N, Procureur J, Bigey F, Gunata Z. A carotenoid cleavage dioxygenase from Vitis vinifera L.: functional characterization and expression during grape berry development in relation to C13-norisoprenoid accumulation. J Exp Bot. 2005 Oct;56:2721-31.

58. Simkin AJ, Underwood BA, Auldridge M, Loucas HM, Shibuya K, Schmelz E, Clark DG, Klee HJ. Circadian regulation of the PhCCD1 carotenoid cleavage dioxygenase controls emission of beta-ionone, a fragrance volatile of petunia flowers. Plant Physiol. 2004 Nov;136:3504-14.

59. Vogel JT, Tan BC, McCarty DR, Klee HJ. The carotenoid cleavage dioxygenase 1 enzyme has broad substrate specificity, cleaving multiple carotenoids at two different bond positions. The Journal of biological chemistry. 2008 Apr 25;283:11364-73.

60. Garcia-Limones C, Schnabele K, Blanco-Portales R, Luz Bellido M, Caballero JL, Schwab W, Munoz-Blanco J. Functional characterization of FaCCD1: a carotenoid cleavage dioxygenase from strawberry involved in lutein degradation during fruit ripening. J Agric Food Chem. 2008 Oct 8;56:9277-85.

61. Simkin AJ, Schwartz SH, Auldridge M, Taylor MG, Klee HJ. The tomato carotenoid cleavage dioxygenase 1 genes contribute to the formation of the flavor volatiles beta-ionone, pseudoionone, and geranylacetone. Plant J. 2004 Dec;40:882-92.

62. Scherzinger D, Al-Babili S. In vitro characterization of a carotenoid cleavage dioxygenase from Nostoc sp. PCC 7120 reveals a novel cleavage pattern, cytosolic localization and induction by highlight. Molecular microbiology. 2008 Jul;69:231-44.

63. Marasco EK, Vay K, Schmidt-Dannert C. Identification of carotenoid cleavage dioxygenases from Nostoc sp. PCC 7120 with different cleavage activities. The Journal of biological chemistry. 2006 Oct 20;281:31583-93.

64. Borel P, Grolier P, Mekki N, Boirie Y, Rochette Y, Le Roy B, Alexandre-Gouabau MC, Lairon D, Azais-Braesco V. Low and high responders to pharmacological doses of beta-carotene: proportion in the population, mechanisms involved and consequences on beta-carotene metabolism. Journal of lipid research. 1998 Nov;39:2250-60.

65. Novotny JA, Harrison DJ, Pawlosky R, Flanagan VP, Harrison EH, Kurilich AC. Beta-carotene conversion to vitamin A decreases as the dietary dose increases in humans. J Nutr. 2010 May;140:915-8.

66. Bachmann H, Desbarats A, Pattison P, Sedgewick M, Riss G, Wyss A, Cardinault N, Duszka C, Goralczyk R, Grolier P. Feedback regulation of beta,beta-carotene 15,15'-monooxygenase by retinoic acid in rats and chickens. J Nutr. 2002 Dec;132:3616-22.

67. Lindqvist A, Sharvill J, Sharvill DE, Andersson S. Loss-of-function mutation in carotenoid 15,15'-monooxygenase identified in a patient with hypercarotenemia and hypovitaminosis A. J Nutr. 2007 Nov;137:2346-50.

68. Ferrucci L, Perry JR, Matteini A, Perola M, Tanaka T, Silander K, Rice N, Melzer D, Murray A, et al. Common variation in the beta-carotene 15,15'-monooxygenase 1 gene

affects circulating levels of carotenoids: a genome-wide association study. Am J Hum Genet. 2009 Feb;84:123-33.

69. Leung WC, Hessel S, Meplan C, Flint J, Oberhauser V, Tourniaire F, Hesketh JE, von Lintig J, Lietz G. Two common single nucleotide polymorphisms in the gene encoding beta-carotene 15,15'-monoxygenase alter beta-carotene metabolism in female volunteers. FASEB J. 2009 Apr;23:1041-53.

70. Borel P, Moussa M, Reboul E, Lyan B, Defoort C, Vincent-Baudry S, Maillot M, Gastaldi M, Darmon M, et al. Human fasting plasma concentrations of vitamin E and carotenoids, and their association with genetic variants in apo C-III, cholesteryl ester transfer protein, hepatic lipase, intestinal fatty acid binding protein and microsomal triacylglycerol transfer protein. Br J Nutr. 2009 Mar;101:680-7.

71. Borel P, Moussa M, Reboul E, Lyan B, Defoort C, Vincent-Baudry S, Maillot M, Gastaldi M, Darmon M, et al. Human plasma levels of vitamin E and carotenoids are associated with genetic polymorphisms in genes involved in lipid metabolism. J Nutr. 2007 Dec;137:2653-9.

72. Herbeth B, Gueguen S, Leroy P, Siest G, Visvikis-Siest S. The lipoprotein lipase serine 447 stop polymorphism is associated with altered serum carotenoid concentrations in the Stanislas Family Study. J Am Coll Nutr. 2007 Dec;26:655-62.

73. Zerbib J, Seddon JM, Richard F, Reynolds R, Leveziel N, Benlian P, Borel P, Feingold J, Munnich A, et al. rs5888 variant of SCARB1 gene is a possible susceptibility factor for age-related macular degeneration. PLoS One. 2009;4:e7341.

74. Berry SD, Davis SR, Beattie EM, Thomas NL, Burrett AK, Ward HE, Stanfield AM, Biswas M, Ankersmit-Udy AE, et al. Mutation in bovine beta-carotene oxygenase 2 affects milk color. Genetics. 2009 Jul;182:923-6.

75. Tian R, Pitchford WS, Morris CA, Cullen NG, Bottema CD. Genetic variation in the beta, beta-carotene-9', 10'-dioxygenase gene and association with fat colour in bovine adipose tissue and milk. Animal genetics. 2009 Nov 26;41:253-9.

76. Vage DI, Boman IA. A nonsense mutation in the beta-carotene oxygenase 2 (BCO2) gene is tightly associated with accumulation of carotenoids in adipose tissue in sheep (Ovis aries). BMC genetics. 2010 Feb 2;11:10.

77. Hill F. Xanthophyll pigmentation in sheep fat. Nature. 1962 Jun 2;194:865-6.

78. Eriksson J, Larson G, Gunnarsson U, Bed'hom B, Tixier-Boichard M, Stromstedt L, Wright D, Jungerius A, Vereijken A, et al. Identification of the yellow skin gene reveals a hybrid origin of the domestic chicken. PLoS genetics. 2008 Feb;4:e1000010.

79. Castaneda MP, Hirschler EM, Sams AR. Skin pigmentation evaluation in broilers fed natural and synthetic pigments. Poultry science. 2005 Jan;84:143-7.

80. Mein JR, Lian F, Wang XD. Biological activity of lycopene metabolites: implications for cancer prevention. Nutr Rev. 2008 Dec;66:667-83.

81. Wang XD. Carotenoid Oxidative/Degradative Products and Their Biological Activities. In: Krinsky NI, Mayne, S.T., Sies, H., editor. Carotenoids in Health and Disease. New York: Marcel Dekker; 2004. p. 313-35.

82. Lakshminarayana R, Sathish UV, Dharmesh SM, Baskaran V. Antioxidant and cytotoxic effect of oxidized lutein in human cervical carcinoma cells (HeLa). Food Chem Toxicol. 2010 Apr 13.

83. Kalariya NM, Ramana KV, Srivastava SK, van Kuijk FJ. Carotenoid derived aldehydes-induced oxidative stress causes apoptotic cell death in human retinal pigment epithelial cells. Experimental eye research. 2008 Jan;86:70-80.

84. O'Neill ME, Carroll Y, Corridan B, Olmedilla B, Granado F, Blanco I, Van den Berg H, Hininger I, Rousell AM, et al. A European carotenoid database to assess carotenoid intakes and its use in a five-country comparative study. The British journal of nutrition. 2001 Apr;85:499-507.

85. National Academy of Sciences IoM, Food and Nutrition Board, Panel on Dietary Antioxidants and Related Compounds. Dietary Reference Intakes for Vitamin C, Vitamin E, Selenium, and Carotenoids. Washington, D.C.: National Academy Press; 2000.

86. Talegawkar SA, Johnson EJ, Carithers TC, Taylor HA, Bogle ML, Tucker KL. Carotenoid intakes, assessed by food-frequency questionnaires (FFQs), are associated with serum carotenoid concentrations in the Jackson Heart Study: validation of the Jackson Heart Study Delta NIRI Adult FFQs. Public Health Nutr. 2008 Oct;11:989-97.

87. Mannisto S, Smith-Warner SA, Spiegelman D, Albanes D, Anderson K, van den Brandt PA, Cerhan JR, Colditz G, Feskanich D, et al. Dietary carotenoids and risk of lung cancer in a pooled analysis of seven cohort studies. Cancer epidemiology, biomarkers & prevention : a publication of the American Association for Cancer Research, cosponsored by the American Society of Preventive Oncology. 2004 Jan;13:40-8.

88. Gallicchio L, Boyd K, Matanoski G, Tao XG, Chen L, Lam TK, Shiels M, Hammond E, Robinson KA, et al. Carotenoids and the risk of developing lung cancer: a systematic review. Am J Clin Nutr. 2008 Aug;88:372-83.

89. The effect of vitamin E and beta carotene on the incidence of lung cancer and other cancers in male smokers. The Alpha-Tocopherol, Beta Carotene Cancer Prevention Study Group. The New England journal of medicine. 1994 Apr 14;330:1029-35.

90. Omenn GS, Goodman GE, Thornquist MD, Balmes J, Cullen MR, Glass A, Keogh JP, Meyskens FL, Valanis B, et al. Effects of a combination of beta carotene and vitamin A on lung cancer and cardiovascular disease. The New England journal of medicine. 1996 May 2;334:1150-5.

91. Kim Y, Chongviriyaphan N, Liu C, Russell RM, Wang XD. Combined antioxidant (beta-carotene, alpha-tocopherol and ascorbic acid) supplementation increases the levels of lung retinoic acid and inhibits the activation of mitogen-activated protein kinase in the ferret lung cancer model. Carcinogenesis. 2006 Jul;27:1410-9.

92. Liu C, Wang XD, Bronson RT, Smith DE, Krinsky NI, Russell RM. Effects of physiological versus pharmacological beta-carotene supplementation on cell proliferation and histopathological changes in the lungs of cigarette smoke-exposed ferrets. Carcinogenesis. 2000 Dec;21:2245-53.

93. Liu C, Russell RM, Wang XD. Low dose beta-carotene supplementation of ferrets attenuates smoke-induced lung phosphorylation of JNK, p38 MAPK, and p53 proteins. J Nutr. 2004 Oct;134:2705-10.

94. Liu C, Russell RM, Wang XD. Alpha-tocopherol and ascorbic acid decrease the production of beta-apo-carotenals and increase the formation of retinoids from beta-carotene in the lung tissues of cigarette smoke-exposed ferrets in vitro. J Nutr. 2004 Feb;134:426-30.

95. Liu C, Russell RM, Wang XD. Exposing ferrets to cigarette smoke and a pharmacological dose of beta-carotene supplementation enhance in vitro retinoic acid catabolism in lungs via induction of cytochrome P450 enzymes. J Nutr. 2003 Jan;133:173-9.

96. Wang XD, Liu C, Bronson RT, Smith DE, Krinsky NI, Russell M. Retinoid signaling and activator protein-1 expression in ferrets given beta-carotene supplements and exposed to tobacco smoke. Journal of the National Cancer Institute. 1999 Jan 6;91:60-6.

97. Lietz G, Lange J, Rimbach G. Molecular and dietary regulation of beta,beta-carotene 15,15'-monooxygenase 1 (BCMO1). Arch Biochem Biophys. 2010 Jul 1.

98. Lakshman MR, Liu QH, Sapp R, Somanchi M, Sundaresan PR. The effects of dietary taurocholate, fat, protein, and carbohydrate on the distribution and fate of dietary beta-carotene in ferrets. Nutr Cancer. 1996;26:49-61.

99. Raju M, Lakshminarayana R, Krishnakantha TP, Baskaran V. Micellar oleic and eicosapentaenoic acid but not linoleic acid influences the beta-carotene uptake and its cleavage into retinol in rats. Molecular and cellular biochemistry. 2006 Aug;288:7-15.

100. Parvin SG, Sivakumar B. Nutritional status affects intestinal carotene cleavage activity and carotene conversion to vitamin A in rats. J Nutr. 2000 Mar;130:573-7.

101. van Vliet T, van Vlissingen MF, van Schaik F, van den Berg H. beta-Carotene absorption and cleavage in rats is affected by the vitamin A concentration of the diet. J Nutr. 1996 Feb;126:499-508.

102. Takitani K, Zhu CL, Inoue A, Tamai H. Molecular cloning of the rat beta-carotene 15,15'-monooxygenase gene and its regulation by retinoic acid. Eur J Nutr. 2006 Sep;45:320-6.

103. During A, Fields M, Lewis CG, Smith JC. Intestinal beta-carotene 15,15'-dioxygenase activity is markedly enhanced in copper-deficient rats fed on high-iron diets and fructose. Br J Nutr. 2000 Jul;84:117-24.

104. Chichili GR, Nohr D, Schaffer M, von Lintig J, Biesalski HK. beta-Carotene conversion into vitamin A in human retinal pigment epithelial cells. Investigative ophthalmology & visual science. 2005 Oct;46:3562-9.

105. Takitani K, Zhu CL, Inoue A, Tamai H. Molecular cloning of the rat beta-carotene 15, 15'-monooxygenase gene and its regulation by retinoic acid. European journal of nutrition. 2006 May 13.

106. Choi MY, Romer AI, Hu M, Lepourcelet M, Mechoor A, Yesilaltay A, Krieger M, Gray PA, Shivdasani RA. A dynamic expression survey identifies transcription factors relevant in mouse digestive tract development. Development (Cambridge, England). 2006 Oct;133:4119-29.

107. During A, Harrison EH. Mechanisms of provitamin A (carotenoid) and vitamin A (retinol) transport into and out of intestinal Caco-2 cells. Journal of lipid research. 2007 Oct;48:2283-94.

108. van Bennekum A, Werder M, Thuahnai ST, Han CH, Duong P, Williams DL, Wettstein P, Schulthess G, Phillips MC, Hauser H. Class B scavenger receptor-mediated intestinal absorption of dietary beta-carotene and cholesterol. Biochemistry. 2005 Mar 22;44:4517-25.

109. Seino Y, Miki T, Kiyonari H, Abe T, Fujimoto W, Kimura K, Takeuchi A, Takahashi Y, Oiso Y, et al. Isx participates in the maintenance of vitamin A metabolism by regulation of beta-carotene 15,15'-monooxygenase (Bcmo1) expression. The Journal of biological chemistry. 2008 Feb 22;283:4905-11.

110. Boulanger A, McLemore P, Copeland NG, Gilbert DJ, Jenkins NA, Yu SS, Gentleman S, Redmond TM. Identification of beta-carotene 15, 15'-monooxygenase as a peroxisome proliferator-activated receptor target gene. Faseb J. 2003 Jul;17:1304-6.

111. Gong X, Tsai SW, Yan B, Rubin LP. Cooperation between MEF2 and PPARgamma in human intestinal beta,beta-carotene 15,15'-monooxygenase gene expression. BMC molecular biology. 2006;7:7.

112. Zaripheh S, Nara TY, Nakamura MT, Erdman JW, Jr. Dietary lycopene downregulates carotenoid 15,15'-monooxygenase and PPAR-gamma in selected rat tissues. J Nutr. 2006 Apr;136:932-8.

113. Ziouzenkova O, Orasanu G, Sharlach M, Akiyama TE, Berger JP, Viereck J, Hamilton JA, Tang G, Dolnikowski GG, et al. Retinaldehyde represses adipogenesis and diet-induced obesity. Nature medicine. 2007 Jun;13:695-702.

114. Ziouzenkova O, Orasanu G, Sukhova G, Lau E, Berger JP, Tang G, Krinsky NI, Dolnikowski GG, Plutzky J. Asymmetric cleavage of beta-carotene yields a transcriptional repressor of retinoid X receptor and peroxisome proliferator-activated receptor responses. Molecular endocrinology (Baltimore, Md. 2007 Jan;21:77-88.

115. Ziouzenkova O, Plutzky J. Retinoid metabolism and nuclear receptor responses: New insights into coordinated regulation of the PPAR-RXR complex. FEBS Lett. 2008 Jan 9;582:32-8.

116. Liu C, Lian F, Smith DE, Russell RM, Wang XD. Lycopene supplementation inhibits lung squamous metaplasia and induces apoptosis via up-regulating insulin-like growth factor-binding protein 3 in cigarette smoke-exposed ferrets. Cancer Res. 2003 Jun 15;63:3138-44.

117. Matulka RA, Hood AM, Griffiths JC. Safety evaluation of a natural tomato oleoresin extract derived from food-processing tomatoes. Regulatory toxicology and pharmacology : RTP. 2004 Jun;39:390-402.

118. Mein JR, Chongvirihaphan N, Wang XD. The effect of combined antioxidant supplementation (beta-carotene, ascorbic acid and alpha-tocopherol) on the expression of CMO1 and CMO2 in smoke-exposed ferrets. American Association of Cancer Research: Frontiers in Cancer Prevention Research Meeting. Boston, MA; 2006.

119. Luvizotto RA, Nascimento AF, Veeramachaneni S, Liu C, Wang XD. Chronic Alcohol Intake Upregulates Hepatic Expressions of Carotenoid Cleavage Enzymes and PPAR in Rats. J Nutr. 2010 Aug 11.

120. Shmarakov I, Fleshman MK, D'Ambrosio DN, Piantedosi R, Riedl KM, Schwartz SJ, Curley RW, Jr., von Lintig J, Rubin LP, et al. Hepatic stellate cells are an important cellular site for beta-carotene conversion to retinoid. Arch Biochem Biophys. 2010 May 12.

Chapter 3

Methods

INTRODUCTION

Detailed knowledge of the quantitative and qualitative distribution of carotenoids in biologic systems requires the systematic utilization of robust analytical methods. This aspect becomes evermore a challenge when interested in apo-carotenoid metabolites, which are present in minute quantities. The analytic methods employed must possess sufficient precision and sensitivity for detection of low abundance compounds and unequivocal identification of novel compounds.

The use of high-performance liquid chromatography (HPLC) is well characterized in carotenoid research. However, the molecular characteristics of the apo-carotenoid metabolites of interest can have a dramatic effect on the strategy employed for carotenoid separation. The separation of apo-carotenoids by HPLC is influenced mainly by chain length and number and nature of functional groups. Enzymatic cleavage of carotenoids by CMO2 results in the formation of both C_{13} and C_{27} compounds (1, 2). The initial products formed possess both ketone and aldehyde functional groups. It is has been demonstrated both *in vitro* and *in vivo* that apo-carotenal and apo-lycopenal products can be reduced or oxidized to the corresponding alcohol or carboxylic acid function group (1-3). In the case of lutein, possessing both ε- and β-ionone terminal ring structures, optical rotation characteristics must be taken into account. Thus, there is a broad range of functional and optical groups with very different polar properties. Any method utilized must be robost enough to capture the products formed. In this part of my dissertation, I have developed several new analytical methods with these characteristics in mind.

METHODS AND MATERIALS

Sample Extraction

All samples were prepared and extracted under red or subdued light conditions to prevent photooxidation of carotenoids or apo-carotenoid products photooxidation. Briefly, tissue samples (100 mg) or plasma samples (1 ml) were homogenized in 3 ml saline:ethanol (2:1, v/v). The neutral lipids were extracted using 5 ml hexane and ether (1:1, v/v) by vortexing for one minute, centrifuging for 10 min. at 2,500 rpm at 4°C and collecting the upper layer. Samples were extracted twice, upper layers pooled and dryed under nitrogen gas, and reconstituted in 100 μl ethanol:ether (1:1, v/v). A 50 μl sample of the final extract was injected into the HPLC system.

Previous HPLC Analysis

A gradient reverse phase HPLC system consisting of a Waters 2695 separations module and a Waters 2998 photodiode array detector was used for carotenoid analysis as previously described (Wang et al., 1999). Intact carotenoids and apo-carotenoid metabolites were separated on a reverse phase C_{18} column (4.6 x 250 mm, 5 μM) (Vydac 201TP54, Grace Discovery Sciences, Inc.) fitted with a Pecosphere C_{18} guard column (PerkinElmer, CT.) with a flow rate of 1.00 ml/min. The gradient procedure is as follows: 1) 100% solvent A (Acetonitrile, Tetrahydrafuran, Water, 50 mM ammonium acetate, 50:20:30, v/v/v) for 4 minutes followed by a 6 minute linear gradient to 50% solvent A and 50% solvent B (Acetonitrile, Tetrahydrafuran, Water, 50 mM ammonium acetate, 50:44:6, v/v/v); 2) a 9 minute hold followed by a 2 minute linear gradient to 100% solvent B; 3) a 14 minute hold followed by a 3 minute linear gradient to 100%

solvent A; 4) a 12 minute hold at 100% solvent A before next sample injection. The Waters 2998 programmable photodiode array detector was set at 450 nm and 296 nm for intact carotenoid and apo-carotenoid monitoring.

New HPLC Analysis

A gradient reverse phase HPLC system was used for quantitative analysis of carotenoids and their polar metabolites. The gradient reverse phase HPLC system consists of a Waters 2695 separations module and a Waters 2998 photodiode array detector. The enzymatic cleavage products of zeaxanthin, lutein and β-cryptoxanthin were analyzed on a reverse phase C_{18} column (4.6 x 250 mm, 5 μM) (Vydac 201TP54, Grace Discovery Sciences, Inc.) fitted with a Pecosphere C_{18} guard column (PerkinElmer, CT.) with a flow rate of 1.00 ml/min. The gradient procedure is as follows: 1) 50% solvent A (100% Water, 50mM ammonium acetate) and 50% solvent B (100% Acetonitrile) for 4 minutes followed by a 6 minute linear gradient to 20% solvent A and 80% solvent B; 2) a 9-minute hold followed by a 11-min linear gradient to 90% Solvent B and 10% Solvent C (Acetonitrile, Tetrahydrofuran, H_2O, 50 mM ammonium acetate, 50:44:6, v/v/v); 3) a 3-min hold followed by an 11-min linear gradient to100% solvent C; 4) a 4-min hold followed by a 10 minute linear gradient to 50% solvent A and 50% solvent B; and 5) a 12-min hold on 50% solvent A and 50% solvent B before the next injection. The Waters 2998 programmable photodiode array detector was set at 450 nm and 296 nm for carotenoid metabolite and related volatile analysis. Carotenoid metabolites were identified on the basis of relative retention times (RT) and by comparison of spectra with those of pure standards.

LC-MS Analysis

The LC system consisted of an Agilent 1100 quaternary pump and UV-Vis diode array detector (Agilent Technologies, Palo Alto, CA). The column was a Vydac C_{18} 201TP54 column (4.6 x 250 mm, 5 μM) (Grace Discovery Sciences, Inc.). HPLC-MS separations were monitored at 450 nm. Mass spectra data was obtained with an Agilent 1100 MSD equipped with an atmospheric pressure chemical ionization (APCI) ion source operating in positive ion mode. The quadrupole was scanned *m/z* 100 - 600. The capillary was 2500 V and the temperature of the drying gas (N_2) was 350 °C at a flow rate of 9.0 L/min. The corona discharge voltage was optimized resulting in a current of 6.0 μA. The chromatographic conditions were similar to those used for HPLC analysis.

GC-MS Analysis

Cleavage assays were extracted and 50 μl was subjected to HPLC analysis as indicated above. HPLC flow-through containing peaks identified as putative volatile cleavage products were collected on ice and extracted twice with hexane:methyl-*tert* butyl ether (1:1, v/v). The combined extracts were dried by N_2 under red light. The residue was reconstituted in diethyl ether, dried over anhydrous sodium sulfate, concentrated to dryness by N_2, and dissolved in hexane for injection. GC-MS analysis was performed with an Agilent 5973N Mass Selective Detector coupled with an Agilent 6890 Series GC Detector. The oven was kept at 40 °C for 3 min and then increased to 250 °C at 5 °C min^{-1} with a helium carrier gas flow of 1.5 mL/min. One microliter of each sample was injected on a Supleco SAC-5 (Sigma-Aldrich, St. Louis, MO) capillary

column (30 m × 0.25 mm i.d., 0.25 μm film thickness). Mass spectra were recorded in electron impact (EI) ionization mode at 70 eV. Identifications were carried out by comparison of EI mass data with published data or with data from authentic standards (4, 5).

LC-MS/MS Analysis

Apo-carotenoid metabolite analysis was performed on an Applied Biosystems (ABI) 5500 quadrupole-linear ion trap (QTRAP) mass spectrometer coupled to an Agilent 1200 binary pump (Agilent Technologies, Palo Alto, CA). The LC system was fitted with a Vydac C_{18} 201TP54 column (4.6 x 250 mm, 5 μM) (Grace Discovery Sciences, Inc.) fitted with a Pecosphere C_{18} guard column (PerkinElmer, CT.) with a flow rate of 1.00 ml/min. The gradient procedure is as follows: 1) 100% solvent A (Acetonitrile, H_2O, 50mM ammonium acetate, 90:10, v/v) for 4 minutes followed by a 15 minute linear gradient to 50% solvent A and 50% solvent B (100% Tetrahydrafuran); 2) a 6 minute hold of 50% solvent A and 50% solvent B followed by a 5 minute linear gradient to 100% solvent A before the next injection. The injection volume was 20 μl. For all runs, the MS instrument was equipped with an atmospheric pressure chemical ionization source operated in positive ion mode. High purity nitrogen served as the collison-induced dissociation (CAD) gas (simplified setting: high) and curtain gas (set at 10 psi). The nebulizer temperature and current were maintained at 400 °C and 5.0 amp. Mass-dependent parameters for both β-apo-10'-carotenal and 3-OH-β-apo-10'carotenal were obtained by direct infusion of the standards (2 ng/μl) diluted in acetonitrile and water (90:10, v/v). The following transitions were determined for quantitative analyses:

393.4 → 301.3 for 3-OH-β-apo-10'-carotenal and 377.5 → 285.1 for β-apo-10'-carotenal. The collison energy (CE) and collison extraction potential (CXP) were set at 11.0 and 13.0 V, respectively. The entrance potential (EP) and declustering potential (DP) were set at 4.0 and 78.0 V, respectively, for both 3-OH-β-apo-10'-carotenal and β-apo-10'-carotenal.

RESULTS

For the identification and quantification of potential apo-carotenoid cleavage products resulting from the cleavage of β-cryptoxanthin, lutein and zeaxanthin by CMO2, a systematic approach employing the development of HPLC, LC-MS, GC-MS and LC-MS/MS methods was undertaken. The previous HPLC has been used primarily for the separation and quantification of intact carotenoids (6). However, it has been used with minor modifications for the detection and quantification of β-apo-10'-carotenoids (7) but has never been employed for the separation of 3-OH-β-apo-10'-carotenoids. Using the previously developed method, there was a separation of 6 min between 3-OH-β-apo-10'-carotenal and β-apo-10'-carotenal eluting at 6.1 min and at 12.1 min, respectively (Figure 1). However, using the newly developed method there was a separation of 7.9 min between 3-OH-β-apo-10'-carotenal and β-apo-10'-carotenal eluting at 25.5 min and at 33.1 min, respectively (Figure 2), resulting an increase of separation of 2 minutes. There were no differences in absorption spectra between the two methods as expected. However, the utility of the new method is the increased ability to detect more polar apo-carotenoid compounds, as evidenced by the increase in retention time of 3-OH-β-apo-10'carotenal, which is delayed 21 min in relation to the solvent front as compared with 3

min using the previous method. Apo-carotenoids can undergo oxidation or reduction both *in vitro* and *in vivo* (1, 3), thus, the increased retention times increases the likelihood of detecting these compounds. In addition, this becomes of practical importance when trying to identify the volatile apo-carotenoids β-ionone. Using the previous method, β-ionone standard elutes at 4.5 min at 296 nm (Figure 1) while using the new method it elutes at 11.6 min (Figure 3). This results in an increase in retention time of 7.1 min and an increase in retention of 7.5 min in relation to the solvent front compared to 1.2 min using the previous method. This becomes an important increase in retention time when trying to identify the 3-OH-β-ionone.

In addition to the HPLC method, several MS methods were developed to aid in the identification of apo-carotenoid products formed from enzymatic cleavage by CMO2. GC-MS was used to identify volatile apo-carotenoids like β-ionone (Figure 3). Using the β-ionone standard, a peak with a retention time of 23.2 min showed a fragmentation pattern that matched previously published β-ionone MS β-ionone (5). Using this method, it is expected that 3-OH-β-ionone, which is less volatile than β-ionone, will elute later in the run. This was evidenced in Chapter 4. This method may prove useful in the study of other volatile apo-carotenoid products.

LC-MS and LC-MS/MS methods were developed for the *in vitro* identification of the non-volatile C_{27} apo-carotenoids, such as 3-OH-β-apo-10'-carotenal and β-apo-10'-carotenal. A MS method was multiplexed to the newly developed HPLC method. For both 3-OH-β-apo-10'-carotenal and β-apo-10'-carotenal, respectively, mass spectra matching the predicted *m/z* of 393 $(M+H)^+$ and 377 $(M+H)^+$ were evidenced (Figure 2). While the developed LC-MS method was sufficient for the identification of apo-

carotenoids *in vitro*, its utility *in vivo* is questionable. The length of the LC program (70 min) and ineffectiveness of a single quadrapole for quantification are major limitations of this method. Thus, a LC-MS/MS method was developed for potential application to *in vivo* bioanalysis. The increased sensitivity, quantitative ability, and decreased run time make this an attractive method for further development. For both 3-OH-β-apo-10'-carotenal and β-apo-10'-carotenal, fragmentation patterns were optimized using the linear ion trap and transitions were identified for each compound. For 3-OH-β-apo-10'-carotenal the transition ion 301.3 was identified (Figure 4) while for β-apo-10'-carotenal, the transition ion 285.3 was used for identification (Figure 5). Additionally, the LC method used was sufficient for complete separation of both compounds, thereby decreasing the total run by allowing for switching the detector for different parent ions in the same run using the ion trap. This LC-MS/MS method should further validated and optimized for *in vivo* bioanalysis of apo-carotenoid metabolites.

SUMMARY

While the *in vitro* formation of apo-carotenoids is indisputable, a major challenge to their study is the availability of analytical methods for the identification and quantification of the diverse array of metabolites. The methods described herein provide a powerful means for the identification and quantification of a number of apo-carotenoid metabolites. While the methods developed for this dissertation were primarily developed with the *in vitro* identification of apo-carotenoids in mind, a number of recent studies have begun to employ LC-MS and LC-MS/MS methods for the detection of apo-carotenoids and apo-lycopenoids *in vivo* (8, 9). The LC-MS/MS method in particular

represents a potentially powerful method for the study of apo-carotenoids *in vivo* and should be further validated for this purpose.

REFERENCES

1. Hu KQ, Liu C, Ernst H, Krinsky NI, Russell RM, Wang XD. The biochemical characterization of ferret carotene-9',10'-monooxygenase catalyzing cleavage of carotenoids in vitro and in vivo. The Journal of biological chemistry. 2006 Jul 14;281:19327-38.

2. Kiefer C, Hessel S, Lampert JM, Vogt K, Lederer MO, Breithaupt DE, von Lintig J. Identification and characterization of a mammalian enzyme catalyzing the asymmetric oxidative cleavage of provitamin A. The Journal of biological chemistry. 2001 Apr 27;276:14110-6.

3. Sharma RV, Mathur SN, Dmitrovskii AA, Das RC, Ganguly J. Studies on the metabolism of beta-carotene and apo-beta-carotenoids in rats and chickens. Biochim Biophys Acta. 1976 Jan 18;486:183-94.

4. Garcia-Limones C, Schnabele K, Blanco-Portales R, Luz Bellido M, Caballero JL, Schwab W, Munoz-Blanco J. Functional characterization of FaCCD1: a carotenoid cleavage dioxygenase from strawberry involved in lutein degradation during fruit ripening. J Agric Food Chem. 2008 Oct 8;56:9277-85.

5. Vogel JT, Tan BC, McCarty DR, Klee HJ. The carotenoid cleavage dioxygenase 1 enzyme has broad substrate specificity, cleaving multiple carotenoids at two different bond positions. The Journal of biological chemistry. 2008 Apr 25;283:11364-73.

6. Wang XD, Liu C, Bronson RT, Smith DE, Krinsky NI, Russell M. Retinoid signaling and activator protein-1 expression in ferrets given beta-carotene supplements and exposed to tobacco smoke. J Natl Cancer Inst. 1999 Jan 6;91:60-6.

7. Liu C, Russell RM, Wang XD. Exposing ferrets to cigarette smoke and a pharmacological dose of beta-carotene supplementation enhance in vitro retinoic acid catabolism in lungs via induction of cytochrome P450 enzymes. J Nutr. 2003 Jan;133:173-9.

8. Kopec RE, Riedl KM, Harrison EH, Curley RW, Hruszkewycz DP, Clinton SK, Schwartz SJ. Identification and Quantification of Apo-lycopenals in Fruits, Vegetables, and Human Plasma. J Agric Food Chem. 2010 Mar 24;58:3290-6.

9. Shmarakov I, Fleshman MK, D'Ambrosio DN, Piantedosi R, Riedl KM, Schwartz SJ, Curley RW, Jr., von Lintig J, Rubin LP, et al. Hepatic stellate cells are an important cellular site for beta-carotene conversion to retinoid. Arch Biochem Biophys. 2010 May 12.

10. Wang XD, Liu C, Bronson RT, Smith DE, Krinsky NI, Russell M. Retinoid signaling and activator protein-1 expression in ferrets given beta-carotene supplements and exposed to tobacco smoke. Journal of the National Cancer Institute. 1999 Jan 6;91:60-6.

Figure Legends

Figure 1. HPLC separation of apo-carotenoid metabolites standards using previously developed HPLC method. HPLC separation of 3-OH-β-apo-10'-carotenal (*peak 1*) and β-apo-10'-carotenal (*peak 2*) with monitoring at 450 nm (A). HPLC separation of β-

ionone (*peak 3*) standard with monitoring at 296 nm (B). Apo-carotenoid metabolites were separated using a previously developed HPLC method as described (10).

Figure 2. HPLC separation and LC-MS analysis of apo-carotenoid metabolites standards using newly developed HPLC method. HPLC separation of 3-OH-β-apo-10'-carotenal (*peak 1*) and β-apo-10'-carotenal (*peak 2*) with monitoring at 450 nm (A). Absorption spectral analysis of 3-OH-βapo-10'-carotenal (B) and β-apo-10'-carotenal (C). LC-MS analysis 3-OH-β-apo-10'-carotenal (D) and β-apo-10'-carotenal (E).

Figure 3. HPLC separation and GC-MS analysis of β-ionone standard using newly developed HPLC and GC-MS method. HPLC separation of β-ionone (*peak 1*) with monitoring at 296 nm (A). GC-MS chromatogram of β-ionone standard (B). Absorption spectrum (C) and mass spectra of β-ionone standard (D).

Figure 4. HPLC-MS/MS chromatogram (A) and mass spectra (B) of 3-OH-β-apo-10'-carotenal.

Figure 5. HPLC-MS/MS chromatogram (A) and mass spectra (B) of β-apo-10'-carotenal.

Figure 1.

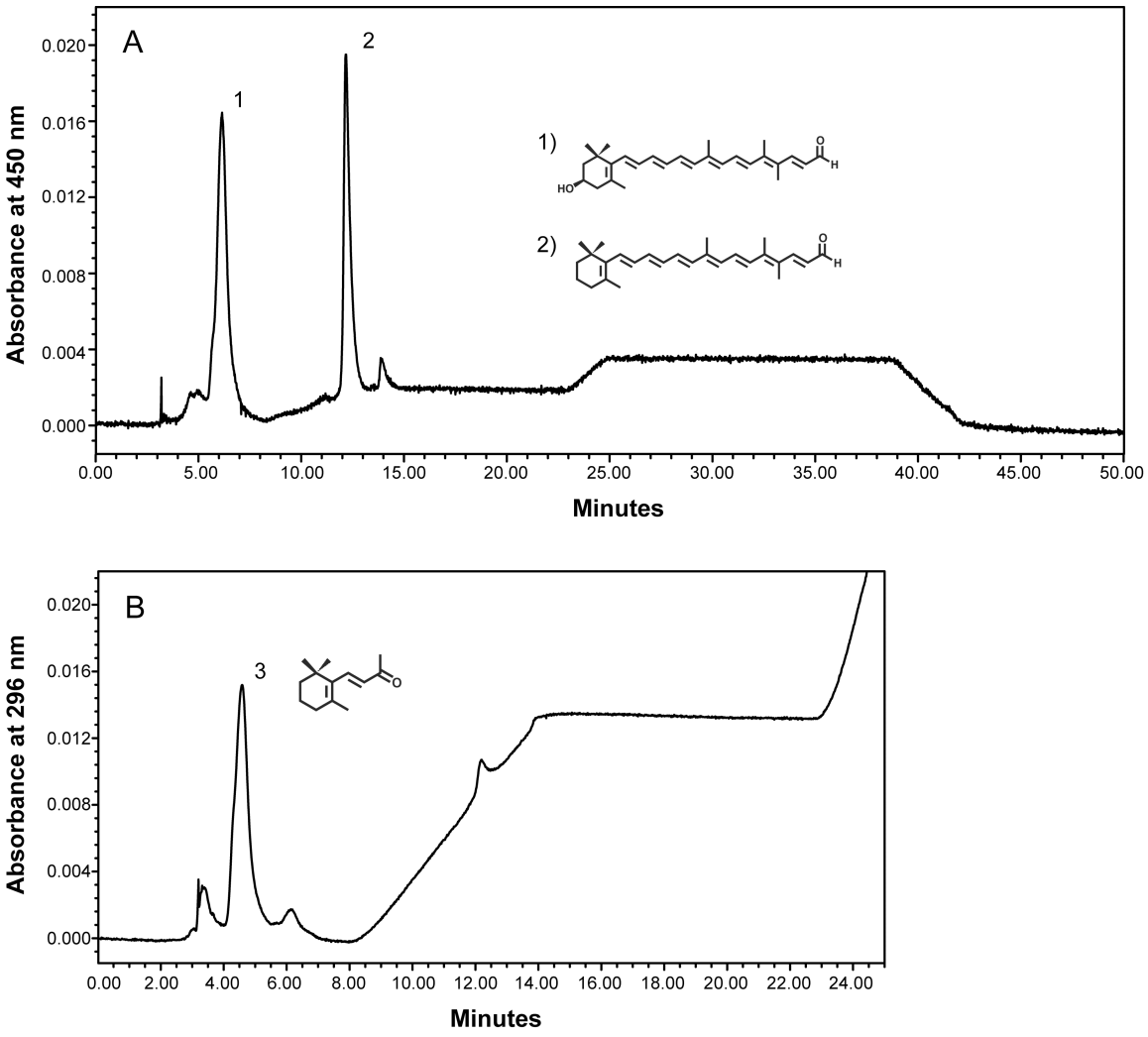
A
1
2
1)
2)
HO
O
H
Absorbance at 450 nm
0.020
0.016
0.012
0.008
0.004
0.000
0.00
5.00
10.00
15.00
20.00
25.00
30.00
35.00
40.00
45.00
50.00
Minutes
B
3
O
Absorbance at 296 nm
0.020
0.016
0.012
0.008
0.004
0.000
0.00
2.00
4.00
6.00
8.00
10.00
12.00
14.00
16.00
18.00
20.00
22.00
24.00
Minutes

Figure 2.

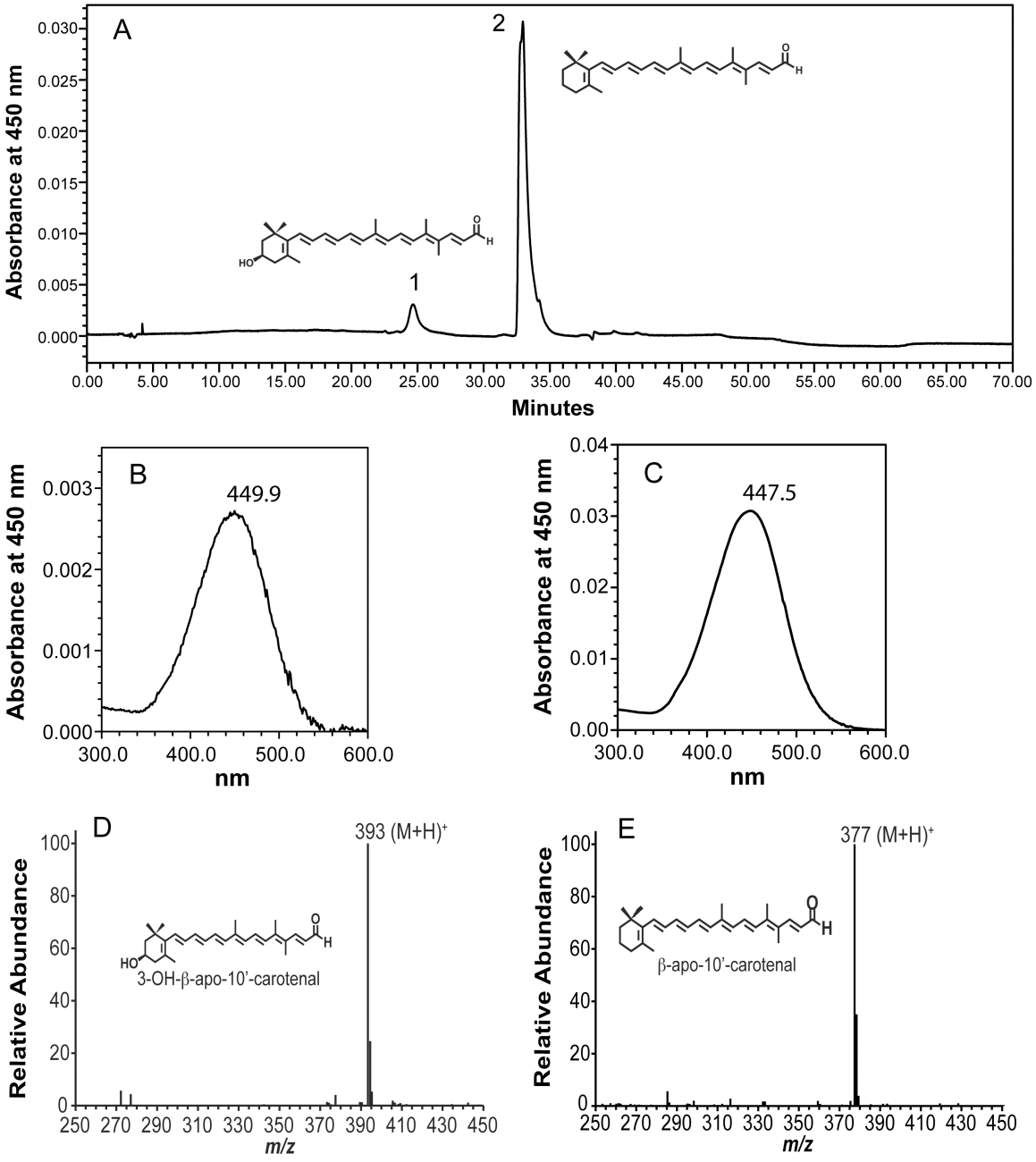
A
1
2
Absorbance at 450 nm
Minutes
B
449.9
Absorbance at 450 nm
nm
C
447.5
Absorbance at 450 nm
nm
D
393 (M+H)+
3-OH-β-apo-10'-carotenal
Relative Abundance
m/z
E
377 (M+H)+
β-apo-10'-carotenal
Relative Abundance
m/z

Figure 3.

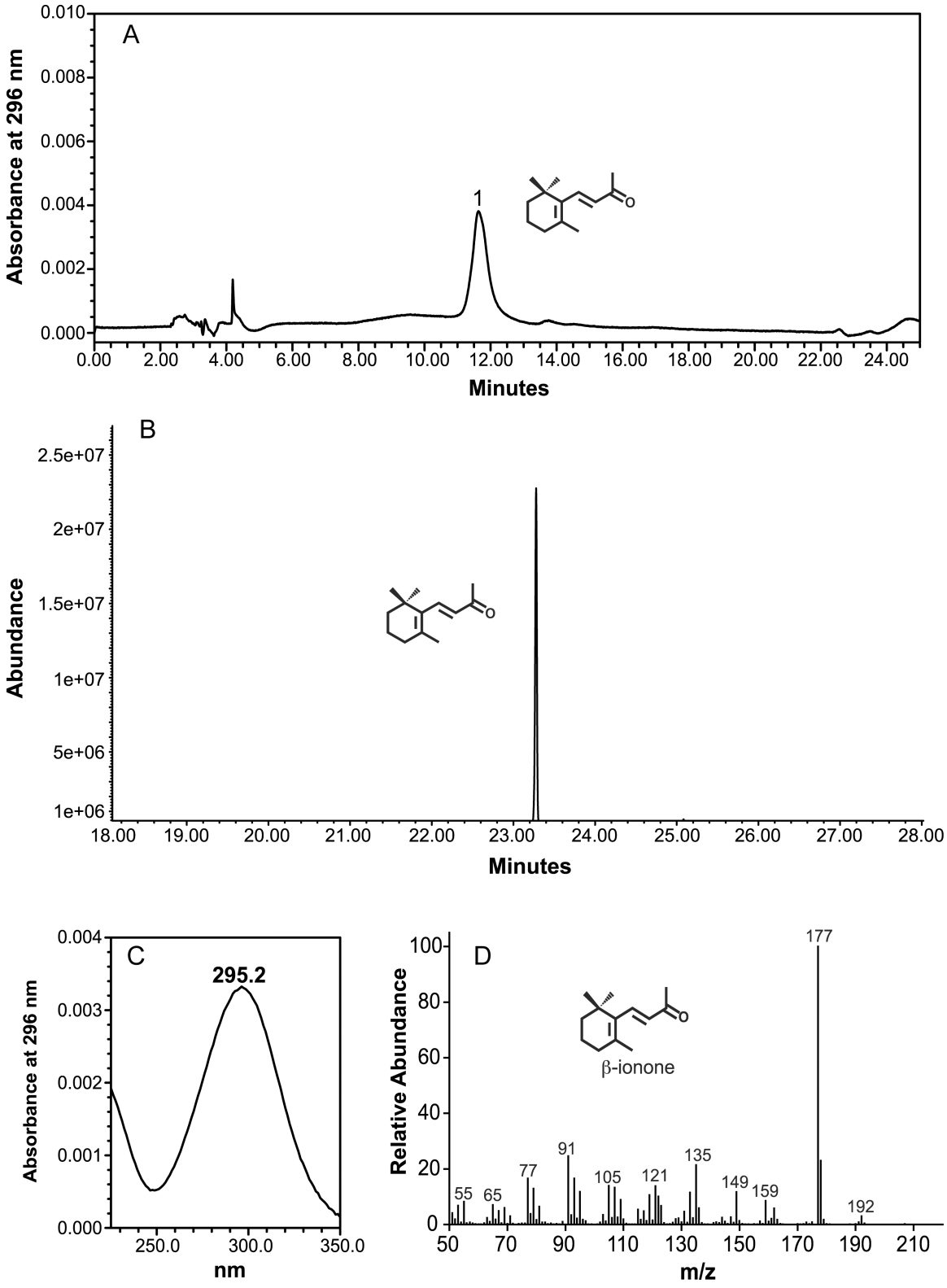
A
Absorbance at 296 nm
0.010
0.008
0.006
0.004
0.002
0.000
1
0.00 2.00 4.00 6.00 8.00 10.00 12.00 14.00 16.00 18.00 20.00 22.00 24.00
Minutes
B
Abundance
2.5e+07
2e+07
1.5e+07
1e+07
5e+06
1e+06
18.00 19.00 20.00 21.00 22.00 23.00 24.00 25.00 26.00 27.00 28.00
Minutes
C
295.2
Absorbance at 296 nm
0.004
0.003
0.002
0.001
0.000
250.0 300.0 350.0
nm
D
Relative Abundance
100
80
60
40
20
0
β-ionone
177
91
135
77
105
121
149
159
55
65
192
50 70 90 110 130 150 170 190 210
m/z

Figure 4.

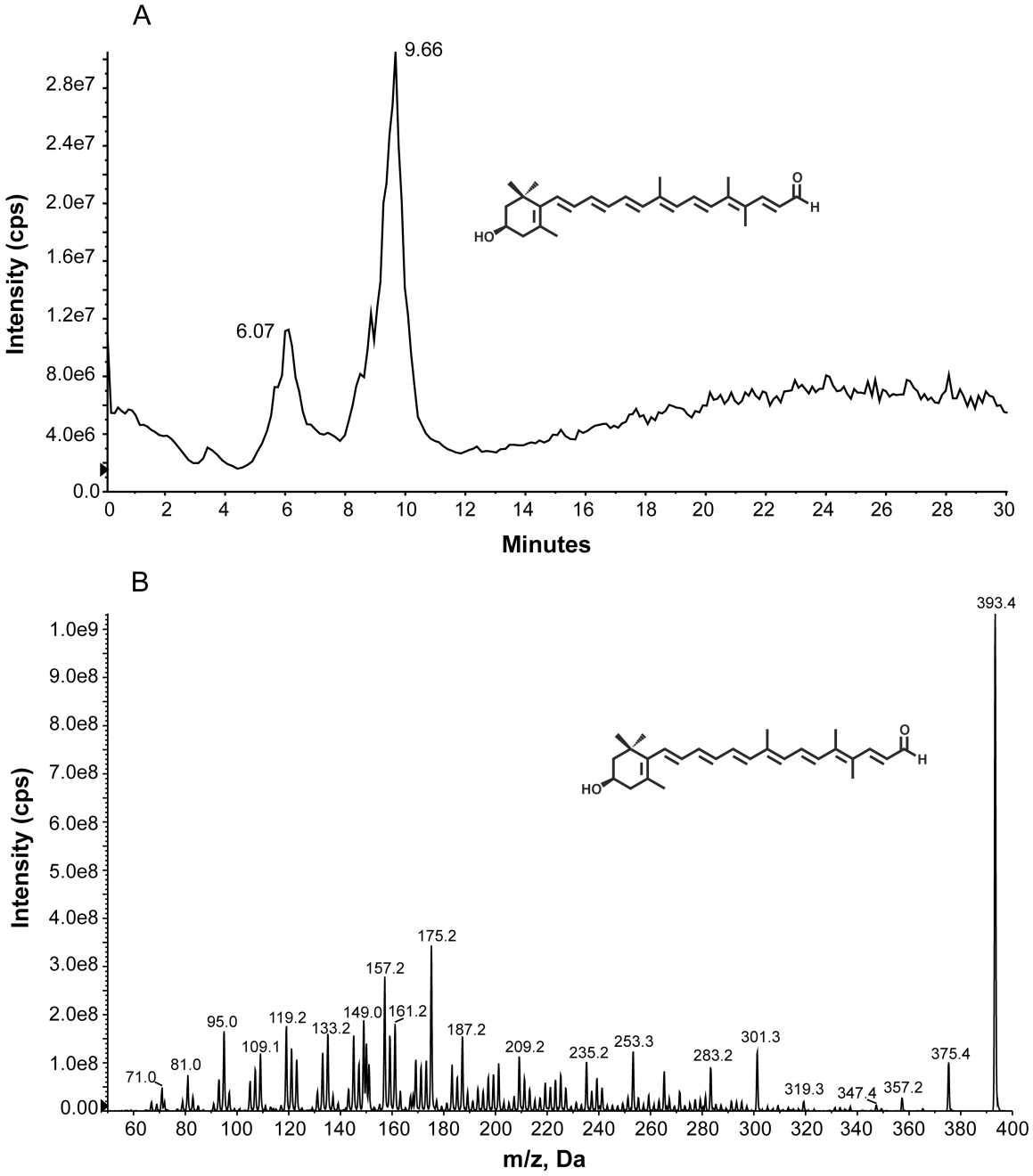
A
9.66
6.07
Intensity (cps)
Minutes
B
393.4
175.2
157.2
95.0
119.2
149.0
161.2
133.2
109.1
187.2
209.2
235.2
253.3
283.2
301.3
375.4
71.0
81.0
319.3
347.4
357.2
Intensity (cps)
m/z, Da

Figure 5.

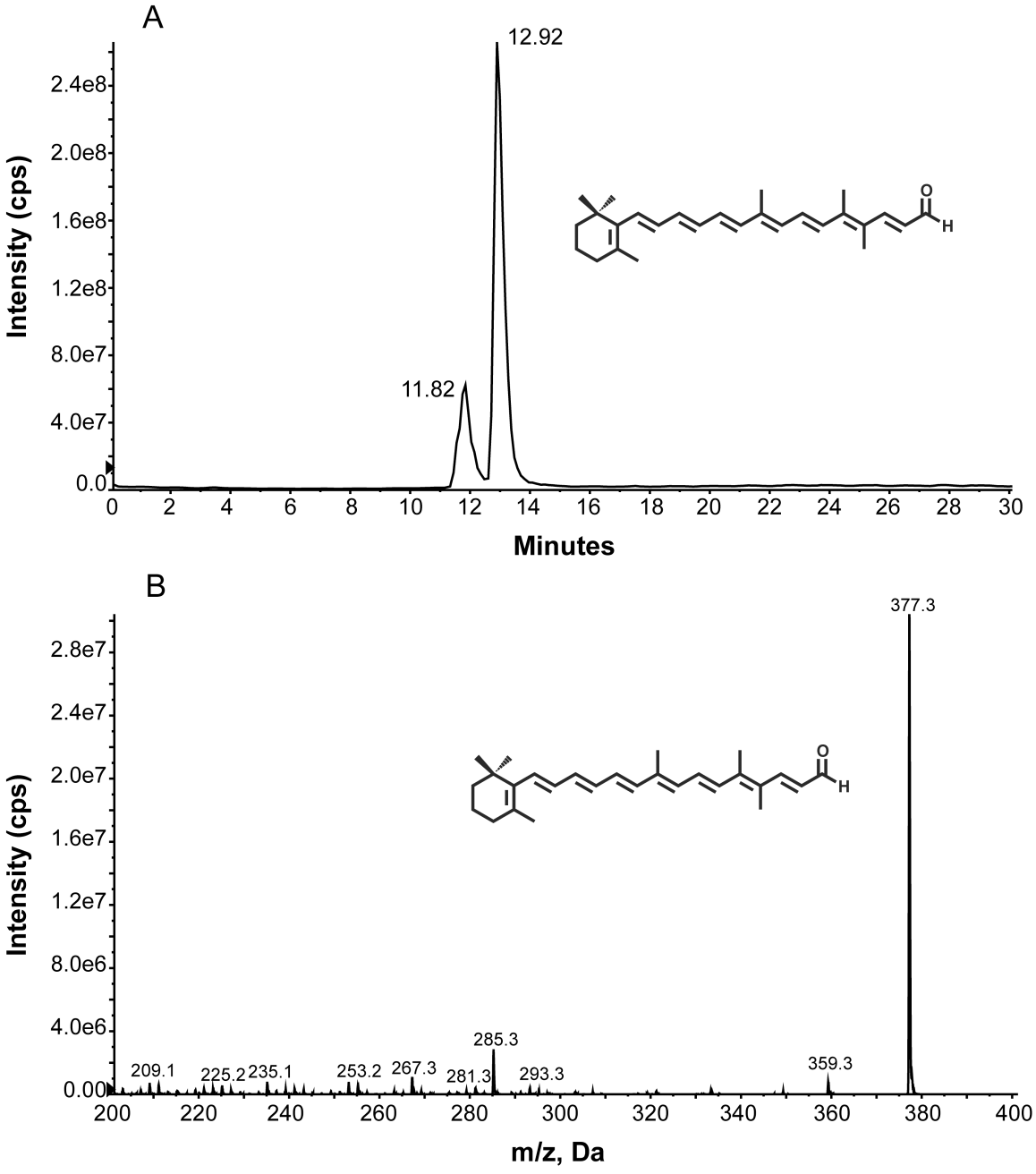
A
12.92
11.82
Intensity (cps)
2.4e8
2.0e8
1.6e8
1.2e8
8.0e7
4.0e7
0.0
0
2
4
6
8
10
12
14
16
18
20
22
24
26
28
30
Minutes
O
H
B
377.3
285.3
359.3
209.1
225.2
235.1
253.2
267.3
281.3
293.3
Intensity (cps)
2.8e7
2.4e7
2.0e7
1.6e7
1.2e7
8.0e6
4.0e6
0.00
200
220
240
260
280
300
320
340
360
380
400
m/z, Da
O
H

Chapter 4

Enzymatic Formation of Apo-Carotenoids from the Xanthophyll Carotenoids Lutein, Zeaxanthin and β-Cryptoxanthin by Ferret Carotene-9',10'-Monooxygenase

ABSTRACT

Xanthophyll carotenoids, such as lutein, zeaxanthin and β-cryptoxanthin, may provide potential health benefits against chronic and degenerative diseases. Investigating pathways of xanthophyll metabolism are important to understanding their biological functions. Carotene-15,15'-monooxygenase (CMO1) has been shown to be involved in vitamin A formation, while recent studies suggest that carotene-9',10'-monooxygenase (CMO2) may have a broader substrate specificity than previously recognized. In this *in vitro* study, we investigated baculovirus-generated recombinant ferret CMO2 cleavage activity towards the carotenoid substrates zeaxanthin, lutein and β-cryptoxanthin. Utilizing HPLC, LC-MS and GC-MS, we identified both volatile and non-volatile apocarotenoid products including 3-OH-β-ionone, 3-OH-α-ionone, β-ionone, 3-OH-α-apo-10'-carotenal, 3-OH-β-apo-10'-carotenal, and β-apo-10'-carotenal, indicating cleavage at both the 9,10 and 9',10' carbon-carbon double bond. Enzyme kinetic analysis indicated the xanthophylls zeaxanthin and lutein are preferentially cleaved over β-cryptoxanthin, indicating a key role of CMO2 in non-provitamin A carotenoid metabolism. Furthermore, incubation of 3-OH-β-apo-10'-carotenal with CMO2 lysate resulted in the formation of 3-OH-β-ionone. In the presence of NAD^+, *in vitro* incubation of 3-OH-β-apo-10'-carotenal with ferret hepatic homogenates formed 3-OH-β-apo-10'-carotenoic acid. Since apo-carotenoids serve as important signaling molecules in a variety of biological processes, enzymatic cleavage of xanthophylls by mammalian CMO2 represents a new avenue of research regarding vertebrate carotenoid metabolism and biological function.

Introduction

Many epidemiological studies have indicated that increased dietary intake of carotenoids may offer protection against the development of several chronic and degenerative diseases, including cardiovascular disease (1), age-related macular degeneration (2) and certain cancers (3). There are six major carotenoids that can be routinely found in human plasma and tissues (4, 5), which can be divided into two major structural groups: 1) xanthophylls, which include the oxygenated carotenoids lutein, zeaxanthin, and β-cryptoxanthin; and 2) carotenes, which include hydrocarbon carotenoids that are either cyclized, such as β-carotene or α-carotene, or linear, like lycopene. The vast amount of carotenoid research efforts have focused on the provitamin A carotenoids, which includes β-carotene, α-carotene, and β-cryptoxanthin, due to their ability to be metabolized to the essential nutrient vitamin A. The non-provitamin A carotenoids, which includes lutein, zeaxanthin, and lycopene, cannot be metabolized to vitamin A but have demonstrated potentially significant impact on human health and disease prevention and progression.

Carotenoids are lipophilic polyisoprenoid plant pigments typically containing a series of conjugated double bonds in the central chain of the molecule, making them susceptible to oxidative cleavage. Although any of the conjugated double bonds within the carotenoid molecule can be cleaved, many biologically active apocarotenoids are formed via site-specific cleavage (6, 7). Oxidative cleavage of carotenoids results in the formation of apocarotenoid metabolites, which may have important biological roles different than their parent compound. The biological significance of carotenoid

metabolite generation, especially the differential effects of small and large quantities of oxidative metabolites, has been recently reviewed (8, 9).

Carotenoid cleavage oxygenases (CCOs) mediate the site-specific cleavage of carotenoid substrates, forming important apocarotenoid products. CCOs belong to an ancient and highly conserved family with members in plants, animals and bacteria. The maize 9-cis-epoxycarotenoid dioxygenase *Viviparous14* (VP14) was the first CCO to be cloned and characterized (10). VP14 catalyzes asymmetric cleavage of the 11,12 double bond of neoxanthin and/or violaxanthin forming abscisic acid, which acts as a hormone in plants, promoting senescence and abscission of leaves and dormancy induction in buds and seeds. Sequence homology with VP14 led to the cloning and characterization of the Drosophila carotene-15,15'-monooxygenase (CMO1), which is responsible for vitamin A biosynthesis from β-carotene (11). CMO1 orthologues have since been cloned and characterized in several species, including mice and humans (12-16). The presence of at least one unsubstituted β-ionone ring has been recognized as a requisite for cleavage by CMO1 (12), limiting cleavage to provitamin A carotenoid substrates such as β-carotene and β-cryptoxanthin and identifying central cleavage via CMO1 as the major pathway leading to vitamin A formation. Indeed, no cleavage activity was detected when lycopene or zeaxanthin was used as a substrate (14).

An alternative metabolic pathway for β-carotene, termed the excentric cleavage pathway, was proposed (17). Existence of the excentric cleavage pathway was confirmed by the isolation of a second carotenoid cleaving enzyme, termed carotene-9',10'-monooxygenase (CMO2), which has been identified in humans, mice and ferrets (18, 19). CMO2 cleaves β-carotene at the 9',10' double bond forming β-apo-10'-carotenal and β-

ionone. β-Apo-10'-carotenal can be further oxidized to β-apo-10'-carotenoic acid (20), which can be shortened to retinoic acid via a mechanism similar to β-oxidation (21). This suggests excentric cleavage of β-carotene as an alternative pathway in retinoic acid formation (22). The contribution of CMO2 in vitamin A biosynthesis remains a controversial issue (23). Recently a quantitative trait locus (QTL) associated with yellow adipose tissue and milk color was identified to contain a premature stop codon mutation in the bovine CMO2 gene. This results in increased adipose, serum, and milk β-carotene concentrations and decreased liver retinol compared to wild types, yet no developmental or physiologic abnormalities in CMO2 mutants were observed (24, 25). In addition to β-carotene, CMO2 cleaves *cis*-isomers of lycopene generating apo-10'-lycopenoids (18), which have displayed unique biological activities *in vitro* and *in vivo* (26-28). A series of apo-lycopenals, including apo-10'-lycopenal, have recently been identified in human plasma, yet whether they originate from enzymatic cleavage or from consumption of apo-lycopenal-containing fruits and vegetables is unclear (29). The cleavage of both β-carotene and lycopene suggests that CMO2 may accept a wider variety of substrates than previously recognized (18, 19).

Recent genetic analyses have provided further evidence that CMO2 plays a broader role in carotenoid metabolism. A single nucleotide polymorphism (SNP) in the sheep (*Ovis aries*) CMO2 gene, resulting in a premature stop codon, was shown to be associated with an increase in adipose carotenoid accumulation (30). Lutein and flavoxanthin are the predominant carotenoids accumulated within sheep adipose tissue (31). A SNP in the CMO2 gene was also identified in domestic chickens (*Gallus gallus*) leading to lower tissue specific expression of CMO2 in the skin (32). The decrease in

skin CMO2 leads to the yellow skin pigmentation of domestic chickens, suggesting a decreased ability to cleave the xanthophylls lutein and zeaxanthin, which are the major accumulated carotenoids in chicken skin (33). However, no biochemical evidence is available demonstrating cleavage of hydroxy carotenoids by CMO2, in particular the xanthophylls lutein and zeaxanthin, which are concentrated in human macula and retina of the eye and provide potential protection against age-related macular degeneration (2, 34).

In the present study, using recombinant ferret CMO2, we identified cleavage products via HPLC, LC-MS and GC-MS and characterized the kinetic properties of CMO2 using zeaxanthin, lutein and β-cryptoxanthin as substrates *in vitro*. Furthermore, we identified and characterized the oxidation of the 3-OH-β-apo-10'-carotenal to 3-OH-β-apo-10'-carotenoic acid *in vitro*.

Materials and Methods

Materials

(3R)-β-Cryptoxanthin (96.8%), zeaxanthin (96%), β-apo-10'-carotenal, and 3-hydroxy(OH)-β-apo-10'-carotenal were kindly provided by BASF Inc., Ludwigshafen, Germany. (3R,3'R)-Lutein (96.4%) was purchased from Chromadex, Inc. (Irvine, CA). β-Ionone (96.4%) was purchased from Spectrum Chemical (Gardena, CA). Ammonium acetate was purchased from Sigma Chemical (St. Louis, MO). HPLC-grade solvents were obtained from J. T. Baker Chemical (Philipsburg, NJ) and Sigma-Aldrich Chemical (Milwaukee, WI). Substrate stock solutions were prepared in anhydrous tetrahydrofuran (THF) under red light and stored at -80°C until use.

Expression of Ferret CMO2 in Sf9 cells

The complete ferret CMO2 coding sequence (Genbank™ AY527150.1) was subcloned from pRcHA-fCMO2 plasmid into the baculovirus expression vector pFastBac1 (Invitrogen) by PCR using the BamHI/SpeI site as previously described (18). Briefly, *Spodoptera frugiperda 9* (Sf9) cells were tansfected with the ferret CMO2 bacmid DNA, and the recombinant ferret CMO2 viral titer was amplified by propagation in Sf9 cells. Flasks (225 cm^2) were seeded and infected at a multiplicity of infection (MOI) of 10. Four days post-infection, cell pellets were collected, centrifuged, washed 1X with cold PBS, and stored at -80°C until further use. Expression of ferret CMO2 protein in Sf9 cells was confirmed by both Coomassie Blue staining and Western Blotting analysis with a purified polyclonal antibody against ferret CMO2 (18).

Enzymatic Kinetic Assay

All procedures of enzyme preparation were conducted on ice. The Sf9 cell pellets containing either uninfected or infected recombinant ferret CMO2 baculovirus were suspended in 0.5 ml of lysis buffer (20 mM Tris-HCl; pH 8.0, 150 mM KCl, 0.1% Tween 20) and homogenized in a Potter-Elvehjem homogenizer for 60s. The homogenates were clarified by centrifugation at 10,000 × *g* for 30 minutes at 4°C. Supernatants were collected and either used immediately for enzymatic assays or stored at -80°C until further use. The substrate aliquots of carotenoids in anhydrous THF (β-cryptoxanthin, lutein and zeaxanthin) were dried by N_2 under red light and subsequently prepared in 4% Tween 40 in acetone, which is again evaporated by N_2. The dried substrates were solubilized in buffer (20 mM Tris-HCl; pH 8.5, 150 mM KCl) and sonicated to obtain a clear micellar solution. All enzymatic assays were performed in a final volume of 1 ml

containing assay buffer (20 mM Tris-HCl; pH 8.5, 150 mM KCl, 10 μM $FeSO_4$, 3 mM NAD^+, 0.3 mM DTT) and ~ 2 mg of enzyme supernatant (or various concentrations as indicated). Mixtures were pre-incubated for 5 min. at 37°C, and the cleavage reaction was initiated by adding 100 μl of substrate (β-cryptoxanthin, lutein, zeaxanthin or 3-OH-β-apo-10'-carotenal at various concentrations). After incubation for 30 min. (or various time points as indicated) at 37°C in the dark with gentle shaking, reactions were terminated by addition of 1.5 ml absolute ethanol. Incubation mixtures were extracted 2X with 5 ml hexane:methyl-*tert* butyl ether (1:1, v/v). The combined extracts were dried by N_2 under red light and dissolved in 200 μl ethanol:methyl-*tert* butyl ether (1:1, v/v) and analyzed by HPLC or LC-MS as described herein.

HPLC Analysis

A gradient reverse phase HPLC system was used for quantitative analysis of carotenoids and their polar metabolites. Briefly, the gradient reverse phase HPLC system consists of a Waters 2695 separations module and a Waters 2998 photodiode array detector. The enzymatic cleavage products of zeaxanthin, lutein and β-cryptoxanthin were analyzed on a reverse phase C_{18} column (4.6 x 250 mm, 5 μM) (Vydac 201TP54, Grace Discovery Sciences, Inc.) fitted with a Pecosphere C_{18} guard column (PerkinElmer, CT.) with a flow rate of 1.00 ml/min. The gradient procedure is as follows: 1) 50% solvent A (100% Water, 50mM ammonium acetate) and 50% solvent B (100% Acetonitrile) for 4 minutes followed by a 6 minute linear gradient to 20% solvent A and 80% solvent B; 2) a 9-minute hold followed by a 11-min linear gradient to 90% Solvent B and 10% Solvent C (Acetonitrile, Tetrahydrofuran, H_2O, 50 mM ammonium acetate, 50:44:6, v/v/v); 3) a 3-min hold followed by an 11-min linear gradient to100% solvent C;

4) a 4-min hold followed by a 10 minute linear gradient to 50% solvent A and 50% solvent B; and 5) a 12-min hold on 50% solvent A and 50% solvent B before the next injection. The Waters 2998 programmable photodiode array detector was set at 450 nm and 296 nm for carotenoid metabolite and related volatile analysis. Carotenoid metabolites were identified on the basis of relative retention times (RT) and by comparison of spectra with those of pure standards.

LC-MS Analysis

The LC system consisted of an Agilent 1100 quaternary pump and UV-Vis diode array detector (Agilent Technologies, Palo Alto, CA). The column was a Vydac C_{18} 201TP54 column (4.6 x 250 mm, 5 μM) (Grace Discovery Sciences, Inc.). HPLC-MS separations were monitored at 450 nm. Mass spectra data was obtained with an Agilent 1100 MSD equipped with an atmospheric pressure chemical ionization (APCI) ion source operating in positive ion mode. The quadrupole was scanned *m/z* 100 - 600. The capillary was 2500 V and the temperature of the drying gas (N_2) was 350 °C at a flow rate of 9.0 L/min. The corona discharge voltage was optimized resulting in a current of 6.0 μA. The chromatographic conditions were similar to those used for HPLC analysis.

GC-MS Analysis

Cleavage assays were extracted and 50 μl was subjected to HPLC analysis as indicated above. HPLC flow-through containing peaks identified as putative volatile cleavage products were collected on ice and extracted twice with hexane:methyl-*tert* butyl ether (1:1, v/v). The combined extracts were dried by N_2 under red light. The residue was reconstituted in diethyl ether, dried over anhydrous sodium sulfate, concentrated to dryness by N_2, and dissolved in hexane for injection. GC-MS analysis

were performed with an Agilent 5973N Mass Selective Detector coupled with an Agilent 6890 Series GC Detector. The oven was kept at 40 °C for 3 min and then increased to 250 °C at 5 °C min^{-1} with a helium carrier gas flow of 1.5 mL/min. One microliter of each sample was injected on a Supleco SAC-5 (Sigma-Aldrich, St. Louis, MO) capillary column (30 m × 0.25 mm i.d., 0.25 μm film thickness). Mass spectra were recorded in electron impact (EI) ionization mode at 70 eV. Identifications were carried out by comparison of EI mass data with published data or with data from authentic standards.

Incubation of 3-OH-β-apo-10'-carotenal with the S9 Fraction of Ferret Liver

Ferret liver (~1g) was homogenized with 5 ml of cold Tris Buffer A (20 mM Tris-HCl, 150 mM KCl, 0.5 mM DTT, pH 8.0) using an Ultra Turrax T8 Homogenizer (IKA, Germany). The homogenate was centrifuged at 9000 × *g* at 4 °C for 30 min and the supernatant is collected. The supernatant represented a mixture of microsomes and cytosol, containing aldehyde dehydrogenase (18, 35). Reactions were carried out in a final volume of 1 ml of Buffer A containing 4 mg of S9 liver homogenates with or without added cofactors (3 mM NAD^+). The mixtures were pre-incubated for 5 min at 37 °C before addition of substrates. Incubations were initiated by addition of 20 μl of 3-OH-β-apo-10'-carotenal as the substrate at the indicated concentrations. After 1 hr of shaking in a 37 °C water bath under red light, the incubations were terminated by addition of 1.5 ml of ethanolic KOH (20 mM KOH). Carotenoid metabolites were extracted twice with 5 ml hexane, combined and dried by N_2. The remaining aqueous fraction was acidified by addition of 120 μl of 4 M HCL and extracted twice with 5 ml hexane and combined with the previous extraction. The dried fraction was dissolved in 100 μl ethanol:methyl-*tert* butyl ether (1:1, v/v) and subjected to HPLC and LC/MS analysis as described.

Solid phase extraction (SPE) of apo-carotenoic acid derivatives

To facilitate the positive identification of oxidative apo-carotenoic acid derivatives, acidic extracts were applied to an aminopropyl SPE column (36). Briefly, 3-hydroxy-β-apo-10'-carotenal was incubated with ferret liver S9, extracted, and dried by N_2 as before. The dried extracts were reconstituted in chloroform and applied to pre-conditioned aminopropyl SPE columns (Strata NH2, Phenomenex, USA) and placed in the Vac Elut apparatus and washed twice with hexane. A chloroform:isopropanol (2:1, v/v) mixture was next applied to the column, eluting the neutral lipid layer, which was discarded. 3-OH-β-apo-10'-carotenoic acid was eluted with diethyl ether (containing 5% acetic acid), collected and dried under N_2, reconstituted in 100 μl ethanol:methyl-*tert* butyl ether (1:1, v/v) and subjected to HPLC and LC/MS analysis as described.

RESULTS

Cleavage of Zeaxanthin, Lutein and β-Cryptoxanthin using Recombinant Ferret CMO2 and Identification of Cleavage Products

To confirm expression of the recombinant ferret CMO2 in the baculovirus system, we demonstrated, using both Coomassie Blue staining and immunobloting with a polyclonal-CMO2 antibody (Figure 1), expression of a protein of approximately 60 kDa, which is the predicted molecular mass of ferret CMO2 protein (18). To demonstrate enzymatic cleavage activity, insect cell homogenates infected with ferret CMO2 baculovirus were incubated with zeaxanthin, lutein or β-cryptoxanthin at varying concentrations. For zeaxanthin, HPLC separation with monitoring at 450 nm revealed the production of a new peak in the incubations containing CMO2-infected Sf9 cell

lysates. The RT (25.5 min.) and absorption spectrum (UV_{max} 449.9 nm) of the new peak matched the RT (25.5 min.) and absorption spectrum (UV_{max} 449.9 nm) of the authentic 3-OH-β-apo-10'-carotenal standard (Figure 2). To identify corresponding cleavage products, samples were subjected to LC-MS analyses, and since the system was operated in $APCI^+$ mode, quasimolecular ions generally appeared as $(M+H)^+$ signals. LC-MS analysis of the new peak identified a quasimolecular ion of *m/z* 393 $(M+H)^+$ (Figure 2), which corresponds to the quasimolecular ion of the authentic 3-OH-β-apo-10'-carotenal standard, confirming the formation of 3-OH-β-apo-10'-carotenal.

In addition to formation of the 3-OH-β-apo-10'-carotenal product, cleavage of zeaxanthin at 9',10' (9,10) double bond results in the formation of the C_{13} compound 3-OH-β-ionone. HPLC analysis with monitoring at 296 nm revealed the presence of a new peak with a RT of 3.9 min (Figure 3B) and UV_{max} of 294.1 nm (Figure 3E), which is similar to published chromatographic data of 3-OH-β-ionone (37). Due to the absence of a 3-OH-β-ionone authentic standard, the identity of the new peak was investigated by GC-MS analysis after HPLC separation. The collected peak was identified by the presence of the major ions of *m/z* 193 and *m/z* 175, with a parent molecular ion of *m/z* 208 (Figure 3G), which are indicative of 3-OH-β-ionone (38, 39). Taken together, the analyses clearly demonstrate cleavage of zeaxanthin at the 9',10' (9,10) double bond by ferret CMO2, resulting in the formation of 3-OH-β-apo-10'-carotenal and 3-OH-β-ionone (Figure 11A).

Lutein and zeaxanthin are constitutional isomers, differing in orientation of the ionone ring system. These differences may have an impact on functional roles (40). Therefore, we investigated cleavage activity of ferret CMO2 towards lutein. HPLC

separation with monitoring at 450 nm revealed the formation of two new peaks when incubated with ferret CMO2 (Figure 4). Peak 1 was shifted 2.5 min. earlier in RT (23.0 min.) and had an absorption spectrum 4.8 nm shorter (UV_{max} 445.1 nm) than the 3-OH-β-apo-10'-carotenal standard (Figure 4). The RT (25.5 min.) and absorption spectra (UV_{max} 449.9 nm) of peak 2 matched the RT and absorption spectra of the authentic 3-OH-β-apo-10'-carotenal standard. Lutein possesses an allylic hydroxyl group at the C-3' position of the ε-ring, and due to the shift in the C-5' - C-4' double bond, the loss of water from the protonated parent ion in $APCI^+$ mode gives a more stable allylic radical cation (41). Thus, $APCI^+$-MS analysis allows differentiation of cleavage at either the 9,10 or 9',10' carbon-carbon double bond. Peak 1 possessed a base peak of *m/z* 375, corresponding to the $(M+H-H_2O)^+$ ion, confirming the presence of the 3'-OH-α-apo-10-carotenal product. Peak 2 was confirmed by the presence of a quasimolecular ion at *m/z* 393 $(M+H)^+$, which corresponds to the quasimolecular ion of the 3-OH-β-apo-10'-carotenal standard.

Cleavage of lutein at the 9,10 and 9',10' double is expected to produce both 3-OH-β-ionone and 3'-OH-α-ionone. HPLC separation with monitoring at 296 nm revealed the presence of a new peak with a RT of 3.9 min. (Figure 3D) and a UV_{max} of 294.1 nm (Figure 3F), similar to that observed with zeaxanthin yet displaying a broader spectrum indicating additional compounds (Figure 3). Our HPLC program did not allow separation of 3-OH-β-ionone and 3'-OH-α-ionone, thus, the peak was collected, extracted and subjected to GC-MS. The presence of 3-OH-β-ionone was confirmed by the presence of major ions at *m/z* 193 and *m/z* 175 (Figure 3G) while 3'-OH-α-ionone was confirmed by the presence of major ions at *m/z* 109 and *m/z* 175, with a parent molecular ion at *m/z* 208 (Figure 3H) (38). Taken together, these analyses demonstrate

cleavage of lutein by ferret CMO2 at both the 9,10 and 9',10' double bond, forming 3-OH-β-apo-10'-carotenal, 3'-OH-α-ionone, 3'-OH-α-10-carotenal, and 3-OH-β-ionone (Figure 11B).

For β-Cryptoxanthin, HPLC separation revealed the production of four new peaks in the incubations containing CMO2-infected Sf9 cell lysates. At 450 nm, the RT (25.5 and 33.4 min) and absorption spectra (UV_{max} 449.9 nm and 447.5 nm) of peaks 1 and 2 matched the RT and absorption spectra of the 3-OH-β-apo-10'-carotenal and β-apo-10'-carotenal authentic standards, respectively (Figure 5). The identity of peaks 1 and 2 were further verified by their quasimolecular ions at *m/z* 393 $(M+H)^+$ and 377 $(M+H)^+$, respectively (Figure 4), which correspond to the quasimolecular ions of the authentic 3-OH-β-apo-10'-carotenal and β-apo-10'-carotenal standards, respectively. At 296 nm, the RT (3.9 min.) and absorption spectra (UV_{max} 294.1 nm) of peak 1 was similar to that of the identified 3-OH-β-ionone. The RT (11.9 min.) and absorption spectra (UV_{max} 295.2 nm) of peak 2 matched the RT and absorption spectra of the authentic β-ionone standard (Figure 6). GC-MS analysis revealed the presence of a major ion at *m/z* 177 indicating the presence of β-ionone (39), while the presence of major ions of *m/z* 193 and *m/z* 175 confirmed the presence of 3-OH-β-ionone (39). The above analyses demonstrate that ferret CMO2 cleaves β-cryptoxanthin at the 9,10 and 9',10' double bond forming 3-OH-β-apo-10'-carotenal, β-ionone, β-apo-10-carotenal, and 3-OH-β-ionone (Figure 11C). The formation of β-apo-10'-carotenal and 3-OH-β-apo-10'-carotenal was significantly decreased by the deletion of Fe^{2+} from the incubation mixture (78%, 71%, and 67% lower from three independent experiments, compared with that of the complete reaction), indicating that iron was an essential co-factor for the reaction, as previously described

(18). Only trace amounts of other peaks were detected in two control reactions done with uninfected cell homogenates or without cell homogenates. These trace peaks likely represent non-enzymatic cleavage of carotenoids, as previously described (7, 18).

In Vitro Kinetic Analysis

To estimate the substrate specificity and kinetic constants for recombinant ferret CMO2, we performed *in vitro* assays with zeaxanthin, lutein and β-cryptoxanthin as substrates. Using β-cryptoxanthin as the substrate (~50 μM), the production of β-apo-10'-carotenal was linear up 10 mg/ml (Figure 7) while formation of 3-OH-β-apo-10'-carotenal was linear up to 2 mg/ml with only a slight increase in formation up to 10 mg/ml. The production of β-apo-10'-carotenal from β-cryptoxanthin was linear up to 90 minutes while 3-OH-β-apo-10'-carotenal formation was linear up to 30 min (Figure 7). The production of 3-OH-β-apo-10'-carotenal from zeaxanthin (~50 μM) was linear up to 4 mg/ml with only a slight increase up to 10 mg/ml (Figure 8). The production of 3-OH-β-apo-10'-carotenal and 3'-OH-α-apo-10'-carotenal from lutein (~50 μM) was linear up to 4 mg/ml with only a slight increase up to 10 mg/ml (Figure 8). Using 2 mg/ml ferret CMO2 lysate, formation of 3-OH-β-apo-10'-carotenal and 3'-OH-α-apo-10-carotenal was linear up to 30 min. using zeaxanthin and lutein as substrates (Figure 8), respectively. To ensure less than 10% substrate conversion for all substrates investigated, incubations were carried out with 2 mg/ml ferret CMO2 lysate over a 30 min. period.

Kinetic constants for recombinant ferret CMO2 were estimated by varying the concentrations of carotenoid substrates. Reaction curves displayed a sigmoidal shape for all substrates, thus kinetic parameters were estimated from a positive cooperativity allosteric kinetic model (GraphPad Prism, version 5.02, San Diego, CA, USA). All

kinetic constants are identified as apparent $K_{0.5}$ and apparent V_{max}. Production of 3-OH-β-apo-10'-carotenal from zeaxanthin (0 – 200 μM) was fit to an allosteric enzyme kinetic model and apparent $K_{0.5}$ and V_{max} values of 51.49 ± 3.66 μM and 48.40 ± 2.28 μM pmol of 3-OH-β-apo-10'-carotenal mg^{-1} min^{-1} were estimated (Figure 9A). Using Lutein as the substrate (0 – 225 μM), formation of 3-OH-β-apo-10'-carotenal had estimated apparent $K_{0.5}$ and V_{max} values of 47.97 ± 2.40 μM and 31.91 ± 1.14 pmol mg^{-1} min^{-1} while formation of 3-OH-β-apo-10'-carotenal had estimated apparent $K_{0.5}$ and V_{max} values of 51.10 ± 2.10 μM and 38.0 ± 1.13 pmol mg^{-1} min^{-1}. The combined kinetics had estimated apparent $K_{0.5}$ and V_{max} values of 49.60 ± 1.93 μM and 69.87 ± 1.95 pmol of 3-OH-β-apo-10'-carotenal and 3-OH-α-apo-10-carotenal mg^{-1} min^{-1} (Figure 9B). Using β-cryptoxanthin as the substrate (0 – 450 μM), production of β-apo-10'-carotenal had estimated apparent $K_{0.5}$ and V_{max} values of 79.29 ± 2.87 μM and 31.45 ± 0.74 pmol mg^{-1} min^{-1} while production of 3-OH-β-apo-10'-carotenal had estimated apparent $K_{0.5}$ and V_{max} values of 110.0 ± 7.96 μM and 2.92 ± 0.13 pmol mg^{-1} min^{-1}. The combined kinetics had estimated apparent $K_{0.5}$ and V_{max} values of 80.83 ± 2.96 μM and 34.26 ± 0.8117 pmol of β-apo-10'-carotenal and 3-OH-β-apo-10'-carotenal mg^{-1} min^{-1} (Figure 9C). Hill coefficients of h = 1.95, h = 2.13 and h = 2.44 were estimated for zeaxanthin, lutein and β-cryptoxanthin, respectively.

Cleavage of 3-OH-β-apo-10'-carotenal using Recombinant Ferret CMO2

Initial velocity determination revealed a discord between protein- and time-dependent formation of β-apo-10'-carotenal and 3-OH-β-apo-10'-carotenal from β-cryptoxanthin (Figure 7), suggesting potential cleavage of 3-OH-β-apo-10'-carotenal by CMO2. Thus, cleavage of 3-OH-β-apo-10'-carotenal by CMO2 was investigated. 3-OH-

β-apo-10'-carotenal (5 μM) was incubated with 2 mg ferret CMO2 lysate, uninfected Sf9 lysates or buffer alone for 30 min. Cleavage activity was quantified as percent parent remaining and normalized to buffer alone (100%). Incubation of 3-OH-β-apo-10'-carotenal with uninfected Sf9 insect cell lysate resulted in 45% decrease in the parent compound, indicating that the 3-OH-apo-10'-carotenal metabolite is highly unstable. However, when 3-OH-apo-10'-carotenal was incubated with CMO2 lysate, there was a 67% decrease in the parent compound (Supplementary Table 1), accompanied by appearance of 3-OH-β-ionone (Supplementary Figure 1), indicating the further cleavage of 3-OH-β-apo-10'-carotenal by CMO2 at the 9,10 double bond. However, we did not detect the expected apo-10,10'-carotenedialdehyde product in addition to 3-OH-β-ionone.

In Vitro Oxidation of 3-OH-β-apo-10'-carotenal by Ferret Hepatic Homogenates

Acid derivatives of apocarotenoid products have been identified as biologically active metabolites, serving as intermediates in retinoic acid formation and possessing unique biological activities (42). Therefore, we sought to determine the *in vitro* conversion of 3-OH-β-apo-10'-carotenal to 3-OH-β-apo-10'-carotenoic acid. When NAD^+ (3 mM) was present in the reaction mixture, incubation of 3-OH-β-apo-10'-carotenal (2 or 10 μM) with ferret liver S9 homogenate resulted in the formation of 3-OH-β-apo-10'-carotenoic acid (Figure 10). The new peak had a retention time of 16 min and UV_{Max} of 416 nm (Figure 10D, *Inset*). The new peak was retained when subjected to aminopropyl SPE (data not shown), and LC-MS analysis identified quasimolecular ions at *m/z* 409 $(M + H)^+$ and 391 $(M+H-H_2O)^+$ (Figure 10D). In the presence of the aldehyde dehydrogenase inhibitor citral (1 mM), which blocks conversion of retinal to retinoic acid (35), 3-OH-β-apo-10'-carotenoic acid formation was completely inhibited (Figure 10C),

indicating enzymatic conversion of 3-OH-β-apo-10'-carotenal into 3-OH-β-apo-10'-carotenoic acid.

DISCUSSION

The present study is the first documentation of excentric enzymatic cleavage of xanthophyll carotenoids by a vertebrate carotenoid cleavage oxygenase, adding to the accumulating evidence that CMO2 plays a key role in carotenoid metabolism, especially of non-provitamin A carotenoids. We demonstrate that ferret CMO2 catalyzes the excentric cleavage of hydroxy carotenoids, including the non-provitamin A zeaxanthin and lutein, and provitamin A β-cryptoxanthin, at both the 9,10 and 9',10' double bond producing both volatile and non-volatile apocarotenoid cleavage products (Figure 11**)**. Importantly, we showed the xanthophylls zeaxanthin and lutein are preferentially cleaved over the mono-hydroxy β-cryptoxanthin. This provides strong biochemical evidence supporting the recent genetic evidence that accumulation of the xanthophylls lutein and zeaxathin in adipose tissue and skin are due to mutations in the CMO2 gene (30, 32). Considering the possible beneficial effects of lutein, zeaxanthin and β-cryptoxanthin in human health (1-3), enzymatic cleavage of xanthophylls by CMO2 represents a new avenue of research regarding vertebrate carotenoid metabolism and biological function.

While previous studies have shown a key role for CMO1 in catalyzing the symmetric cleavage of provitamin A carotenoids to vitamin A (11, 23, 43), similar evidence for a definitive role of CMO2 in carotenoid metabolism has been lacking. The presence of at least one unsubstituted β-ionone ring has been proposed to be sufficient for cleavage of carotenoids by CMO1 (12, 14), and indeed, low or no cleavage activity was

detected when all-trans lycopene or zeaxanthin was investigated as a substrate (14). In contrast, previous investigations of vertebrate CMO2 substrate recognition demonstrated cleavage of both β-carotene and cis-isomers of lycopene, respectively (18, 19), suggesting both the central polyene chain backbone and the ionone-ring structures are important in substrate specificity. In the present study, we demonstrate that the xanthophylls zeaxanthin and lutein are preferentially cleaved over the mono-hydroxy β-cryptoxanthin, indicating an important role of substitution of the ionone ring structures in CMO2 cleavage (Figure 11). There was little difference in cleavage activity between the β- and ε-ionone ring of lutein indicating little effect of ring orientation on cleavage activity. However, symmetry of substitution of the ionone ring in β-cryptoxanthin had a major influence on cleavage activity, i.e. 10-fold greater formation of β-apo-10'-carotenal compared to 3-OH-β-apo-10'-carotenal formation (data not shown). These results suggest that symmetry of substitution and not simply substitution alone is important in CMO2 substrate recognition.

In the present study, ferret CMO2 cleaved zeaxanthin into 3-OH-β-apo-10'carotenal and 3-OH-β-ionone, indicating cleavage at either the 9'10' or 9,10 carbon-carbon double bond. However, lutein was converted into 3-OH-β-apo-10'carotenal, 3'-OH-α-apo-10-carotenal, 3-OH-β-ionone, and 3'-OH-α-ionone while β-cryptoxanthin was converted into β-apo-10'-carotenal, 3-OH-β-apo-10-carotenal, β-ionone, and 3-OH-β-ionone indicating cleavage at both the 9,10 and 9',10' carbon-carbon double bond. This is supported by our further observation of CMO2 cleavage activity towards 3-OH-β-apo-10'-carotenal, forming 3-OH-β-ionone. Members of the plant carotenoid cleavage dioxygenase 1 (CCD1) family of CCOs display a similar pattern of carotenoid cleavage,

cleaving multiple substrates at both the 9,10 and 9',10' double bond [44]. However, the main products of CCD1 cleavage are C_{14} dialdehydes and C_{13} volatile compounds, indicating both C40 and C27 compounds can serve as substrates for CCD1 orthologues. However, we did not detect any C_{14} dialdehydes in our cleavage reactions, which could be due to further degradation, nor did we detect any cleavage products when β-apo-8'-carotenal as the substrate (data not shown). Our data demonstrates that cleavage by CMO2 at either the 9,10 or 9',10' double bond is mutually exclusive. Whether CMO2 can cleave additional substrates clearly needs further investigation.

Our kinetic analyses indicate that ferret CMO2 cleavage activity was higher toward zeaxanthin and lutein than β-cryptoxanthin *in vitro*. While the estimated apparent $K_{0.5}$ concentrations obtained in the current study are higher than concentrations achieved *in vivo* (e.g., 1 – 2 μM for lutein and zeaxathin [45, 46]), studies investigating recombinant CMO1 cleavage activity towards β-carotene estimated K_m values ranging from 6 – 31 μM [47], which is significantly higher than *in vivo* β-carotene concentrations [48]. These studies have contributed greatly to the understanding of the mechanisms and substrate specificity of CMO1. In the current study when zeaxanthin, lutein and β-cryptoxanthin where used as substrates, however, substrate-dependent cleavage did not follow Michaelis-Menten kinetics. Comparison of kinetic models indicated that an allosteric model of positive cooperativity was a more appropriate fit of enzymatic activity. Human CMO1 was shown to be a tetrameric enzyme *in vitro* [12] yet displayed Michaeli-Menten kinetics. However, one of the limitations of the current study, especially in regards to estimating kinetic parameters, is the use of crude enzyme lysates. Crude enzyme lysates can give the impression of allosteric kinetics due to the low

percentage of enzyme present, especially at lower substrate concentrations [49]. This combination decreases the interaction between substrate and enzyme, and thus, a lower rate is observed (an especially pertinent observation with carotenoids, which must be micellized for solubilization). In the current study, protein and time-dependency were markedly different between 3-OH-β-apo-10'-carotenal and β-apo-10'-carotenal formation (Figure 7). The increased protein concentration and incubation time led to an increase in 3-OH-β-apo-10'-carotenal cleavage, necessitating the use of shorter incubations and decreased protein concentrations for kinetic estimations. This becomes an issue when the substrate is substantially diluted. The lag in activity displayed in the kinetic curves could in fact be due to the substrate and protein dilution. While the procurement of purified CMO2 remains a significant challenge [18, 19], investigations using purified CMO2 enzyme need to be carried out to further clarify the kinetics of CMO2.

In the present study, we demonstrate *in vitro* oxidation of 3-OH-β-apo-10'-carotenal to the 3-OH-β-apo-10'-carotenoic acid product. Feeding of apocarotenals results in the formation of apo-carotenoic acids *in vivo* (7, 20, 35), suggesting formation of acid products as the first step in further metabolic transformation of apocarotenoid products. Apocarotenoids are important bioactive mediators in plants and animals. In plants, they play key roles in reproduction, defense, and architecture (51). 3-OH-β-Apo-10'-carotenoic acid has been identified in *Boronia megastigma* (Nees) during flower development, indicating cleavage of xanthophylls and oxidation of cleavage products (52, 53). In animals, a number of studies have identified a broad array of apocarotenoids and apolycopenoids with potential biological activities (7, 18, 20, 54, 55). Non-volatile apo-

carotenoids and apo-lycopenoids, such as apo-10', apo-12'-, and apo-14'-, can inhibit cell growth (26, 56-58), stimulate differentiation (59), transactivate nuclear receptors (26) or antagonize nuclear receptor activation (60) and induce expression of phase II enzymes via activation of the Nrf2 transcription factor (27). Recently, we observed that 3-OH-β-apo-10'-carotenal exerts a dose-dependent effect on both growth inhibitory effect and induction of cell death in HepG2 liver cancer cells, BEAS-2B immortalized bronchial epithelial cells and A549 lung cancer cell lines (Mein et al., unpublished data). These ongoing studies implicate a role for 3-OH-β-apo-10'-carotenal in the regulation of cell proliferation and apoptosis. The volatile apo-carotenoid β-ionone has also been shown to inhibit cell proliferation and induce apoptosis both *in vitro* (61-64) and *in vivo* (65) and induce expression of phase I and phase II enzymes in rats and mice (66-68). In previous studies, β-cryptoxanthin dose-dependently increased RARE-dependent promoter activity in cells co-transfected with RAR expression vector (69) and was shown to bind and activate RAR receptors using a yeast two-hybrid system (70). Whether the activity of β-cryptoxanthin in these systems could be due to its conversion to apo-carotenoic acid metabolites is unclear. We clearly demonstrate excentric cleavage of β-cryptoxanthin, forming both apo-carotenoids and 3-OH-apo-carotenoids, which can be further oxidized to 3-OH-apo-carotenoic acids. While the activity of β-apo-10'-carotenoids has been investigated, research regarding the biological activity of 3-OH-apo-carotenoid products is clearly needed.

Cleavage of lutein and zeaxanthin by CMO2 raises important questions as to the role of zeaxanthin and lutein in the eye. Several carotenoids, including lutein, zeaxanthin, β-carotene, α-carotene, and lycopene, have been identified in the ciliary body

and human retinal pigment epithelia (RPE) of the eye (34). Both CMO1 and CMO2 are strongly expressed in the RPE (71, 72), and CMO1 actively converts β-carotene and β-cryptoxanthin into all-*trans*-retinal (73, 74), which is isomerized to the visual pigment chromophore 11-*cis*-retinal by RPE65 (75). In flies, an 11-cis-configuration of 3-OH-retinal is essential for visual pigment biogenesis (76). Although no apocarotenoids resulting from excentric cleavage by CMO2 have been identified in the RPE (77), 3-OH-β-apo-14'-carotenal and 3-OH-β-ionone have been identified in cadaver retinas (78). In addition, several non-dietary lutein and zeaxanthin metabolites, including 3'-epilutein, 3-OH-β,ε-caroten-3'-one and meso-zeaxanthin, have also been identified in these regions (34). The physiologic relevance of these metabolites is unknown, yet they are most likely formed by oxidation-reduction and isomerization reactions of lutein and zeaxanthin. Recently, non-specific oxidation products of β-carotene, lutein and zeaxanthin demonstrated activity in cultured RPE cells, indicating potential proinflammatory effects of non-specific carotenoid-derived aldehyde oxidation products (79). However, the susceptibility of lutein and zeaxanthin to degradation in the RPE may be limited by protein binding (80, 81). Nonetheless, the identification of 3-OH-apo-carotenoids *in vivo* remains a significant challenge. We did not detect any 3-OH-apo-carotenoids in mice or ferrets supplemented with either lutein or β-cryptoxanthin (unpublished data). This could be due to the detection limitations of our analytical systems, difficulty of extraction from complex biological matrices or stability of metabolites. Clearly, the development and utilization of more sensitive techniques for the identification and detection of apo-carotenoids *in vivo* (29) will greatly enhance research in this area.

Taken together, the broad substrate specificity of CMO2 demonstrated herein may help us understand the potential biologic role of CMO2 in carotenoid metabolism and function. Recent experimental data suggests that carotenoid metabolites may have more important biological roles than their parent compounds (8, 42). However, excessive accumulation of excentric carotenoid cleavage products has also demonstrated potential harmful effects (9, 82), especially when coupled with a highly oxidative environment (*e.g*. the lungs of a cigarette smoker or liver of an excessive alcohol drinker) (83-85). Therefore, depending on the dose, these metabolites may have specific actions on several important cellular signaling pathways and molecular targets. In considering the efficacy and complex biological functions of carotenoids in human chronic disease prevention, future investigations of carotenoids must take into account the regulatory mechanisms and carotenoid cleavage activity of CMO2 and further metabolic transformation of carotenoid metabolites.

References

1. Johnson EJ, Krinsky N.I. Carotenoids and Coronary Heart Disease. In: Britton G, Liaaen-Jensen, S., Pfander, H., editor. Carotenoids Volume 5: Nutrition and Health. Basel: Birkhäuser Verlag; 2009. p. 287-300.

2. Schalch W, Landrum, J.T., Bone, R.A. The Eye. In: Britton G, Liaaen-Jensen, S., Pfander, H., editor. Carotenoids Volume 5: Nutrition and Health. Basel: Birkhäuser Verlag; 2009. p. 301-34.

3. Rock CL. Carotenoids and Cancer. In: Britton G, Liaaen-Jensen, S., Pfander, H., editor. Carotenoids Volume 5: Nutrition and Health. Basel: Birkhäuser Verlag; 2009. p. 269-86.

4. Bendich A. Symposium conclusions: biological actions of carotenoids. J Nutr. 1989 Jan;119:135-6.

5. Khachik F, Spangler CJ, Smith JC, Jr., Canfield LM, Steck A, Pfander H. Identification, quantification, and relative concentrations of carotenoids and their metabolites in human milk and serum. Analytical chemistry. 1997 May 15;69:1873-81.

6. Tang GW, Wang XD, Russell RM, Krinsky NI. Characterization of beta-apo-13-carotenone and beta-apo-14'-carotenal as enzymatic products of the excentric cleavage of beta-carotene. Biochemistry. 1991 Oct 15;30:9829-34.

7. Wang XD, Tang GW, Fox JG, Krinsky NI, Russell RM. Enzymatic conversion of beta-carotene into beta-apo-carotenals and retinoids by human, monkey, ferret, and rat tissues. Arch Biochem Biophys. 1991 Feb 15;285:8-16.

8. Mein JR, Lian F, Wang XD. Biological activity of lycopene metabolites: implications for cancer prevention. Nutr Rev. 2008 Dec;66:667-83.

9. Wang XD. Carotenoid Oxidative/Degradative Products and Their Biological Activities. In: Krinsky NI, Mayne, S.T., Sies, H., editor. Carotenoids in Health and Disease. New York: Marcel Dekker; 2004. p. 313-35.

10. Schwartz SH, Tan BC, Gage DA, Zeevaart JA, McCarty DR. Specific oxidative cleavage of carotenoids by VP14 of maize. Science (New York, NY. 1997 Jun 20;276:1872-4.

11. von Lintig J, Vogt K. Filling the gap in vitamin A research. Molecular identification of an enzyme cleaving beta-carotene to retinal. The Journal of biological chemistry. 2000 Apr 21;275:11915-20.

12. Lindqvist A, Andersson S. Biochemical properties of purified recombinant human beta-carotene 15,15'-monooxygenase. The Journal of biological chemistry. 2002 Jun 28;277:23942-8.

13. Paik J, During A, Harrison EH, Mendelsohn CL, Lai K, Blaner WS. Expression and characterization of a murine enzyme able to cleave beta-carotene. The formation of retinoids. The Journal of biological chemistry. 2001 Aug 24;276:32160-8.

14. Redmond TM, Gentleman S, Duncan T, Yu S, Wiggert B, Gantt E, Cunningham FX, Jr. Identification, expression, and substrate specificity of a mammalian beta-carotene 15,15'-dioxygenase. The Journal of biological chemistry. 2001 Mar 2;276:6560-5.

15. Wyss A, Wirtz GM, Woggon WD, Brugger R, Wyss M, Friedlein A, Riss G, Bachmann H, Hunziker W. Expression pattern and localization of beta,beta-carotene 15,15'-dioxygenase in different tissues. The Biochemical journal. 2001 Mar 15;354:521-9.

16. Yan W, Jang GF, Haeseleer F, Esumi N, Chang J, Kerrigan M, Campochiaro M, Campochiaro P, Palczewski K, Zack DJ. Cloning and characterization of a human beta,beta-carotene-15,15'-dioxygenase that is highly expressed in the retinal pigment epithelium. Genomics. 2001 Mar 1;72:193-202.

17. Glover J. The conversion of beta-carotene into vitamin A. Vitamins and hormones. 1960;18:371-86.

18. Hu KQ, Liu C, Ernst H, Krinsky NI, Russell RM, Wang XD. The biochemical characterization of ferret carotene-9',10'-monooxygenase catalyzing cleavage of carotenoids in vitro and in vivo. The Journal of biological chemistry. 2006 Jul 14;281:19327-38.

19. Kiefer C, Hessel S, Lampert JM, Vogt K, Lederer MO, Breithaupt DE, von Lintig J. Identification and characterization of a mammalian enzyme catalyzing the asymmetric oxidative cleavage of provitamin A. The Journal of biological chemistry. 2001 Apr 27;276:14110-6.

20. Sharma RV, Mathur SN, Dmitrovskii AA, Das RC, Ganguly J. Studies on the metabolism of beta-carotene and apo-beta-carotenoids in rats and chickens. Biochim Biophys Acta. 1976 Jan 18;486:183-94.

21. Wang XD, Russell RM, Liu C, Stickel F, Smith DE, Krinsky NI. Beta-oxidation in rabbit liver in vitro and in the perfused ferret liver contributes to retinoic acid biosynthesis from beta-apocarotenoic acids. The Journal of biological chemistry. 1996 Oct 25;271:26490-8.

22. Napoli JL, Race KR. Biogenesis of retinoic acid from beta-carotene. Differences between the metabolism of beta-carotene and retinal. The Journal of biological chemistry. 1988 Nov 25;263:17372-7.

23. Hessel S, Eichinger A, Isken A, Amengual J, Hunzelmann S, Hoeller U, Elste V, Hunziker W, Goralczyk R, et al. CMO1 deficiency abolishes vitamin A production from beta-carotene and alters lipid metabolism in mice. The Journal of biological chemistry. 2007 Nov 16;282:33553-61.

24. Berry SD, Davis SR, Beattie EM, Thomas NL, Burrett AK, Ward HE, Stanfield AM, Biswas M, Ankersmit-Udy AE, et al. Mutation in bovine beta-carotene oxygenase 2 affects milk color. Genetics. 2009 Jul;182:923-6.

25. Tian R, Pitchford WS, Morris CA, Cullen NG, Bottema CD. Genetic variation in the beta, beta-carotene-9', 10'-dioxygenase gene and association with fat colour in bovine adipose tissue and milk. Animal genetics. 2009 Nov 26;41:253-9.

26. Lian F, Smith DE, Ernst H, Russell RM, Wang XD. Apo-10'-lycopenoic acid inhibits lung cancer cell growth in vitro, and suppresses lung tumorigenesis in the A/J mouse model in vivo. Carcinogenesis. 2007 Jul;28:1567-74.

27. Lian F, Wang XD. Enzymatic metabolites of lycopene induce Nrf2-mediated expression of phase II detoxifying/antioxidant enzymes in human bronchial epithelial cells. International journal of cancer. 2008 Jun 19;123:1262-8.

28. Mein JR, Wang XD. Oxidative Metabolites of Lycopene and Their Biological Functions. In: Landrum JT, editor. Carotenoids: Physical, Chemical, and Biological Functions and Properties: CRC Press; 2010. p. 417-35.

29. Kopec RE, Riedl KM, Harrison EH, Curley RW, Hruszkewycz DP, Clinton SK, Schwartz SJ. Identification and Quantification of Apo-lycopenals in Fruits, Vegetables, and Human Plasma. J Agric Food Chem. 2010 Mar 24;58:3290-6.

30. Vage DI, Boman IA. A nonsense mutation in the beta-carotene oxygenase 2 (BCO2) gene is tightly associated with accumulation of carotenoids in adipose tissue in sheep (Ovis aries). BMC genetics. 2010 Feb 2;11:10.

31. Hill F. Xanthophyll pigmentation in sheep fat. Nature. 1962 Jun 2;194:865-6.

32. Eriksson J, Larson G, Gunnarsson U, Bed'hom B, Tixier-Boichard M, Stromstedt L, Wright D, Jungerius A, Vereijken A, et al. Identification of the yellow skin gene reveals a hybrid origin of the domestic chicken. PLoS genetics. 2008 Feb;4:e1000010.

33. Castaneda MP, Hirschler EM, Sams AR. Skin pigmentation evaluation in broilers fed natural and synthetic pigments. Poultry science. 2005 Jan;84:143-7.

34. Bernstein PS, Khachik F, Carvalho LS, Muir GJ, Zhao DY, Katz NB. Identification and quantitation of carotenoids and their metabolites in the tissues of the human eye. Experimental eye research. 2001 Mar;72:215-23.

35. Wang XD, Krinsky NI, Tang GW, Russell RM. Retinoic acid can be produced from excentric cleavage of beta-carotene in human intestinal mucosa. Arch Biochem Biophys. 1992 Mar;293:298-304.

36. Tang GW, Russell RM. 13-cis-retinoic acid is an endogenous compound in human serum. Journal of lipid research. 1990 Feb;31:175-82.

37. Scherzinger D, Al-Babili S. In vitro characterization of a carotenoid cleavage dioxygenase from Nostoc sp. PCC 7120 reveals a novel cleavage pattern, cytosolic localization and induction by highlight. Molecular microbiology. 2008 Jul;69:231-44.

38. Garcia-Limones C, Schnabele K, Blanco-Portales R, Luz Bellido M, Caballero JL, Schwab W, Munoz-Blanco J. Functional characterization of FaCCD1: a carotenoid cleavage dioxygenase from strawberry involved in lutein degradation during fruit ripening. J Agric Food Chem. 2008 Oct 8;56:9277-85.

39. Vogel JT, Tan BC, McCarty DR, Klee HJ. The carotenoid cleavage dioxygenase 1 enzyme has broad substrate specificity, cleaving multiple carotenoids at two different bond positions. The Journal of biological chemistry. 2008 Apr 25;283:11364-73.

40. Landrum JT, Chatfield DC, Mebel AM, Alvarez-Calderon F, Fernandez MV. The conformation of end-groups is one determinant of carotenoid topology suitable for high fidelity molecular recognition: a study of beta- and epsilon-end-groups. Arch Biochem Biophys. 2010 Jan 15;493:169-74.

41. Dachtler M, Glaser T, Kohler K, Albert K. Combined HPLC-MS and HPLC-NMR on-line coupling for the separation and determination of lutein and zeaxanthin stereoisomers in spinach and in retina. Analytical chemistry. 2001 Feb 1;73:667-74.

42. Wang XD. Biological Activities of Carotenoid Metabolites. In: Britton G, Liaaen-Jensen, S., Pfander, H., editor. Carotenoids Volume 5: Nutrition and Health. Basel: Birkhäuser Verlag; 2009. p. 383-408.

43. von Lintig J, Wyss A. Molecular analysis of vitamin A formation: cloning and characterization of beta-carotene 15,15'-dioxygenases. Arch Biochem Biophys. 2001 Jan 1;385:47-52.

44. Kloer DP, Schulz GE. Structural and biological aspects of carotenoid cleavage. Cell Mol Life Sci. 2006 Oct;63:2291-303.

45. Bone RA, Landrum JT. Dose-dependent response of serum lutein and macular pigment optical density to supplementation with lutein esters. Arch Biochem Biophys. 2010 Jun 22.

46. Bone RA, Landrum JT, Guerra LH, Ruiz CA. Lutein and zeaxanthin dietary supplements raise macular pigment density and serum concentrations of these carotenoids in humans. J Nutr. 2003 Apr;133:992-8.

47. Lietz G, Lange J, Rimbach G. Molecular and dietary regulation of beta,beta-carotene 15,15'-monooxygenase 1 (BCMO1). Arch Biochem Biophys. 2010 Jul 1.

48. National Academy of Sciences IoM, Food and Nutrition Board, Panel on Dietary Antioxidants and Related Compounds. Dietary Reference Intakes for Vitamin C, Vitamin E, Selenium, and Carotenoids. Washington, D.C.: National Academy Press; 2000.

49. Monod J, Changeux JP, Jacob F. Allosteric proteins and cellular control systems. Journal of molecular biology. 1963 Apr;6:306-29.

50. Rogers AaG, Y. Enzyme Kinetics: Theory and Practice. In: Schwender J, editor. Plant Metabolic Networks. New York: Springer; 2009. p. 98-100.

51. Bouvier F, Isner JC, Dogbo O, Camara B. Oxidative tailoring of carotenoids: a prospect towards novel functions in plants. Trends in plant science. 2005 Apr;10:187-94.

52. Cooper CM, Davies NW, Menary RC. C-27 apocarotenoids in the flowers of Boronia megastigma (Nees). J Agric Food Chem. 2003 Apr 9;51:2384-9.

53. Cooper CM, Davies NW, Menary RC. Changes in some carotenoids and apocarotenoids during flower development in Boronia megastigma (Nees). J Agric Food Chem. 2009 Feb 25;57:1513-20.

54. al-Hasani SM, Parrish DB. Forms of vitamin A and of carotenoids in tissues, blood serum and yolk of eggs from Cotournix coturnix japonica fed -apo-carotenals. J Nutr. 1972 Nov;102:1437-40.

55. Zaripheh S, Boileau TW, Lila MA, Erdman JW, Jr. [14C]-lycopene and [14C]-labeled polar products are differentially distributed in tissues of F344 rats prefed lycopene. J Nutr. 2003 Dec;133:4189-95.

56. Suzuki T, Matsui M, Murayama A. Biological activity of (all-E)-beta-apo-12'-carotenoic acid and the geometrical isomers on human acute promyelocytic leukemia cell line HL-60. Journal of nutritional science and vitaminology. 1995 Dec;41:575-85.

57. Tibaduiza EC, Fleet JC, Russell RM, Krinsky NI. Excentric cleavage products of beta-carotene inhibit estrogen receptor positive and negative breast tumor cell growth in vitro and inhibit activator protein-1-mediated transcriptional activation. J Nutr. 2002 Jun;132:1368-75.

58. Prakash P, Liu C, Hu KQ, Krinsky NI, Russell RM, Wang XD. Beta-carotene and beta-apo-14'-carotenoic acid prevent the reduction of retinoic acid receptor beta in benzo[a]pyrene-treated normal human bronchial epithelial cells. J Nutr. 2004 Mar;134:667-73.

59. Winum JY, Kamal M, Defacque H, Commes T, Chavis C, Lucas M, Marti J, Montero JL. Synthesis and biological activities of higher homologues of retinoic acid. Farmaco. 1997 Jan;52:39-42.

60. Ziouzenkova O, Orasanu G, Sukhova G, Lau E, Berger JP, Tang G, Krinsky NI, Dolnikowski GG, Plutzky J. Asymmetric cleavage of beta-carotene yields a transcriptional repressor of retinoid X receptor and peroxisome proliferator-activated receptor responses. Molecular endocrinology (Baltimore, Md. 2007 Jan;21:77-88.

61. Duncan RE, Lau D, El-Sohemy A, Archer MC. Geraniol and beta-ionone inhibit proliferation, cell cycle progression, and cyclin-dependent kinase 2 activity in MCF-7 breast cancer cells independent of effects on HMG-CoA reductase activity. Biochemical pharmacology. 2004 Nov 1;68:1739-47.

62. Liu J, Li B, Ma R, Chen B. [Inhibitory effect on mammary carcinoma cells induced by beta-ionone]. Wei sheng yan jiu = Journal of hygiene research. 2004 Mar;33:151-3, 7.

63. Liu JR, Chen BQ, Yang BF, Dong HW, Sun CH, Wang Q, Song G, Song YQ. Apoptosis of human gastric adenocarcinoma cells induced by beta-ionone. World J Gastroenterol. 2004 Feb 1;10:348-51.

64. Mo H, Elson CE. Apoptosis and cell-cycle arrest in human and murine tumor cells are initiated by isoprenoids. J Nutr. 1999 Apr;129:804-13.

65. Liu JR, Sun XR, Dong HW, Sun CH, Sun WG, Chen BQ, Song YQ, Yang BF. beta-Ionone suppresses mammary carcinogenesis, proliferative activity and induces apoptosis in the mammary gland of the Sprague-Dawley rat. International journal of cancer. 2008 Jun 15;122:2689-98.

66. Aoki K, Takimoto M, Ota H, Yoshida T. Participation of CYP2A in cocaine-induced hepatotoxicity in female mice. Pharmacology & toxicology. 2000 Jul;87:26-32.

67. Jeong TC, Kim HJ, Yun CH, Lee SS, Yang KH, Han SS, Roh JK. Induction of liver cytochrome P450 2B1 by beta-ionone in Sprague Dawley rats. Biochem Biophys Res Commun. 1995 Nov 2;216:198-202.

68. Liu JR, Dong HW, Sun XR, Wang Q, Sun WG, Parry JW, Liu Q, Han XH, Sun CH, et al. Effects of beta-ionone on mammary carcinogenesis and antioxidant status in rats treated with DMBA. Nutr Cancer. 2010;62:58-65.

69. Lian F, Hu KQ, Russell RM, Wang XD. Beta-cryptoxanthin suppresses the growth of immortalized human bronchial epithelial cells and non-small-cell lung cancer cells and up-regulates retinoic acid receptor beta expression. International journal of cancer. 2006 Nov 1;119:2084-9.

70. Matsumoto A, Mizukami H, Mizuno S, Umegaki K, Nishikawa J, Shudo K, Kagechika H, Inoue M. beta-Cryptoxanthin, a novel natural RAR ligand, induces ATP-

binding cassette transporters in macrophages. Biochemical pharmacology. 2007 Jul 15;74:256-64.

71. Lindqvist A, Andersson S. Cell type-specific expression of beta-carotene 15,15'-mono-oxygenase in human tissues. J Histochem Cytochem. 2004 Apr;52:491-9.

72. Lindqvist A, He YG, Andersson S. Cell type-specific expression of beta-carotene 9',10'-monooxygenase in human tissues. J Histochem Cytochem. 2005 Nov;53:1403-12.

73. Bhatti RA, Yu S, Boulanger A, Fariss RN, Guo Y, Bernstein SL, Gentleman S, Redmond TM. Expression of beta-carotene 15,15' monooxygenase in retina and RPE-choroid. Investigative ophthalmology & visual science. 2003 Jan;44:44-9.

74. Chichili GR, Nohr D, Schaffer M, von Lintig J, Biesalski HK. beta-Carotene conversion into vitamin A in human retinal pigment epithelial cells. Investigative ophthalmology & visual science. 2005 Oct;46:3562-9.

75. Moiseyev G, Takahashi Y, Chen Y, Gentleman S, Redmond TM, Crouch RK, Ma JX. RPE65 is an iron(II)-dependent isomerohydrolase in the retinoid visual cycle. The Journal of biological chemistry. 2006 Feb 3;281:2835-40.

76. Voolstra O, Oberhauser V, Sumser E, Meyer NE, Maguire ME, Huber A, von Lintig J. NinaB is essential for Drosophila vision but induces retinal degeneration in opsin-deficient photoreceptors. The Journal of biological chemistry. 2010 Jan 15;285:2130-9.

77. Khachik F, de Moura FF, Zhao DY, Aebischer CP, Bernstein PS. Transformations of selected carotenoids in plasma, liver, and ocular tissues of humans and in nonprimate animal models. Investigative ophthalmology & visual science. 2002 Nov;43:3383-92.

78. Prasain JK, Moore R, Hurst JS, Barnes S, van Kuijk FJ. Electrospray tandem mass spectrometric analysis of zeaxanthin and its oxidation products. J Mass Spectrom. 2005 Jul;40:916-23.

79. Kalariya NM, Ramana KV, Srivastava SK, van Kuijk FJ. Carotenoid derived aldehydes-induced oxidative stress causes apoptotic cell death in human retinal pigment epithelial cells. Experimental eye research. 2008 Jan;86:70-80.

80. Bhosale P, Bernstein PS. Vertebrate and invertebrate carotenoid-binding proteins. Arch Biochem Biophys. 2007 Feb 15;458:121-7.

81. Loane E, Nolan JM, O'Donovan O, Bhosale P, Bernstein PS, Beatty S. Transport and retinal capture of lutein and zeaxanthin with reference to age-related macular degeneration. Survey of ophthalmology. 2008 Jan-Feb;53:68-81.

82. Siems W, Wiswedel I, Salerno C, Crifo C, Augustin W, Schild L, Langhans CD, Sommerburg O. Beta-carotene breakdown products may impair mitochondrial functions--potential side effects of high-dose beta-carotene supplementation. The Journal of Nutritional Biochemistry. 2005 Jul;16:385-97.

83. Liu C, Russell RM, Wang XD. Exposing ferrets to cigarette smoke and a pharmacological dose of beta-carotene supplementation enhance in vitro retinoic acid catabolism in lungs via induction of cytochrome P450 enzymes. J Nutr. 2003 Jan;133:173-9.

84. Veeramachaneni S, Ausman LM, Choi SW, Russell RM, Wang XD. High dose lycopene supplementation increases hepatic cytochrome P4502E1 protein and inflammation in alcohol-fed rats. J Nutr. 2008 Jul;138:1329-35.

85. Wang XD, Liu C, Bronson RT, Smith DE, Krinsky NI, Russell M. Retinoid signaling and activator protein-1 expression in ferrets given beta-carotene supplements and exposed to tobacco smoke. J Natl Cancer Inst. 1999 Jan 6;91:60-6.

Figure Legends

Figure 1. Expression of ferret CMO2 in Sf9 insect cells. Ferret CMO2 was expressed in Sf9 insect cells using a baculovirus system as described under "Experimental Procedures." The cell lysates from uninfected (lane 1) and ferret CMO2 baculovirus-infected (lane 2) insect cells were boiled in reducing sample buffer and subjected to 10% SDS-PAGE. The protein expression was detected by Coomassie Blue stain (A) and by detection with a CMO2-specific polyclonal antibody after transfer to a polyvinylidene difluoride membrane (B).

Figure 2. Identification of cleavage products from zeaxanthin by HPLC and LC-MS analysis. Zeaxanthin (20 μM) was incubated with the homogenates from either uninfected (A) or ferret CMO2-baculovirus infected (B) insect cells for 30 min. at 37°C as described in "Experimental Procedures". The cleavage products were extracted from the incubation mixture and separated by reverse-phase HPLC using a C_{18} column. Peaks corresponding to the authentic 3-OH-β-apo-10'-carotenal standard (C) were detected at 450 nm only in the incubation mixture with the homogenates of ferret CMO2-baculovirus infected cells (B), but not in that of the uninfected cells (A). D, spectral analysis of the cleavage product (blue line) of zeaxanthin vs. 3-OH-β-apo-10'-carotenal standard (red line). Both the RT and absorption spectrum of the product matched exactly with that of the 3-OH-β-

apo-10'-carotenal standard. LC-MS analysis (E) of the cleavage product showed a base peak of *m/z* 393, which corresponds to the protonated molecule $(M+H)^+$ of the authentic 3-OH-β-apo-10'-carotenal standard.

Figure 3. Identification of volatile cleavage products from zeaxanthin and lutein by HPLC and GC-MS analysis. Zeaxanthin (20 μM) and Lutein (20 μM) were incubated with homogenates from either uninfected (A and C) or ferret CMO2-baculovirus infected (B and D) insect cell lysates for 30 min. at 37°C as described in "Experimental Procedures". The cleavage products were extracted from the incubation mixture and separated by reverse-phase HPLC using a C_{18} column. Unknown reaction products 1 and 2 were detected at 296 nm only in the incubation mixtures with ferret CMO2-baculovirus infected cells (B and D) but not in that of the uninfected cells (A and C). Spectral analysis of reaction products 1 (E) and 2 (F) indicated the presence of ionone compounds. GC-MS analysis of reactions product 1 (B) from zeaxanthin cleavage indicated the presence of 3-OH-β-ionone (G) and GC-MS analysis of reaction product 2 (C) from lutein cleavage indicated the presence of both 3-OH-βionone (G) and 3'-OH-α-ionone (H). The EI mass spectra were matched to previously published spectra (38, 39).

Figure 4. Identification of cleavage products from lutein by HPLC and LC-MS analysis. Lutein (20 μM) was incubated with the homogenates from either uninfected (A) or ferret CMO2-baculovirus infected (B) insect cells for 30 min. at 37°C as described in "Experimental Procedures". The cleavage products were extracted from the incubation mixture and separated by reverse-phase HPLC using a C_{18} column. Two reaction

products (1 and 2) were detected at 450 nm only in the incubation mixture with the homogenates of ferret CMO2-baculovirus infected cells (B), but not in that of the uninfected cells (A). D, spectral analysis of the cleavage products (blue line, 1 and 2) of lutein vs. 3-OH-β-apo-10'-carotenal standard (red line). Both the RT and absorption spectrum of the peak 2 matched exactly with that of the 3-OH-β-apo-10'-carotenal standard (C). LC-MS analysis (E) of peak 1 displayed a base peak of *m/z* 375, corresponding to the $(M+H-H_2O)^+$ ion of the 3'-OH-α-apo-10-carotenal product, while peak 2 (F) displayed a base peak of *m/z* 393, which corresponds to the $(M+H)^+$ ion of the authentic 3-OH-β-apo-10'-carotenal standard.

Figure 5. Identification of cleavage products from β-cryptoxanthin by HPLC and LC-MS analysis. β-Cryptoxanthin (100 μM) was incubated with the homogenates from either uninfected (A) or ferret CMO2-baculovirus infected (B) insect cells for 30 min. at 37°C as described in "Experimental Procedures". The cleavage products were extracted from the incubation mixture and separated by reverse-phase HPLC using a C_{18} column. Two reaction products (1 and 2) were detected at 450 nm in the incubation mixture containing ferret CMO2-baculovirus infected cell homogenate (B) but not the uninfected SF9 cell homogenate (A). D and E, spectral analysis of the cleavage products (blue line, 1 and 2) of β-cryptoxanthin vs. 3-OH-β-apo-10'-carotenal standard (red line, D) and β-apo-10'-carotenal standard (red line, E). Both the RT and absorption spectrum of reaction product 1 and 2 matched exactly with that of the 3-OH-β-apo-10'-carotenal and β-apo-10'-carotenal standard (C), respectively. LC-MS analysis (F) of peak 1 displayed a base peak of *m/z* 393, corresponding to $(M+H)^+$ 3-OH-β-apo-10-carotenal product,

while peak 2 (G) displayed a base peak of *m/z* 377, which corresponds to the $(M+H)^+$ of the authentic β-apo-10'-carotenal standard.

Figure 6. Identification of volatile cleavage products from β-cryptoxanthin by HPLC and GC-MS analysis. β-Cryptoxanthin (100 μM) was incubated with homogenates from either uninfected (A) or ferret CMO2-baculovirus infected (B) insect cell lysates for 30 min. at 37°C as described in "Experimental Procedures". The cleavage products were extracted from the incubation mixture and separated by reverse-phase HPLC using a C_{18} column. Unknown reaction products 1 and 2 were detected at 296 nm only in the incubation mixtures with ferret CMO2-baculovirus infected cells (B) but not in that of the uninfected cells (A). Spectral analysis of reaction products 1 (D) and 2 (E), which matched in retention time and absorption spectra of the β-ionone standard, indicated the presence of ionone compounds. GC-MS analysis of reactions product 1 from β-cryptoxanthin cleavage indicated the presence of 3-OH-β-ionone (F) and analysis of reaction product 2 indicated the presence of β-ionone (G). The EI mass spectra were matched to spectra found in literature (38, 39).

Figure 7. Protein- and time-dependent cleavage of β-cryptoxanthin by ferret carotene-9', 10'-oxygenase (CMO2). Reaction velocity as a function of protein concentration (A and C) and time (B and D) is plotted for both β-apo-10'-carotenal and 3-OH-β-apo-10'-carotenal formation. For protein-dependent cleavage, β-cryptoxanthin (50 μM) was incubated with various protein concentrations of cell homogenates expressing ferret CMO2 at 37 °C for 60 min. For time-dependent formation, β-cryptoxanthin (50 μM) was

incubated with ~2 mg of homogenate expressing ferret CMO2 at 37 °C for various time points. Data are the average of two independent experiments performed in duplicate.

Figure 8. Protein- and time-dependent cleavage of zeaxanthin and lutein by ferret carotene-9', 10'-oxygenase (CMO2). Reaction velocity as a function of protein concentration (A) and time (B) is plotted for 3-OH-β-apo-10'-carotenal formation from zeaxanthin cleavage by CMO2. Reaction velocity as a function of protein and time is plotted for 3'-OH-α-apo-10-carotenal (C and D) and 3-OH-β-apo-10'-cartenal (E and F) formation from lutein cleavage by CMO2. For protein-dependent cleavage, zeaxanthin (50 μM) and lutein (50 μM) were incubated with various protein concentrations of cell homogenates expressing ferret CMO2 at 37 °C for 60 min. For time-dependent formation, zeaxanthin (50 μM) and lutein (50 μM) was incubated with ~2 mg of homogenate expressing ferret CMO2 at 37 °C for various time points. Data are the average of two independent experiments performed in duplicate.

Figure 9. *In vitro* kinetic analysis of recombinant ferret CMO2 with carotenoids as substrates. Reaction velocity (pmol product formed/mg/min) as a function of substrate concentration (μM) is plotted for a 30-min reaction with 2 mg of crude lysates of recombinant ferret CMO2 containing 0 – 200 μM zeaxanthin (A) and 0 – 225 μM lutein (B). Structures and estimated relative kinetic constants for zeaxanthin, lutein and β-cryptoxanthin are compared (C). Product quantification was performed by reverse-phase HPLC analysis as described under "Experimental Procedures." These data are the average of four independent experiments performed in duplicate.

Figure 10. 3-OH-β-apo-10'-carotenoic acid is generated from incubation of 3-OH-β-apo-10'-carotenal with ferret liver lysates and NAD^+. Incubation of 3-OH-β-apo-10'-carotenal (10 μM) with ferret liver lysate (1 mg) and NAD^+ (3 mM) resulted in the formation of new peak (B, peak 1), which was not present when incubated without NAD^+ (A). In the presence of the aldehyde dehydrogenase inhibitor citral (1 mM), formation was inhibited (C). *Inset:* spectral anaylsis of oxidation product with UV_{max} of 416. MS analysis (D) identified base peaks of *m/z* 409 and *m/z* 391, corresponding to the protonated ion of the parent compound and loss of water, indicating the presence of 3-OH-β-apo-10'-carotenoic acid.

Figure 11. Metabolism of Hydroxy-Carotenoids by Ferret Carotene-9',10'-Oygenase (CMO2). Enzymatic cleavage of zeaxanthin (A), lutein (B) and β-cryptoxanthin (C) by ferret CMO2.

Figure 1.

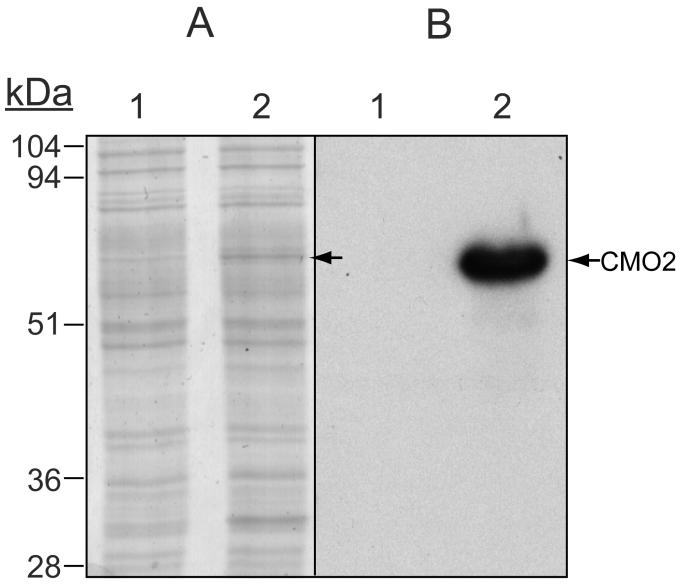

Figure 2.

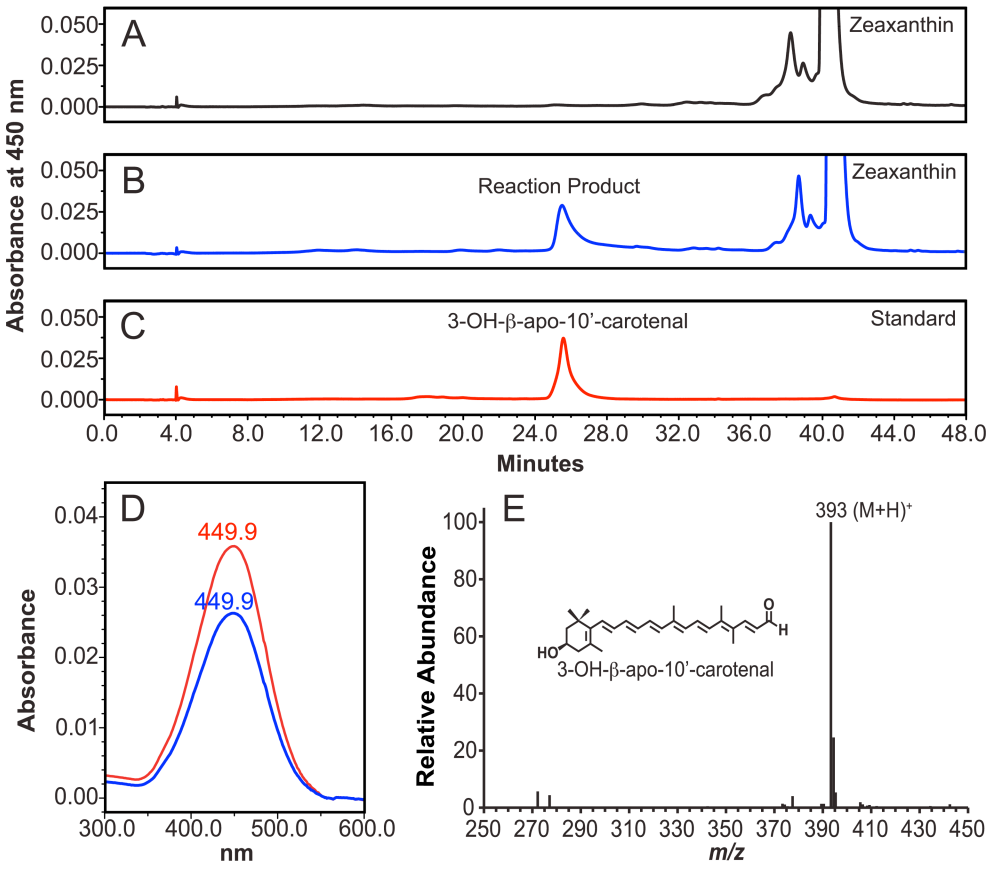
A
Zeaxanthin
B
Reaction Product
Zeaxanthin
C
3-OH-β-apo-10'-carotenal
Standard
Absorbance at 450 nm
0.050
0.025
0.000
0.0 4.0 8.0 12.0 16.0 20.0 24.0 28.0 32.0 36.0 40.0 44.0 48.0
Minutes
D
449.9
449.9
Absorbance
0.04
0.03
0.02
0.01
0.00
300.0 400.0 500.0 600.0
nm
E
393 (M+H)+
Relative Abundance
100
80
60
40
20
0
HO
O
H
3-OH-β-apo-10'-carotenal
250 270 290 310 330 350 370 390 410 430 450
m/z

Figure 3.

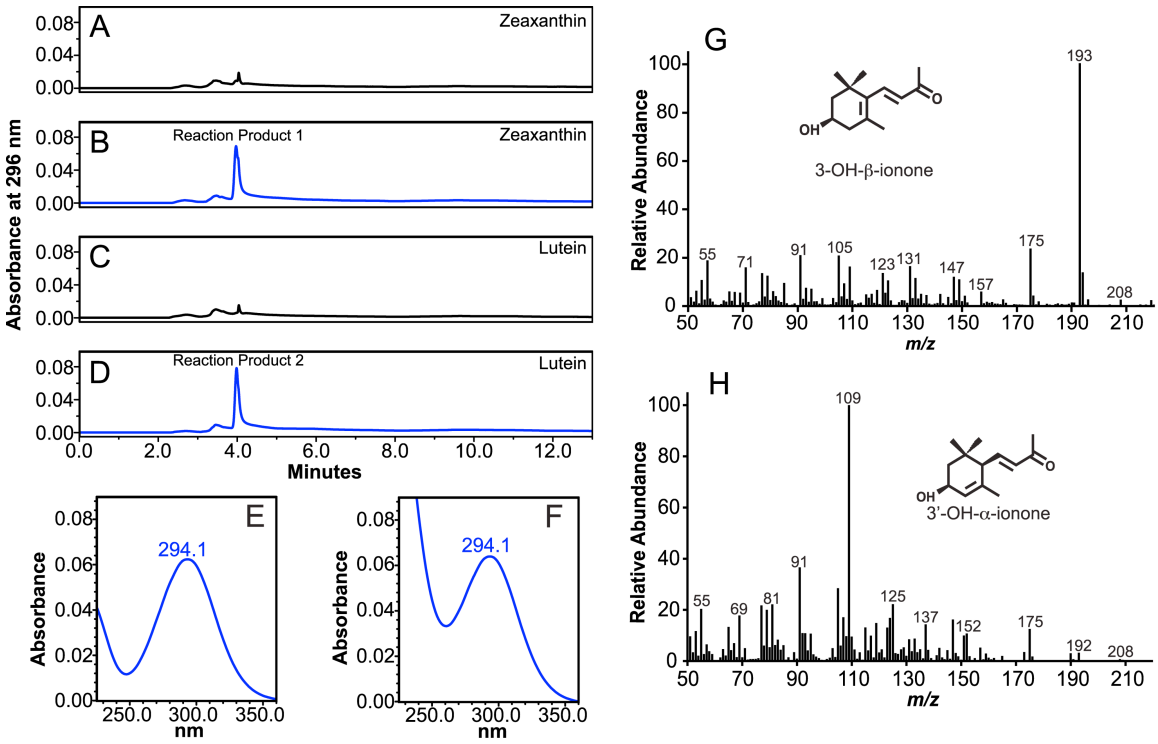
A
Zeaxanthin
B
Reaction Product 1
Zeaxanthin
C
Lutein
D
Reaction Product 2
Lutein
Absorbance at 296 nm
Minutes
E
294.1
F
294.1
Absorbance
nm
G
3-OH-β-ionone
Relative Abundance
m/z
H
3'-OH-α-ionone
Relative Abundance
m/z

Figure 4.

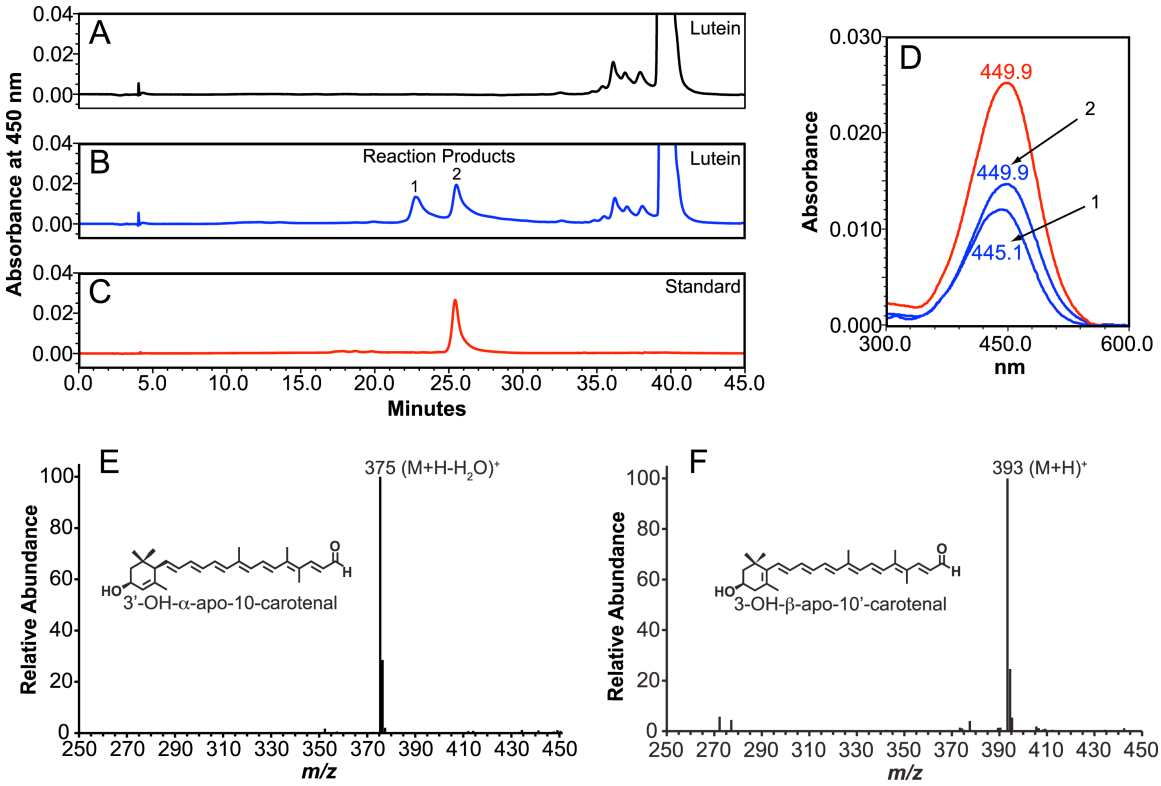
A
Lutein
B
Reaction Products
Lutein
1
2
C
Standard
Absorbance at 450 nm
Minutes
D
449.9
2
449.9
1
445.1
Absorbance
nm
E
375 (M+H-H2O)+
3'-OH-α-apo-10-carotenal
Relative Abundance
m/z
F
393 (M+H)+
3-OH-β-apo-10'-carotenal
Relative Abundance
m/z

Figure 5.

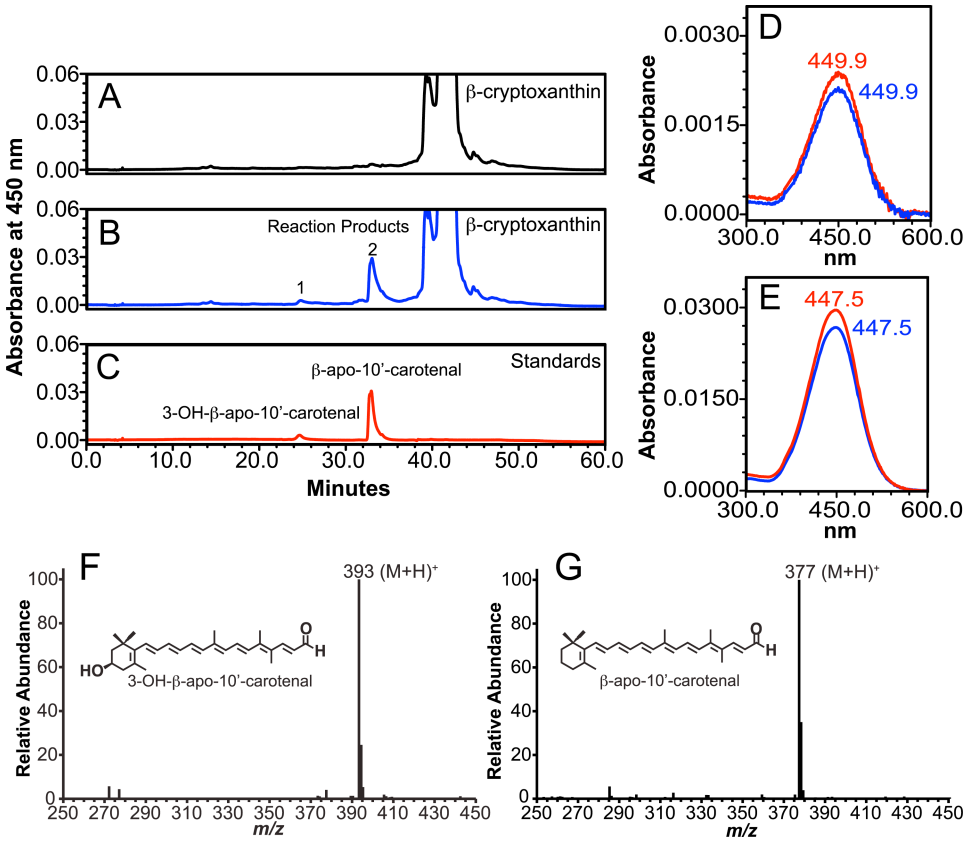
A
β-cryptoxanthin
B
Reaction Products
β-cryptoxanthin
1
2
C
β-apo-10'-carotenal
Standards
3-OH-β-apo-10'-carotenal
Absorbance at 450 nm
Minutes
D
449.9
449.9
Absorbance
nm
E
447.5
447.5
Absorbance
nm
F
393 (M+H)+
3-OH-β-apo-10'-carotenal
Relative Abundance
m/z
G
377 (M+H)+
β-apo-10'-carotenal
Relative Abundance
m/z

Figure 6.

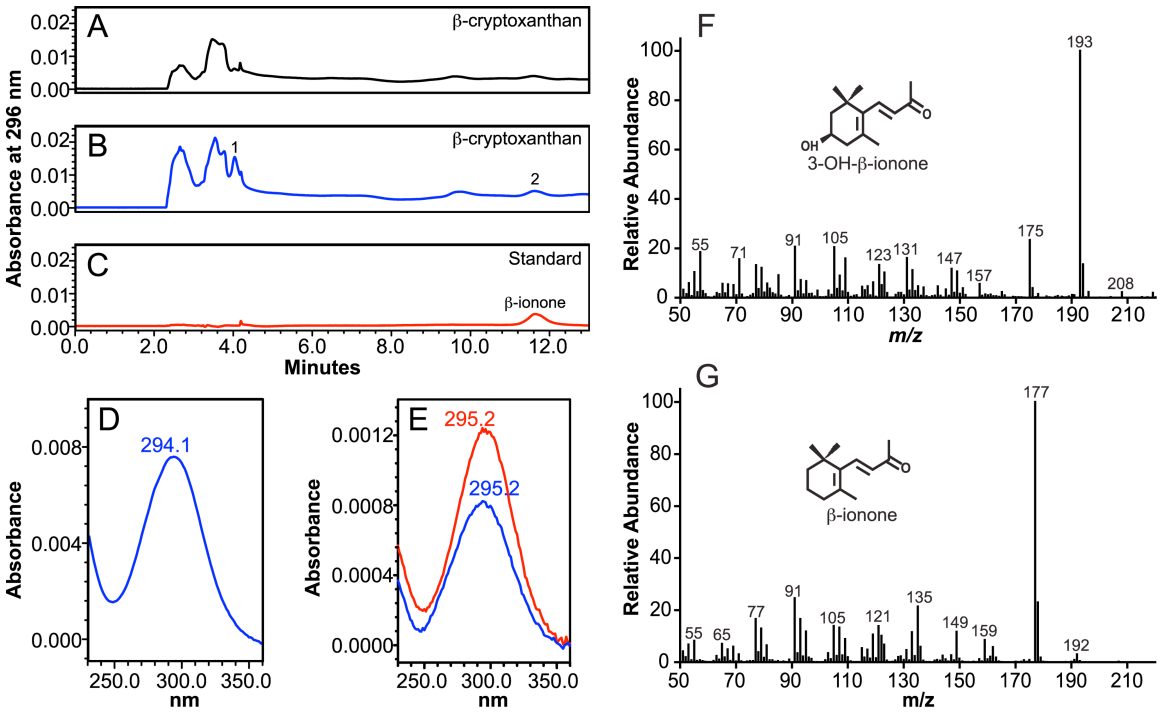
A
β-cryptoxanthan
B
β-cryptoxanthan
1
2
C
Standard
β-ionone
Absorbance at 296 nm
Minutes
D
294.1
Absorbance
nm
E
295.2
295.2
Absorbance
nm
F
3-OH-β-ionone
Relative Abundance
m/z
193
175
208
G
β-ionone
Relative Abundance
m/z
177
192

Figure 7.

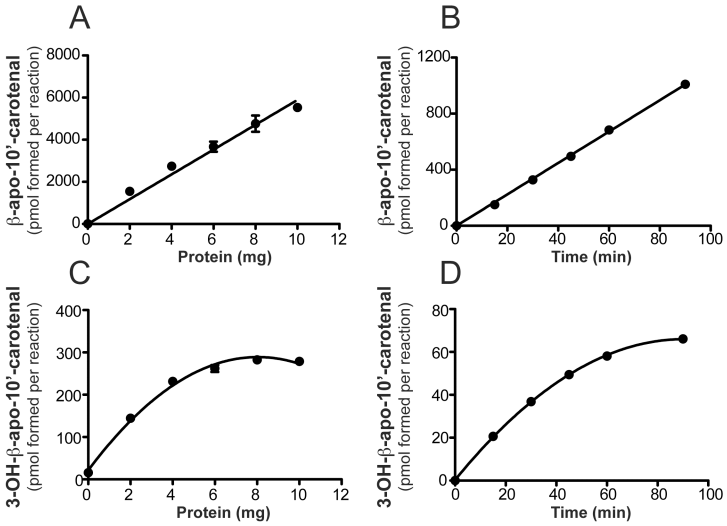
A
β-apo-10'-carotenal
(pmol formed per reaction)
8000
6000
4000
2000
0
0 2 4 6 8 10 12
Protein (mg)
B
β-apo-10'-carotenal
(pmol formed per reaction)
1200
800
400
0
0 20 40 60 80 100
Time (min)
C
3-OH-β-apo-10'-carotenal
(pmol formed per reaction)
400
300
200
100
0
0 2 4 6 8 10 12
Protein (mg)
D
3-OH-β-apo-10'-carotenal
(pmol formed per reaction)
80
60
40
20
0
0 20 40 60 80 100
Time (min)

Figure 8.

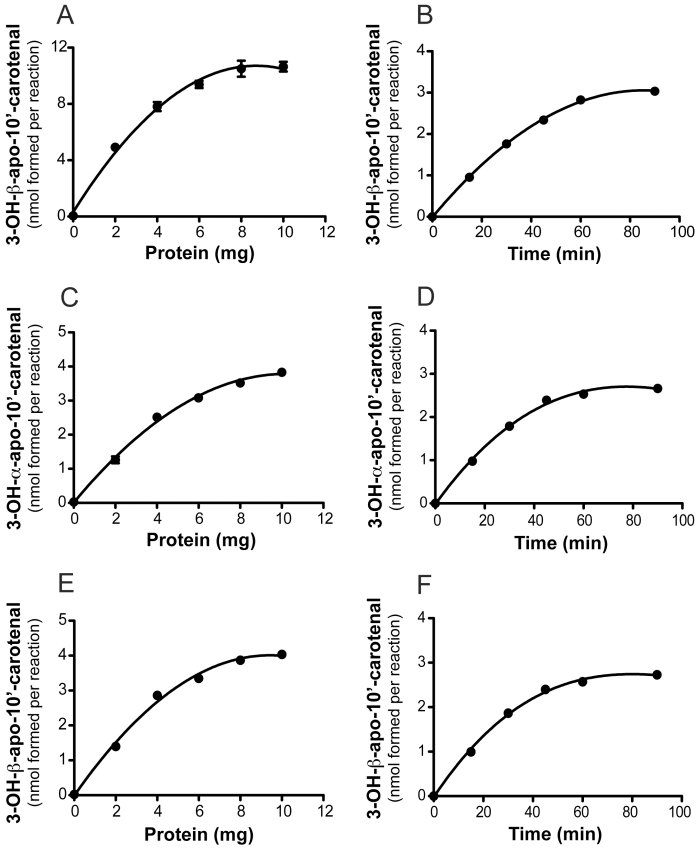
A
B
C
D
E
F
3-OH-β-apo-10'-carotenal
3-OH-α-apo-10'-carotenal
(nmol formed per reaction)
Protein (mg)
Time (min)

Figure 9.

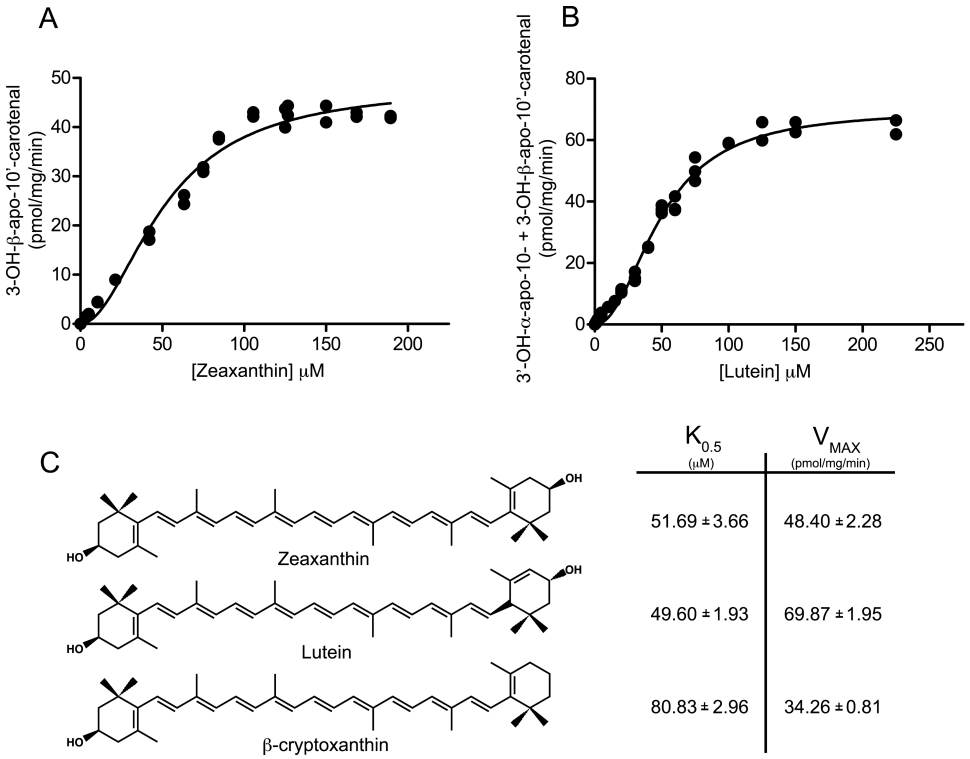

	$K_{0.5}$ (μM)	V_{MAX} (pmol/mg/min)
Zeaxanthin	51.69 ± 3.66	48.40 ± 2.28
Lutein	49.60 ± 1.93	69.87 ± 1.95
β-cryptoxanthin	80.83 ± 2.96	34.26 ± 0.81

Figure 10.

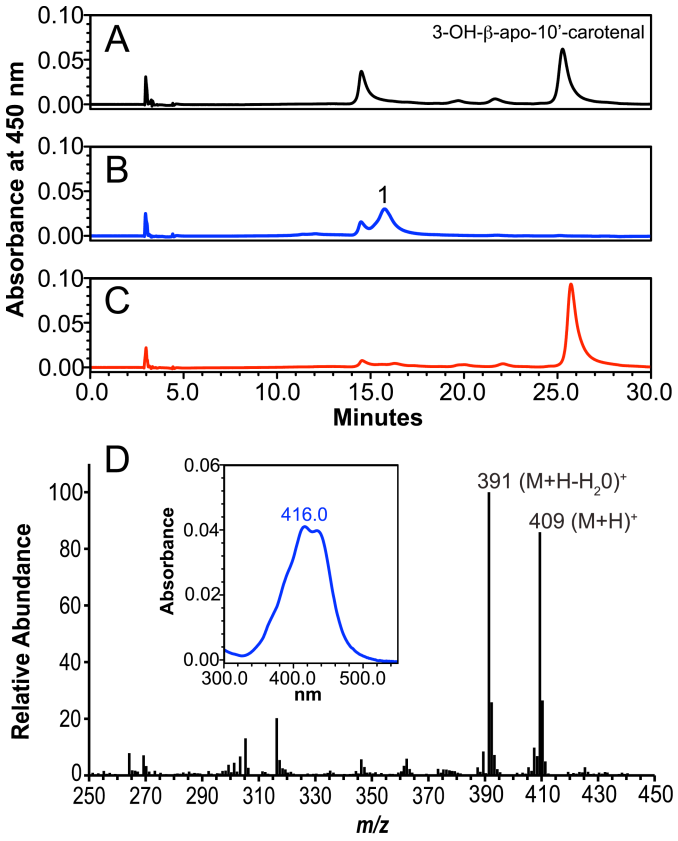
A
3-OH-β-apo-10'-carotenal
B
1
C
Absorbance at 450 nm
0.10
0.05
0.00
0.0
5.0
10.0
15.0
20.0
25.0
30.0
Minutes
D
Relative Abundance
100
80
60
40
20
0
250
270
290
310
330
350
370
390
410
430
450
m/z
391 (M+H-H2O)+
409 (M+H)+
Absorbance
0.06
0.04
0.02
0.00
416.0
300.0
400.0
500.0
nm

Figure 11.

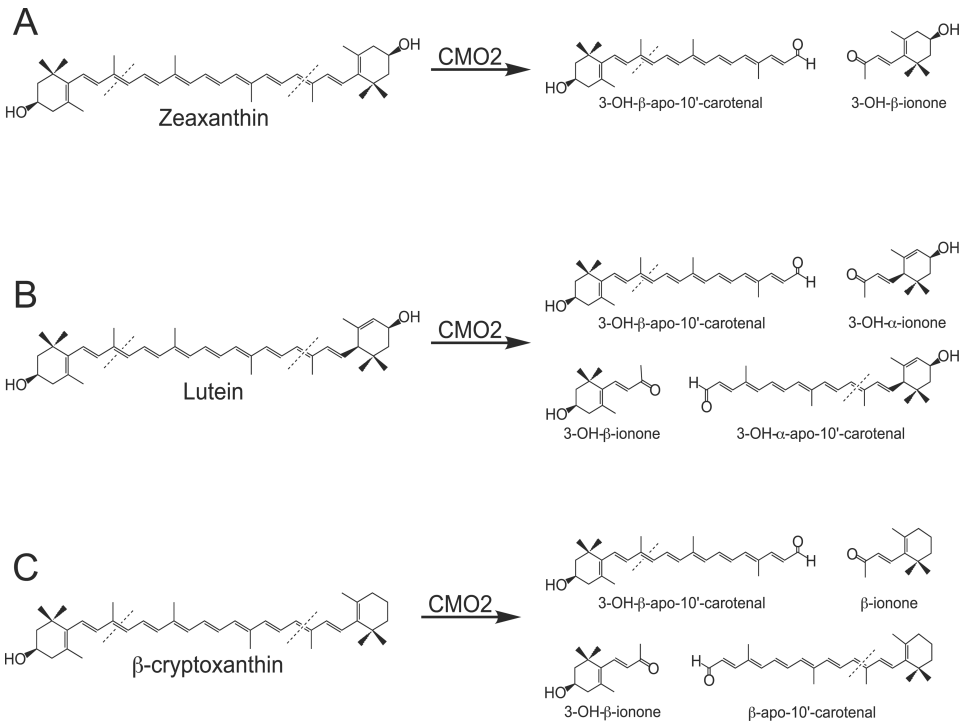
A
Zeaxanthin
CMO2
3-OH-β-apo-10'-carotenal
3-OH-β-ionone
B
Lutein
CMO2
3-OH-β-apo-10'-carotenal
3-OH-α-ionone
3-OH-β-ionone
3-OH-α-apo-10'-carotenal
C
β-cryptoxanthin
CMO2
3-OH-β-apo-10'-carotenal
β-ionone
3-OH-β-ionone
β-apo-10'-carotenal

Chapter 5.

Carotene-15,15'-Monooxygenase (CMO1) and Carotene-9',10'Monooxygenase (CMO2) are differentially expressed in ferret tissues and can be regulated by β-cryptoxanthin supplementation *in vivo*.

ABSTRACT

Several well-implemented cohort studies have shown blood levels and dietary intake of β-cryptoxanthin to be strongly associated with a decreased risk of lung cancer independent of vitamin A. This has raised an important question as to whether the protective effect of β-cryptoxanthin, a provitamin A carotenoid, is due to the intact molecule or from apo-carotenoid metabolites formed via enzymatic cleavage. The objective of this study was assess the regulation of carotene cleavage oxygenase enzyme (β,β-carotene-15,15'-monooxygenase (CMO1) and carotene-9',10'-monooxygenase (CMO2)) expression in selected ferret tissues in response to varying doses of β-cryptoxanthin supplementation. Using the ferret, an animal model that mimics human carotenoid metabolism, we first partially cloned the ferret CMO1 gene and compared the relative abundance of CMO1 and CMO2 expression in various tissues. Tissue-specific comparisons revealed significant differences in expression levels of CMO1 and CMO2. CMO1 expression was significantly higher in the intestinal mucosa while CMO2 expression was significantly higher in the lungs, visceral adipose and kidneys compared to CMO1. Low-dose (7.5 μg/kg body weight per day, n = 6) and high-dose (37.5 μg/kg body weight per day, n = 6) β-cryptoxanthin supplementation for 9 weeks resulted in a dose-dependent increase in β-cryptoxanthin concentrations with no changes in retinyl palmitate in the lungs and other selected tissues. Interestingly, there was a significant decrease in lung CMO2 expression in both low- and high-dose supplementation groups with little changes in CMO1 or CMO2 expression in other tissues. In summary, the abundance of CMO2 expression in the lungs and down-regulation by β-cryptoxanthin

supplementation indicates a potential role of CMO2 in the biological activity of β-cryptoxanthin in human health.

INTRODUCTION

Consumption of fruits and vegetables, especially those rich in carotenoids, has been associated with a reduced risk of a variety of degenerative and chronic diseases, including age-related macular degeneration (1), cardiovascular disease (2) and several cancers (3). Carotenoids are a class of lipophilic compounds with a polyisoprenoid structure found in various fruits and vegetables. There are six major carotenoids that are routinely found in human plasma and tissues (4, 5). Among individual carotenoids, β-cryptoxanthin has demonstrated a strong association with a decreased risk of lung cancer (6, 7). In a pooled analysis of seven large cohort studies in North America and Europe involving 3,155 incident lung cancer cases, β-cryptoxanthin was the only dietary carotenoid associated with a significant decrease in lung cancer risk (RR = 0.76; CI 0.67 – 0.86, highest *vs.* lowest quintile) (8). More recently, dietary intake of β-cryptoxanthin was shown to be significantly associated with a reduced lung cancer risk (RR=0.80, CI 0.72 – 0.89, highest *vs.* lowest quintile) (9). This association remained independent of other provitamin A carotenoids, such as β-carotene, and vitamin A status, suggesting the protective effect of β-cryptoxanthin may be mediated thru metabolic pathways other than vitamin A. While a number of biological functions have been attributed to carotenoids (10), the metabolic pathways involved in carotenoid metabolism are now beginning to be fully investigated, especially for carotenoids other than β-carotene.

Carotenoid cleavage oxygenases (CCOs) represent an ancient family of enzymes with members present in all taxa. In animals, three CCOs have been isolated: carotene-15,15-monooxygenase (CMO1) (11, 12), carotene-9',10'-monooxygenase (CMO2) (13, 14), and the retinoid isomerase retinal pigment epithelium 65 (RPE65) (15, 16). CMO1 cleaves provitamin A carotenoids symmetrically at the 15,15' double bond (11, 17) and is involved in the formation of vitamin A *in vivo* (18). CMO2 excentrically cleaves β-carotene, lycopene and the xanthophylls at the 9', 10'double bond producing apo-10'-carotenoids, apo-10'-lycopenoids and 3-OH-β-apo-carotenoids (13, 14) (Mein et al, Submitted). While both CMO1 and CMO2 enzymatically cleave carotenoids into important apo-carotenoid products, the regulatory mechanisms underlying CMO1 and CMO2 expression remain poorly understood.

Unlike vitamin A, high-dose β-carotene supplementation in humans does not result in hypervitaminosis A or teratogenicity (19), indicating cleavage of β-carotene to vitamin A is tightly regulated. Previous studies have indicated feedback inhibition of CMO1 expression via retinoic acid formation (20, 21), which is the end product of CMO1 activity on β-carotene. The molecular mechanisms and role of retinoic acid in regulation of intestinal CMO1 has recently been clarified (22-24). Retinoic acid, via RARs, induces expression of the intestine specific homeobox transcription factor (ISX), which in turn represses expression of both CMO1 and the scavenger receptor B type 1 (SR-B1). SR-B1 plays an important role in dietary lipid absorption (25), indicating an elegant dietary responsive network controlling lipid absorption and vitamin A production. Whether CMO2 participates in a similar diet-responsive network is unknown.

The molecular regulatory mechanisms underlying CMO2 expression are far less understood. Molecular analyses have failed to identify known regulatory nuclear response elements within the mouse (26) or ferret CMO2 promoter (unpublished data). Dietary interventions have provided some evidence of potential CMO2 regulation in response to carotenoid supplementation. In ferrets supplemented with lycopene (equivalent to 60 mg/d in a 70-kg human) for 9 weeks, there was a 4-fold increase in lung CMO2 expression (13). In F344 rats, lycopene supplementation for various time points resulted in a general decrease in CMO2 expression in various tissues (26). The degree of expression change was dependent on the tissue and length of supplementation, indicating tissue-specific regulation of CMO2. Interestingly, the liver and adrenal gland contain the largest abundance of CMO2 mRNA, yet there were no changes in CMO2 expression in either of the tissues.

The ferret is an excellent animal model for studying the pathways involved in carotenoid metabolism. Unlike most rodent animal models, ferrets share many similarities with humans regarding the absorption and metabolism of intact carotenoids making them a superior model for studying carotenoid metabolism. However, studies investigating the effects of carotenoid supplementation on ferret endogenous carotenoid cleaving enzymes expression have not been fully characterized.

In the present study, we partially cloned the ferret CMO1 gene and investigated the effect of low- (equivalent to 120 μg/d in humans) and high-dose (equivalent to 520 μg/d in humans) β-cryptoxanthin supplementation on expression of the ferret endogenous carotenoid cleavage oxygenase enzymes, CMO1 and CMO2. Furthermore, we examined

the tissue distribution of β-cryptoxanthin and retinoids in response to β-cryptoxanthin supplementation.

MATERIALS AND METHODS

Animals, Diets and Study Groups.

Eighteen adult male ferrets (1.2 – 1.4 kg) were obtained from Marshall Farms (North Rose, NY) and were housed in an American Association of Accreditation of Laboratory Animal Care (AAALAC)-accredited animal facility at the U.S.D.A. Jean Mayer Human Nutrition Research Center on Aging (HNRCA) at Tufts University. Animals were housed in a room with controlled temperature (68 – 72°F), humidity (45 – 55%) and light (12 hour light-dark cycles). Animals were fed a semi-purified ferret diet containing no β-cryptoxanthin (Research Diets, Inc., New Brunswick, NJ) and provided water *ad libitum*. This semi-purified ferret diet is suitable for ferret growth. The diet contains 35.5% protein, 21% fat, 35% carbohydrate and 5% fiber. The animals were acclimatized over one week on the semi-purified diet containing no β-cryptoxanthin after which they were randomly assigned to 3 groups for nine weeks as follows: (i) control (no β-cryptoxanthin), n = 6; (ii) low β-cryptoxanthin (LBC) [7.5 μg/kg body weight per day], n = 6; (iii) high β-cryptoxanthin (HBC) [37.5 μg/kg body weight per day]. β-Cryptoxanthin (99%) (CaroteNature, Lupsingen, Switzerland) was dissolved into 1 ml corn oil and fed orally (not gavaged) to ferrets daily for 9 weeks while control animals were fed 1 ml corn oil without β-cryptoxanthin. Ferrets readily ingest corn oil. According to our previous studies, the average daily food intake of the ferret, with an average body weight of 1.3 kg, is 80 g/day. The low-dose supplementation is based upon

average U.S intakes (27) while the high-dose dose is a 5X factor of the low-dose. During the experimental period, ferret body weights were recorded weekly. After the 9-week experimental period, all ferrets were terminally exsanguinated under deep isoflurane anesthesia. Plasma and tissue samples were snap frozen in liquid nitrogen and stored at -80°C until analyzed.

PCR Cloning of Ferret CMO1.

For identification of ferret CMO1, reverse transcription PCR was carried out using three pairs of primers designed from areas of high homology between from the reported cDNA sequences of CMO1 from humans (GenBank™ accession number NM_017429) and mouse (GenBank™ accession number NM_021486). Ferret liver total RNA was used as the template for first strand cDNA synthesis. Each probe sequence was amplified using PCR. Reaction mixtures containing autoclaved water, 10X Buffer, dNTP, ferret liver cDNA, M-MLV polymerase, and designed primer pairs. PCR products were visualized for purity on 2% agarose gel electrophoresis, isolated and gel purified using High Pure PCR Product Isolation Kit (Roche Dianostics, Indianapolis, IN). Purified PCR products were subcloned into the pCR®2.1-TOPO vector. The recombinant plasmid was transformed into chemically competent TOP10 *E. coli* (Invitrogen, Carlsbad, CA), which were plated onto ampicillin-, X-Gal-, and IPTG-containing agar plates, and incubated overnight at 37 °C.

Ampicillian-resistant white colonies were isolated and grown overnight at 37 °C in LB medium. Media was collected and plasmids were isolated using the High Pure Plasmid Isolation Kit (Roche Diagnostics, Indianapolis, IN) according to manufactures

procedures. The presence, orientation and size of PCR products were confirmed by restriction analysis. Clones were sequenced using an ABI 3130XL DNA sequencer. PCR fragments were then used for further generation of PCR primers with subsequent rounds of PCR employed to obtain a partial CMO1 sequence. The 5'-end of the cDNA was prepared using the 5',3' RACE Kit, 2nd Generation (Roche Diagnostics, Indianapolis, IN) accordingly to the manufacturers protocol.

Tissue preparation and RNA analysis.

Tissues were collected and immediately frozen in liquid nitrogen and stored at -80 °C until use. The intestinal mucosa was flushed with saline, scraped and the entire mucosa was collected. Total cellular RNA was extracted using TriPure isolation reagent (Roche Applied Science, Indianapolis, IN) following the manufacturers procedures. RNA concentrations were determined spectrophotometrically at 260 nm. 260/280 ratios $\geq$ 1.80 were considered sufficient for real-time analysis. First strand cDNA synthesis was performed with M-MLV reverse transcriptase (Invitrogen) using random hexamers (Applied Biosystems) and an automated thermal cycler (MJ Research PTC-200, Bio-Rad Laboratories, Carlsbad, CA). The reaction was carried out at 25 °C for 10 min, 37 °C for 50 min, 70 °C for 15 min, and 4 °C until removed from the thermal cycler. cDNA from the liver of a control animal was used to clone CMO2.

Expressional Analysis

The mRNA levels of CMO1, CMO2 and β-actin were measured by real-time quantitative PCR after the reverse transcription of total RNA. Primers were designed using Primer

Express software version 2.0 (Applied Biosystems, Foster City, CA). The sequences for ferret CMO1 were as follows: sense 5'- ACAGCAAAAGCCCTGAAGGAA-3' and antisense 5'- GGCAGCAAAGACGTAGCGATA-3. The sequences for ferret CMO2 were as follows: sense 5'- TCCGAGGACATTTTCCCAAGT3' and antisense 5'- CCAGCGTGCCAAATTCTGA-3'. The sequenes for β-actin were as follows: sense 5'- TCATCACCATCGGCAACGA-3' and antisense 5'- CCACGTCACACTTCATGATGGA-3'. Real-time PCR reactions were performed on an Applied Biosystems 7000 sequence detection system using Platinum SYBR Green qPCR Kit (Invitrogen) according to the manufacturer's procedures. The mRNA levels of the measured genes relative to β-actin mRNA were determined using the $2^{-\Delta\Delta CT}$ method (28). The mRNA levels were expressed as fold changes relative to the control treatment group.

High Performance Liquid Chromatography (HPLC) Analyses.

Carotenoid and retinoid extraction and analysis were carried out as previously described (29). Briefly, tissue samples (100 mg) or plasma samples (1 ml) were homogenized in 3 ml saline:ethanol (2:1, v/v). The neutral lipids were extracted using 5 ml hexane and ether (1:1, v/v) and by vortexing for one minute, centrifuging for 10 min. at 2,500 rpm at 4°C and collecting the upper layer. Samples were extracted thrice, upper layers pooled and dryed under nitrogen gas, and reconstituted in 100 μl ethanol:ether (1:1, v/v). A 50 μl sample of the final extract was injected into the HPLC system. A gradient reverse phase HPLC system was used for quantitative analysis of carotenoids and retinoids as previously described (30). Briefly, the gradient reverse phase HPLC system consisted of a Waters 2695 separations module and a Waters 2998 photodiode array detector. β-

Cryptoxanthin and retinoids were separated on a reverse phase C_{18} column (4.6 x 250 mm, 5 μM) (Vydac 201TP54, Grace Discovery Sciences, Inc.) fitted with a Pecosphere C_{18} guard column (PerkinElmer, CT.) with a flow rate of 1.00 ml/min. The gradient procedure is as follows: 1) 100% solvent A (Acetonitrile, Tetrahydrafuran, Water, 50 mM ammonium acetate, 50:20:30, v/v/v) for 4 minutes followed by a 6 minute linear gradient to 50% solvent A and 50% solvent B (Acetonitrile, Tetrahydrafuran, Water, 50 mM ammonium acetate, 50:44:6, v/v/v); 2) a 9 minute hold followed by a 2 minute linear gradient to 100% solvent B; 3) a 14 minute hold followed by a 3 minute linear gradient to 100% solvent A; 4) a 12 minute hold at 100% solvent A before next sample injection. The Waters 2998 programmable photodiode array detector was set at 450 nm and 325 nm for β-cryptoxanthin and retinoid monitoring. Using this procedure, β-cryptoxanthin and retinyl palmitate eluted at 22.6 and 26.5 minutes, respectively. Both β-cryptoxanthin and retinyl palmitate were identified by comparison of relative retention time (RT) and absorption spectra with authentic standards. Retinyl acetate and echinenone were used as internal standards to determine extraction efficiency. Extraction efficiency greater than 80% was considered adequate to quantify compounds of interest. All procedures were conducted under red light.

Statistical analysis.

GraphPad PRISM (version 5.02; San Diego, CA, USA) software was used for statistical analyses. The data represent the mean ± standard deviation (SD) or mean ± standard error of the mean (SEM) as indicated. Statistical analyses were made using one-way

ANOVA followed by Tukey's honestly significant differences (HSD) post hoc test to adjust for multiple comparisons. A value of $P < 0.05$ was considered significant.

RESULTS

Partial cloning of the ferret CMO1 gene. The ferret genome remains, as of yet, to be sequenced. Thus, expressional analysis of ferret genes requires the cloning of genes of particular interest. While the ferret CMO2 and β-actin genes have been previously sequenced in our laboratory (13), the ferret CMO1 sequence remained unknown. The approach used for partial cloning of the ferret CMO1 relied on the identification of conserved regions within the mouse and human CMO1 genes. Three sets of primers were used to generate non-overlapping PCR fragments. Generated PCR fragments were then used to generate additional primers in order to fill in gaps between the original PCR fragments. The 5'-end was amplified using 5'-RACE PCR. Cloning of the 3'-end was unsuccessful. The partially cloned ferret CMO1 gene was 1654 bp in length and had an open reading frame that translated into 488 amino acids. Comparison of the human, mouse and rat CMO1 nucleotide sequences demonstrated that the ferret CMO1 shared 87.7% identity with the human CMO1 and 83% identity with the mouse and rat CMO1 genes. The deduced amino acid sequence of the partial ferret CMO1 shared 85.1% identity with the human and mouse CMO1 protein (Figure 1). The partial ferret CMO1 nucleotide sequence has been deposited into the GenBank™ with the accession number HM367090.

Body weights. After nine weeks of treatment, β-cryptoxanthin at both the low- and high-doses had no effect on ferret body weight compared to animals consuming the control diet (Figure 2).

Relative Abundance. The relative abundance of ferret CMO1 and CMO2 mRNA was assessed in the small intestinal mucosa, liver, lung, adipose and kidney in ferrets fed a control diet for 9 weeks (Figure 3). The small intestinal mucosa was used as the reference tissue. The relative abundance of both CMO1 and CMO2 displayed tissue-specific expression patterns. The relative abundance of CMO1 was greatest in the liver and small intestinal mucosa, followed by lower abundance in the kidney, lung and visceral adipose. The relative abundance of CMO2 was greatest in the liver, followed by the visceral adipose, kidney, lung and small intestinal mucosa. Comparison of CMO1 and CMO2 abundance were also conducted in each tissue (Figure 3**)**. Tissue-specific comparison of CMO1 and CMO2 expression revealed significant differences in expression levels. In the intestinal mucosa, CMO1 abundance was significantly greater compared to CMO2. In the liver, however, there was no difference between CMO1 and CMO2 abundance. Relative CMO2 abundance was significantly greater than CMO1 in the visceral adipose, lung and kidney.

Tissue β-cryptoxanthin and Retinyl palmitate concentrations. β-Cryptoxanthin supplementation dose-dependently increased hepatic, lung and intestinal mucosa β-cryptoxanthin tissue concentrations (Table 1). Renal and adipose β-cryptoxanthin concentrations were undetectable with the analytic methods used in the study (data not

shown). The plasma concentrations achieved in the HBC group are lower than plasma β-cryptoxanthin levels observed in both observational (31, 32) and diet intervention trials (33). Since β-cryptoxanthin is a provitamin A carotenoid, it can be cleaved symmetrically by CMO1 to form retinal. β-Cryptoxanthin supplementation did not effect hepatic, intestinal mucosa, lung or plasma retinyl palmitate concentrations (Table 1).

Effect of β-cryptoxanthin on CMO1 and CMO2 gene expression. CMO1 and CMO2 gene expression were assessed using real time quantitative PCR using β-actin as the reference gene. Both low- and high-dose β-cryptoxanthin supplementation had no significant effects on the expression of CMO1 in any tissues analyzed. While there was a trend toward a decrease in expression in the intestinal mucosa, it did not reach significance. CMO2 expression was not effected by β-cryptoxanthin supplementation in the intestinal mucosa, adipose, liver or kidney. However, β-cryptoxanthin supplementation significantly decreased lung CMO2 expression in both the low- and high-dose supplementation treatment groups ($P = 0.02$).

DISCUSSION

Whether the chemopreventive effects of β-cryptoxanthin against lung cancer are due to the intact molecule or formation of metabolites remains unknown. However, understanding the metabolic pathways involved in carotenoid metabolism, especially the regulatory mechanisms involved, is essential to gain a better understanding the potential beneficial biological properties of β-cryptoxanthin. The recent identification of CMO2s broad substrate specificity (Mein et al., 2010 in press), especially of non-provitamin A

carotenoids, suggested that supplementation with the xanthophyll β-cryptoxanthin, which possesses both provitamin A and non-provitamin A activity, may influence CMO1 and CMO2 expression. Previous studies have also demonstrated an influence of carotenoid feeding on the carotenoid cleaving enzymes CMO1 and CMO2. Additionally, the ferret has been utilized as a model organism in the study of carotenoid metabolism and lung cancer chemoprevention by our lab and others. Therefore, we sought to determine the effect of dietary β-cryptoxanthin supplementation on CMO1 and CMO2 expression in the ferret model.

Despite the fact that the ferret has been used in research for decades, little is known about the ferret genome. This has hindered genetic analysis, thus, limiting the usefulness of the ferret model. To gain a better understanding into the metabolic pathways of carotenoid metabolism, we partially cloned the CMO1 gene. The partial ferret CMO1 sequence contained many conserved regions specific to the carotenoid oxygenase family. Ferret CMO1 demonstrated conservation of the acidic residues and three histidine residues, with the fourth remaining out of the partially cloned sequence (Figure 1). These conserved residues are involved in the coordination of iron, which is required for catalytic activity (34-36). In addition, the partial ferret CMO1 sequence contains the conserved domain EDDGIILSAIVS, which is considered the carotene cleavage oxygenase family sequence (35).

Supplementation with varying doses of β-cryptoxanthin over 9 weeks resulted in a dose-dependent increase in tissue accumulation of β-cryptoxanthin. β-Cryptoxanthin dose-dependently increased in the liver, lung, plasma and intestinal mucosa. The plasma values achieved are lower to those observed in observational (31, 32) and intervention

studies (37) in humans. While supplementation resulted in dose-dependent increases in tissue β-cryptoxanthin accumulation, there were no significant differences in tissue retinyl palmitate concentrations. β-Cryptoxanthin is symmetrically cleaved by CMO1, forming retinal and 3-hydroxy(OH)-retinal (11, 17). However, we did not detect any 3-OH-retinal in any of the tissues analyzed by HPLC (data not shown). It has been suggested that β-cryptoxanthin is more efficiently converted to vitamin A than β-carotene (38), yet the efficiency of conversion was carried out in vitamin A deplete animals. The ferrets in the current study were vitamin A sufficient animals consuming a diet replete with vitamin A. Additionally, the dosage used in the current study reflected a dosage that an individual could attain through normal dietary patterns. Whether a higher dosage could increase the amount of vitamin A is unknown.

CMO1 mRNA was significantly greater in the intestinal mucosa compared to CMO2 while no differences in hepatic levels were detected. The high abundance of CMO1 in the liver and intestinal mucosa is expected considering their importance in vitamin A production (34). The expression pattern of CMO1 identified in ferrets is similar to previous findings in other animal models (11, 26, 39). Expression of CMO1 is primarily localized to the epithelial cells of many tissues. The presence of CMO1 in a variety of tissues has been suggested as a source of local vitamin A production in times of low vitamin A intake (39). When compared to CMO1, expression of CMO2 was significantly greater in the visceral adipose, kidneys and lungs. The functional consequences of this are unknown. While CMO2 has also been suggested to function in local vitamin A production (40-42), comparative expression of CMO1 and CMO2 suggests that CMO2 may have different roles in carotenoid metabolism. This observation supports recent

evidence of CMO2's broad substrate specificity (Mein et al., Submitted). However, the biological implications of this relationship need to be further clarified.

Supplementation with both low- and high-dose β-cryptoxanthin significantly decreased lung CMO2 expression but not in other tissues. In our previous study, high-dose lycopene supplementation significantly increased ferret lung CMO2 expression (13). However, CMO1 and CMO2 were significantly decreased in selected rat tissues after lycopene supplementation (26), suggesting species-specific or dose-specific differences in metabolism. In the current study, the changes in lung CMO2 expression suggest that either β-cryptoxanthin alone or metabolism of β-cryptoxanthin may mediate some of the beneficial effects against lung cancer. Intact β-cryptoxanthin has been shown to decrease cell viability and transactivate retinoic acid receptors of several lung cell lines *in vitro* (43). β-Cryptoxanthin also decreased H_2O_2-induced DNA strand breaks and increased DNA damage repair in Caco-2 and HeLa cells, demonstrating a strong antioxidant effect *in vitro*. Recently, it was shown that the CMO2 is a mitochondrial protein in mice (44). High-dose supplementation of the carotenoids impaired mitochondrial function in both *in vitro* and *in vivo* models, resulting in production of ROS. Interestingly, when CMO2 was expressed in HepG2 cells, the impairment in mitochondrial function upon supplementation of carotenoids was ablated (44). We have recently demonstrated that chronic alcohol consumption in rats increased both hepatic CMO2 mRNA and protein expression (45), suggesting that oxidative stress may affect CMO2. High-dose β-carotene supplementation is associated with an increase keto- and epoxy-apo-carotenoid products, which have deleterious cellular effects. CMO2 may in fact function as protective mechanism to prevent excess accumulation to oxidative prone carotenoid or

carotenoid products. Whether the antioxidant capacity, possibly mediated by β-cryptoxanthin, mediates CMO2 expression deserves further inquiry.

The potential influence of apo-carotenoid formation via cleavage of β-cryptoxanthin, however, cannot be ruled out. Our preliminary data suggests that 3-OH-β-apo-10'-carotenal, an excentric cleavage product of β-cryptoxanthin (Mein et al., submitted), may also mediate cell growth and apoptotic effects of lung cell lines *in vitro* (data not shown). Additionally, in CMO1-KO mice supplemented with β-carotene, there was a significant increase in hepatic CMO2 parralleled with a significant increase in apo-carotenoid cleavage products (46). While we have provided evidence for a broader substrate specificity of CMO2, we did not detect any excentric cleavage products in the current study (data not shown). The influence of apo-carotenoids products on carotenoid cleavage enzyme expression and activity needs to be further explored. The relationship between CMO2, β-cryptoxanthin and the lung cancer deserves further investigation.

While lung CMO2 expression was affected by β-cryptoxanthin supplementation, there was little effect on CMO1 expression in selected ferret tissues. While there was a trend toward a decrease of CMO1 in the intestinal mucosa, however, it did not reach significance. All sections of the small intestinal mucosa were pooled for measurement of CMO1 and CMO2 expression. Any potential differences may have been missed due to signal dilution. The highest CMO1 expression is localized to the jujenum and duodenum of mice and rats (47, 48). Whether the same is true for ferrets needs to be further investigated using immunohistochemistry (IHC) or *in situ* hydrization techniques. Potential dilution of CMO1 and CMO2 transcripts in other tissues due to cell-specific expression is further supported by recent reports in mice. It was recently shown that

hepatocytes and hepatic stellate cells (HSC) differentially express CMO1 and CMO2 in the liver (46). In mice, liver CMO1 mRNA and protein expression primarily originated from the hepatic stellate cells. While CMO2 mRNA was present in both hepatocytes and HSC, the majority of expression was due to hepatocyte expression. Future studies in vestigating expression of both CMO1 and CMO2 need to consider cell-specific expression in addition to tissue-specific epression.

In summary, the ferret CMO1 gene shares many common characteristics of the carotene cleavage oxygenase family. The relative abundance of CMO1 and CMO2 is highly tissue-dependent and comparative analysis suggests different functions within the carotenoid metabolic pathway. Low- and high-dose β-cryptoxanthin supplementation results in a dose-dependent increase in β-cryptoxanthin tissue accumulation, yet the levels achieved are lower than those observed in epidemiological studies in humans. There were no changes in retinyl palmitate in any tissues measured. Supplementation with both low- and high-dose β-cryptoxanthin significantly decreased CMO2 expression in the lungs, suggesting a potential role of β-cryptoxanthin in the lungs.

REFERENCES

1. Schalch W, Landrum, J.T., Bone, R.A. The Eye. In: Britton G, Liaaen-Jensen, S., Pfander, H., editor. Carotenoids Volume 5: Nutrition and Health. Basel: Birkhäuser Verlag; 2009. p. 301-34.

2. Johnson EJ, Krinsky N.I. Carotenoids and Coronary Heart Disease. In: Britton G, Liaaen-Jensen, S., Pfander, H., editor. Carotenoids Volume 5: Nutrition and Health. Basel: Birkhäuser Verlag; 2009. p. 287-300.

3. Rock CL. Carotenoids and Cancer. In: Britton G, Liaaen-Jensen, S., Pfander, H., editor. Carotenoids Volume 5: Nutrition and Health. Basel: Birkhäuser Verlag; 2009. p. 269-86.

4. Bendich A. Symposium conclusions: biological actions of carotenoids. J Nutr. 1989 Jan;119:135-6.

5. Khachik F, Spangler CJ, Smith JC, Jr., Canfield LM, Steck A, Pfander H. Identification, quantification, and relative concentrations of carotenoids and their metabolites in human milk and serum. Analytical chemistry. 1997 May 15;69:1873-81.

6. Voorrips LE, Goldbohm RA, Brants HA, van Poppel GA, Sturmans F, Hermus RJ, van den Brandt PA. A prospective cohort study on antioxidant and folate intake and male lung cancer risk. Cancer Epidemiol Biomarkers Prev. 2000 Apr;9:357-65.

7. Yuan JM, Stram DO, Arakawa K, Lee HP, Yu MC. Dietary cryptoxanthin and reduced risk of lung cancer: the Singapore Chinese Health Study. Cancer Epidemiol Biomarkers Prev. 2003 Sep;12:890-8.

8. Mannisto S, Smith-Warner SA, Spiegelman D, Albanes D, Anderson K, van den Brandt PA, Cerhan JR, Colditz G, Feskanich D, et al. Dietary carotenoids and risk of lung cancer in a pooled analysis of seven cohort studies. Cancer epidemiology, biomarkers & prevention : a publication of the American Association for Cancer Research, cosponsored by the American Society of Preventive Oncology. 2004 Jan;13:40-8.

9. Gallicchio L, Boyd K, Matanoski G, Tao XG, Chen L, Lam TK, Shiels M, Hammond E, Robinson KA, et al. Carotenoids and the risk of developing lung cancer: a systematic review. Am J Clin Nutr. 2008 Aug;88:372-83.

10. Krinsky NI, Johnson EJ. Carotenoid actions and their relation to health and disease. Molecular aspects of medicine. 2005 Dec;26:459-516.

11. Redmond TM, Gentleman S, Duncan T, Yu S, Wiggert B, Gantt E, Cunningham FX, Jr. Identification, expression, and substrate specificity of a mammalian beta-carotene 15,15'-dioxygenase. The Journal of biological chemistry. 2001 Mar 2;276:6560-5.

12. Wyss A, Wirtz G, Woggon W, Brugger R, Wyss M, Friedlein A, Bachmann H, Hunziker W. Cloning and expression of beta,beta-carotene 15,15'-dioxygenase. Biochem Biophys Res Commun. 2000 May 10;271:334-6.

13. Hu KQ, Liu C, Ernst H, Krinsky NI, Russell RM, Wang XD. The biochemical characterization of ferret carotene-9',10'-monooxygenase catalyzing cleavage of carotenoids in vitro and in vivo. The Journal of biological chemistry. 2006 Jul 14;281:19327-38.

14. Kiefer C, Hessel S, Lampert JM, Vogt K, Lederer MO, Breithaupt DE, von Lintig J. Identification and characterization of a mammalian enzyme catalyzing the asymmetric oxidative cleavage of provitamin A. The Journal of biological chemistry. 2001 Apr 27;276:14110-6.

15. Hamel CP, Tsilou E, Pfeffer BA, Hooks JJ, Detrick B, Redmond TM. Molecular cloning and expression of RPE65, a novel retinal pigment epithelium-specific microsomal protein that is post-transcriptionally regulated in vitro. The Journal of biological chemistry. 1993 Jul 25;268:15751-7.

16. Jin M, Li S, Moghrabi WN, Sun H, Travis GH. Rpe65 is the retinoid isomerase in bovine retinal pigment epithelium. Cell. 2005 Aug 12;122:449-59.

17. Lindqvist A, Andersson S. Biochemical properties of purified recombinant human beta-carotene 15,15'-monooxygenase. The Journal of biological chemistry. 2002 Jun 28;277:23942-8.

18. Hessel S, Eichinger A, Isken A, Amengual J, Hunzelmann S, Hoeller U, Elste V, Hunziker W, Goralczyk R, et al. CMO1 deficiency abolishes vitamin A production from beta-carotene and alters lipid metabolism in mice. The Journal of biological chemistry. 2007 Nov 16;282:33553-61.

19. Mathews-Roth MM. Carotenoids in erythropoietic protoporphyria and other photosensitivity diseases. Ann N Y Acad Sci. 1993 Dec 31;691:127-38.

20. Bachmann H, Desbarats A, Pattison P, Sedgewick M, Riss G, Wyss A, Cardinault N, Duszka C, Goralczyk R, Grolier P. Feedback regulation of beta,beta-carotene 15,15'-monooxygenase by retinoic acid in rats and chickens. J Nutr. 2002 Dec;132:3616-22.

21. Takitani K, Zhu CL, Inoue A, Tamai H. Molecular cloning of the rat beta-carotene 15,15'-monooxygenase gene and its regulation by retinoic acid. Eur J Nutr. 2006 Sep;45:320-6.

22. Choi MY, Romer AI, Hu M, Lepourcelet M, Mechoor A, Yesilaltay A, Krieger M, Gray PA, Shivdasani RA. A dynamic expression survey identifies transcription factors relevant in mouse digestive tract development. Development (Cambridge, England). 2006 Oct;133:4119-29.

23. Lobo GP, Hessel S, Eichinger A, Noy N, Moise AR, Wyss A, Palczewski K, von Lintig J. ISX is a retinoic acid-sensitive gatekeeper that controls intestinal {beta},{beta}-carotene absorption and vitamin A production. Faseb J. 2010 Jan 8.

24. Seino Y, Miki T, Kiyonari H, Abe T, Fujimoto W, Kimura K, Takeuchi A, Takahashi Y, Oiso Y, et al. Isx participates in the maintenance of vitamin A metabolism by regulation of beta-carotene 15,15'-monooxygenase (Bcmo1) expression. The Journal of biological chemistry. 2008 Feb 22;283:4905-11.

25. Hauser H, Dyer JH, Nandy A, Vega MA, Werder M, Bieliauskaite E, Weber FE, Compassi S, Gemperli A, et al. Identification of a receptor mediating absorption of dietary cholesterol in the intestine. Biochemistry. 1998 Dec 22;37:17843-50.

26. Zaripheh S, Nara TY, Nakamura MT, Erdman JW, Jr. Dietary lycopene downregulates carotenoid 15,15'-monooxygenase and PPAR-gamma in selected rat tissues. J Nutr. 2006 Apr;136:932-8.

27. National Academy of Sciences IoM, Food and Nutrition Board, Panel on Dietary Antioxidants and Related Compounds. Dietary Reference Intakes for Vitamin C, Vitamin E, Selenium, and Carotenoids. Washington, D.C.: National Academy Press; 2000.

28. Livak KJ, Schmittgen TD. Analysis of relative gene expression data using real-time quantitative PCR and the 2(-Delta Delta C(T)) Method. Methods (San Diego, Calif. 2001 Dec;25:402-8.

29. Wang XD, Liu C, Bronson RT, Smith DE, Krinsky NI, Russell M. Retinoid signaling and activator protein-1 expression in ferrets given beta-carotene supplements and exposed to tobacco smoke. J Natl Cancer Inst. 1999 Jan 6;91:60-6.

30. Wang XD, Liu C, Bronson RT, Smith DE, Krinsky NI, Russell M. Retinoid signaling and activator protein-1 expression in ferrets given beta-carotene supplements and exposed to tobacco smoke. Journal of the National Cancer Institute. 1999 Jan 6;91:60-6.

31. Al-Delaimy WK, Ferrari P, Slimani N, Pala V, Johansson I, Nilsson S, Mattisson I, Wirfalt E, Galasso R, et al. Plasma carotenoids as biomarkers of intake of fruits and vegetables: individual-level correlations in the European Prospective Investigation into Cancer and Nutrition (EPIC). European journal of clinical nutrition. 2005 Dec;59:1387-96.

32. Al-Delaimy WK, van Kappel AL, Ferrari P, Slimani N, Steghens JP, Bingham S, Johansson I, Wallstrom P, Overvad K, et al. Plasma levels of six carotenoids in nine European countries: report from the European Prospective Investigation into Cancer and Nutrition (EPIC). Public health nutrition. 2004 Sep;7:713-22.

33. Brevik A, Andersen LF, Karlsen A, Trygg KU, Blomhoff R, Drevon CA. Six carotenoids in plasma used to assess recommended intake of fruits and vegetables in a controlled feeding study. Eur J Clin Nutr. 2004 Aug;58:1166-73.

34. Lakshman MR, Okoh C. Enzymatic conversion of all-trans-beta-carotene to retinal. Methods in enzymology. 1993;214:256-69.

35. Poliakov E, Gentleman S, Cunningham FX, Jr., Miller-Ihli NJ, Redmond TM. Key role of conserved histidines in recombinant mouse beta-carotene 15,15'-monooxygenase-1 activity. The Journal of biological chemistry. 2005 Aug 12;280:29217-23.

36. Schwartz SH, Tan BC, Gage DA, Zeevaart JA, McCarty DR. Specific oxidative cleavage of carotenoids by VP14 of maize. Science (New York, NY. 1997 Jun 20;276:1872-4.

37. Macdonald HM, Hardcastle AC, Duthie GG, Duthie SJ, Aucott L, Sandison R, Shearer MJ, Reid DM. Changes in vitamin biomarkers during a 2-year intervention trial

involving increased fruit and vegetable consumption by free-living volunteers. Br J Nutr. 2009 Nov;102:1477-86.

38. Davis C, Jing H, Howe JA, Rocheford T, Tanumihardjo SA. beta-Cryptoxanthin from supplements or carotenoid-enhanced maize maintains liver vitamin A in Mongolian gerbils (Meriones unguiculatus) better than or equal to beta-carotene supplements. Br J Nutr. 2008 Oct;100:786-93.

39. Lindqvist A, Andersson S. Cell type-specific expression of beta-carotene 15,15'-mono-oxygenase in human tissues. J Histochem Cytochem. 2004 Apr;52:491-9.

40. Napoli JL, Race KR. Biogenesis of retinoic acid from beta-carotene. Differences between the metabolism of beta-carotene and retinal. The Journal of biological chemistry. 1988 Nov 25;263:17372-7.

41. Sharma RV, Mathur SN, Dmitrovskii AA, Das RC, Ganguly J. Studies on the metabolism of beta-carotene and apo-beta-carotenoids in rats and chickens. Biochim Biophys Acta. 1976 Jan 18;486:183-94.

42. Wang XD, Krinsky NI, Tang GW, Russell RM. Retinoic acid can be produced from excentric cleavage of beta-carotene in human intestinal mucosa. Arch Biochem Biophys. 1992 Mar;293:298-304.

43. Lian F, Hu KQ, Russell RM, Wang XD. Beta-cryptoxanthin suppresses the growth of immortalized human bronchial epithelial cells and non-small-cell lung cancer cells and up-regulates retinoic acid receptor beta expression. International journal of cancer. 2006 Nov 1;119:2084-9.

44. Amengual J, Lobo GP, Golczak M, Li HN, Klimova T, Hoppel CL, Wyss A, Palczewski K, von Lintig J. A mitochondrial enzyme degrades carotenoids and protects against oxidative stress. FASEB J. 2010 Nov 24.

45. Luvizotto RA, Nascimento AF, Veeramachaneni S, Liu C, Wang XD. Chronic Alcohol Intake Upregulates Hepatic Expressions of Carotenoid Cleavage Enzymes and PPAR in Rats. J Nutr. 2010 Aug 11.

46. Shmarakov I, Fleshman MK, D'Ambrosio DN, Piantedosi R, Riedl KM, Schwartz SJ, Curley RW, Jr., von Lintig J, Rubin LP, et al. Hepatic stellate cells are an important cellular site for beta-carotene conversion to retinoid. Arch Biochem Biophys. 2010 May 12.

47. Duszka C, Grolier P, Azim EM, Alexandre-Gouabau MC, Borel P, Azais-Braesco V. Rat intestinal beta-carotene dioxygenase activity is located primarily in the cytosol of mature jejunal enterocytes. J Nutr. 1996 Oct;126:2550-6.

48. Wyss A, Wirtz GM, Woggon WD, Brugger R, Wyss M, Friedlein A, Riss G, Bachmann H, Hunziker W. Expression pattern and localization of beta,beta-carotene 15,15'-dioxygenase in different tissues. The Biochemical journal. 2001 Mar 15;354:521-9.

FIGURE LEGENDS

FIGURE 1. Comparison of the deduced amino acid sequences of partial ferret CMO1 and human and mouse CMO1. Nucleotide sequence identity is indicated in *red* between three species and *blue* between two species. The four conserved histidine residues (indicated by bold type and a single asterisk) and conserved acidic residues (indicated by

bold type) were present in the partial ferret CMO1. The CMO family signature sequence is underlined. The partial nucleotide sequence for ferret carotene-15,15'-monooxygenase has been deposited in the GenBank™ with accession number HM367090.

FIGURE 2. Body weights of ferrets after nine weeks of control, low- or high-dose β-cryptoxanthin supplementation. Results are the means ± SEM of weekly body weights (*n* = 6/group).

FIGURE 3. Relative abundance of CMO1 and CMO1 mRNA expression in selected ferret tissues. The relative abundance of CMO1 (A) and CMO2 (B) mRNA was determined in selected ferret tissues receiving control diet for 9 weeks. Intestinal mucosa was used as the reference organ and β-actin served as the reference gene. Tissue comparison of CMO1 and CMO2 expression in selected ferret tissues (C). CMO1 was used as the reference gene for comparison. Expression was detected by real time quantitative PCR as described in 'Materials and Methods'. Values are expressed as mean ± SEM; *n* = 4/group. * $P < 0.05$

FIGURE 4. Effect of β-cryptoxanthin supplementation on relative ferret CMO1 mRNA expression. The effect of control, low- and high-dose β-cryptoxanthin supplementation on the relative expression of CMO1 mRNA in visceral adipose (A), kidney (B), liver (C), lung (D) and intestinal mucosa (E) as determined by real time PCR. Results are the means ± SEM; *n* = 6/group. Bars not sharing a common superscript are significantly different from each other ($P < 0.05$).

FIGURE 5. Effect of β-cryptoxanthin supplementation on relative ferret CMO2 mRNA expression. The effect of control, low- and high-dose β-cryptoxanthin supplementation on the relative expression of CMO1 mRNA in visceral adipose (A), kidney (B), liver (C), lung (D) and intestinal mucosa (E) as determined by real time PCR. Results are the means ± SEM; n = 6/group. Bars not sharing a common superscript are significantly different from each other ($P < 0.05$).

Table 1. β-Cryptoxanthin and retinyl palmitate tissue concentrations in ferrets supplemented with control, low-, or high-dose β-cryptoxanthin for 9 weeks[1].

	Plasma	Lung	Liver	Intestinal Mucosa
β-cryptoxanthin	*nmol/L*		*nmol/kg*	
Control[2]	0	0	0	0
Low β-cryptoxanthin	69 ± 9[a]	31 ± 5[a]	87.06 ± 4.87[a]	31.06 ± 5.23[a]
High β-cryptoxanthin	117 ± 20[b]	63 ± 10[b]	170.88 ± 21.7[b]	58.67 ± 11.0[b]
Retinyl Palmitate	*μmol/L*		*nmol/g*	
Control	4.40 ± 0.93	6.42 ± 1.08	556.1 ± 183	1.59 ± 0.6
Low β-cryptoxanthin	3.95 ± 0.44	12.63 ± 3.49	606.8 ± 202	2.04 ± 0.75
High β-cryptoxanthin	3.81 ± 0.64	7.50 ± 3.80	459.4 ± 56	1.55 ± 0.36

[2]β-cryptoxanthin was not detectable in control fed animals. [1]Values are mean ± SEM; (n = 6).

Means not sharing a common superscript are significantly different ($P < 0.05$) as determined by one-way ANOVA followed by Tukey's Honestly Significant Differences (HSD) test for multiple comparisons.

Figure 1.


Ferret CMO1 (1) MDIIFGRNKKEQLEPVRAKVTGRIPPWLQGTLLRNGPGMHTVGETRYNHWFDGLALLHSFTIRDGEVCYRSKYLR
Human CMO1 (1) MDIIFGRNRKEQLEPVRAKVTGKIPAWLQGTLLRNGPGMHTVGESRYNHWFDGLALLHSFTIRDGEVYYRSKYLR
Mouse CMO1 (1) MEIIFGQNKKEQLEPVQAKVTGSIPAWLQGTLLRNGPGMHTVGESKYNHWFDGLALLHSFSIRDGEVFYRSKYLQ
Ferret CMO1 (76) SDTYKANIEANRIVVSEFGTIAYPDPCKNIFSKAFSYLSHTIPDFTDNCLINIMKCGEDFYATTETNYIRKINPQ
Human CMO1 (76) SDTYNTNIEANRIVVSEFGTMAYPDPCKNIFSKAFSYLSHTIPDFTDNCLINIMKCGEDFYATSETNYIRKINPQ
Mouse CMO1 (76) SDTYIANIEANRIVVSEFGTMAYPDPCKNIFSKAFSYLSHTIPDFTDNCLINIMKCGEDFYATTETNYIRKIDPQ
Ferret CMO1 (151) TLETLEKVDYRNYVTVNLATAHPHYDAAGNVLNMGTSIMDKGKTRYVVFRIPAAVPEDKK-GTNPLKHTEVFCSI
Human CMO1 (151) TLETLEKVDYRKYVAVNLATSHPHYDEAGNVLNMGTSIVEKGKTKYVIFKIPATVPEGKKQGKSPWKHTEVFCSI
Mouse CMO1 (151) TLETLEKVDYRKYVAVNLATSHPHYDEAGNVLNMGTSVVDKGRTKYVIFKIPATVPDSKKKGKSPVKHAEVFCSI
Ferret CMO1 (225) TSRSLLSPSYYHSFGVTENHIVFLEQPFKLDILKMSTAYIRGANWAACLAFHKEDKTYIHVIDQRTRKPLPTKFY
Human CMO1 (226) PSRSLLSPSYYHSFGVTENYVIFLEQPFRLDILKMATAYIRRMSWASCLAFHREEKTYIHIIDQRTRQPVQTKFY
Mouse CMO1 (226) SSRSLLSPSYYHSFGVTENYVVFLEQPFKLDILKMATAYMRGVSWASCMSFDREDKTYIHIIDQRTRKPVPTKFY
Ferret CMO1 (300) TDPMVVFHHVNAYEEDGCLLFDVITYEDSSLYELFYLANLNQDFEENCRLTSIPTLRRFAVPLSVDKNAEAGSNL
Human CMO1 (301) TDAMVVFHHVNAYEEDGCIVFDVIAYEDNSLYQLFYLANLNQDFKENSRLTSVPTLRRFAVPLHVDKNAEVGTNL
Mouse CMO1 (301) TDPMVVFHHVNAYEEDGCVLFDVIAYEDSSLYQLFYLANLNKDFEEKSRLTSVPTLRRFAVPLHVDKDAEVGSNL
Ferret CMO1 (375) IKLTSTTAKALKEKDDQVYCQPELLYEGLELPRINYARNGKRYRYVFAAEVQWSPIPTKILKYDVLTKSSLKWGQ
Human CMO1 (376) IKVASTTATALKEEDGQVYCQPEFLYEGLELPRVNYAHNGKQYRYVFATGVQWSPIPTKIIKYDILTKSSLKWRE
Mouse CMO1 (376) VKVSSTTATALKEKDGHVYCQPEVLYEGLELPRINYAYNGKPYRYIFAAEVQWSPVPTKILKYDILTKSSLKWSE
Ferret CMO1 (450) EHCWPAEPLFVPTLGAQDEDDGIILSAIVSTDPQKLPFL----------
Human CMO1 (451) DDCWPAEPLFVPAPGAKDEDDGVILSAIVSTDPQKLPFLLILDAKSFTELARASVDVDMHMDLHGLFITDMDWDT
Mouse CMO1 (451) ESCWPAEPLFVPTPGAKDEDDGVILSAIVSTDPQKLPFLLILDAKSFTELARASVDADMHLDLHGLFIPDADWNA
Ferret CMO1 (489) ----------
Human CMO1 (526) KKQAASEEQRDRASDCHGAPLT----------
Mouse CMO1 (526) VKQTPAETQEVENSDHPTDPTAPELSHSENDFTAGHGGSSL-

Figure 2.

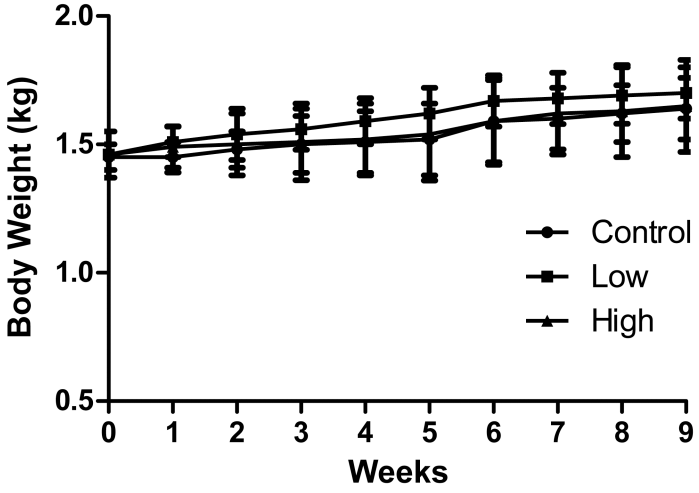

Figure 3.

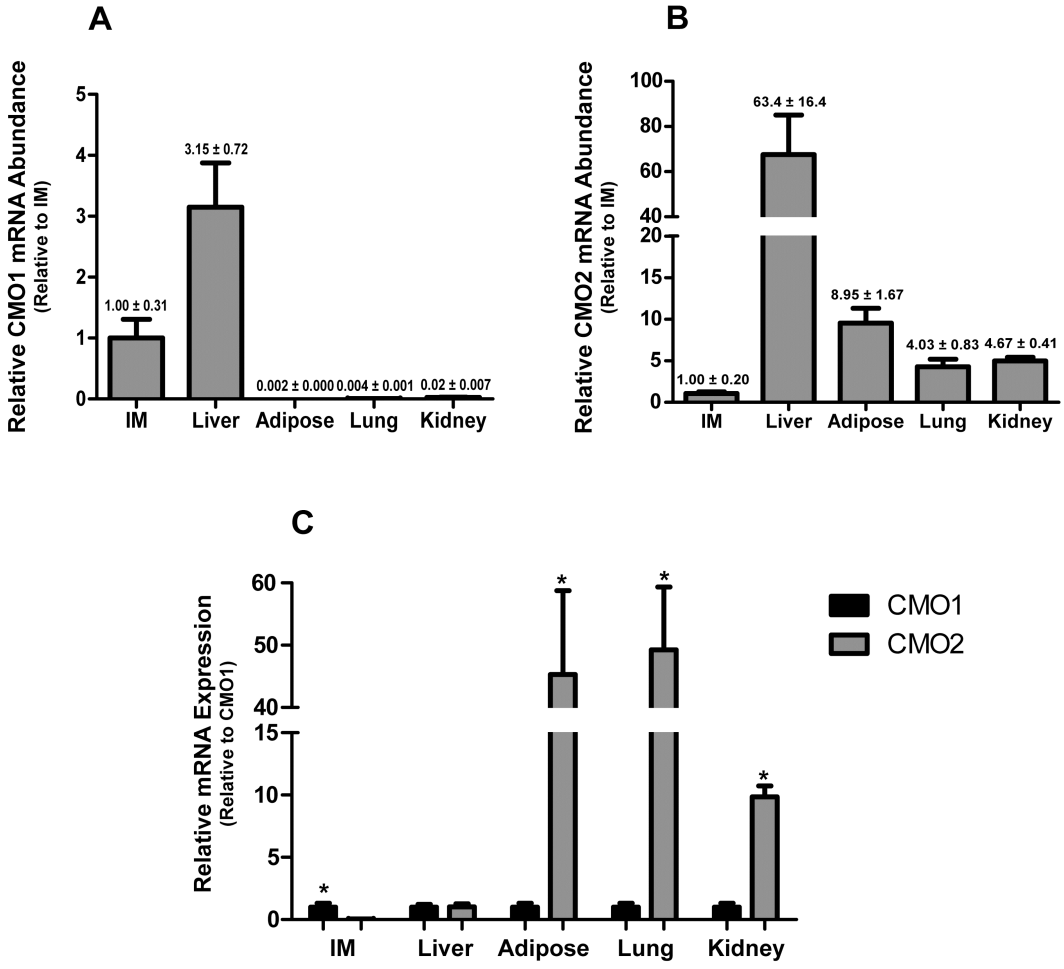
A
Relative CMO1 mRNA Abundance
(Relative to IM)
1.00 ± 0.31
3.15 ± 0.72
0.002 ± 0.000
0.004 ± 0.001
0.02 ± 0.007
IM
Liver
Adipose
Lung
Kidney
B
Relative CMO2 mRNA Abundance
(Relative to IM)
1.00 ± 0.20
63.4 ± 16.4
8.95 ± 1.67
4.03 ± 0.83
4.67 ± 0.41
IM
Liver
Adipose
Lung
Kidney
C
Relative mRNA Expression
(Relative to CMO1)
CMO1
CMO2
IM
Liver
Adipose
Lung
Kidney

Figure 4.

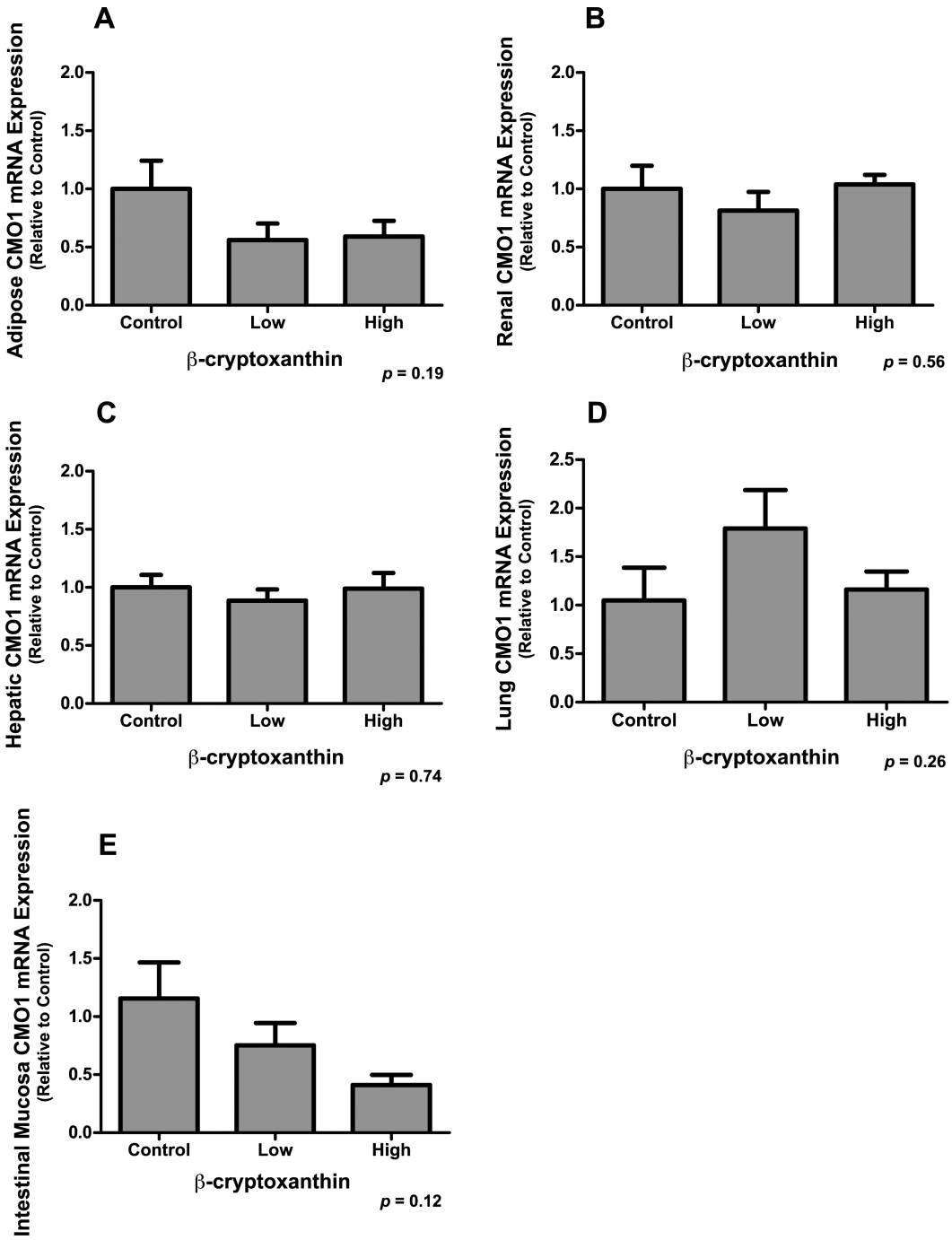
A
Adipose CMO1 mRNA Expression
(Relative to Control)
2.0
1.5
1.0
0.5
0.0
Control
Low
High
β-cryptoxanthin
p = 0.19
B
Renal CMO1 mRNA Expression
(Relative to Control)
2.0
1.5
1.0
0.5
0.0
Control
Low
High
β-cryptoxanthin
p = 0.56
C
Hepatic CMO1 mRNA Expression
(Relative to Control)
2.0
1.5
1.0
0.5
0.0
Control
Low
High
β-cryptoxanthin
p = 0.74
D
Lung CMO1 mRNA Expression
(Relative to Control)
2.5
2.0
1.5
1.0
0.5
0.0
Control
Low
High
β-cryptoxanthin
p = 0.26
E
Intestinal Mucosa CMO1 mRNA Expression
(Relative to Control)
2.0
1.5
1.0
0.5
0.0
Control
Low
High
β-cryptoxanthin
p = 0.12

Figure 5.

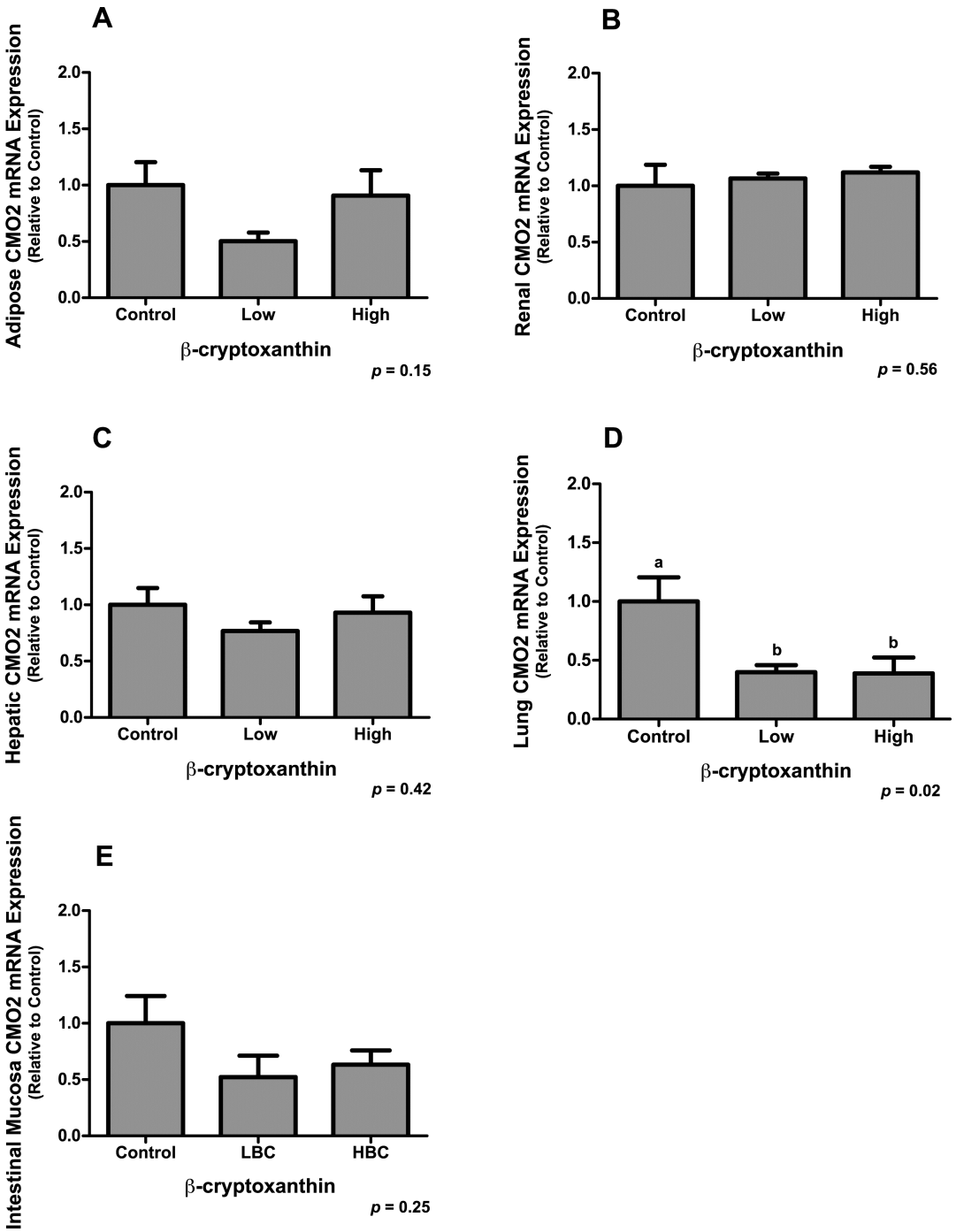
A
Adipose CMO2 mRNA Expression
(Relative to Control)
2.0
1.5
1.0
0.5
0.0
Control
Low
High
β-cryptoxanthin
p = 0.15
B
Renal CMO2 mRNA Expression
(Relative to Control)
Control
Low
High
β-cryptoxanthin
p = 0.56
C
Hepatic CMO2 mRNA Expression
(Relative to Control)
Control
Low
High
β-cryptoxanthin
p = 0.42
D
Lung CMO2 mRNA Expression
(Relative to Control)
a
b
b
Control
Low
High
β-cryptoxanthin
p = 0.02
E
Intestinal Mucosa CMO2 mRNA Expression
(Relative to Control)
Control
LBC
HBC
β-cryptoxanthin
p = 0.25

Chapter 6.

Summary, Discussion and Future Directions

6.1 Summary

This thesis research project investigated the *in vitro* and *in vivo* enzymatic pathways involved in carotenoid metabolism. First, we developed analytical techniques for the identification and characterization of 3-OH-apo-carotenoid metabolites. Second, we produced a functional recombinant ferret CMO2 protein, which was utilized for *in vitro* kinetic characterization using lutein, zeaxanthin and β-cryptoxanthin as substrates. Third, we cloned the ferret CMO1 gene, which displayed conserved regions specific to the carotene oxygenase family. Fourth, we analyzed the CMO1 and CMO2 relative abundance in the ferret model and compared the tissue-specific expression of CMO1 and CMO2. Fifth, we analyzed the effect of β-cryptoxanthin supplementation on CMO1 and CMO2 expression in the ferret model and analyzed tissue accumulation of β-cryptoxanthin and retinyl palmitate. Finally, we conducted initial studies into the biological activity of 3-OH-β-apo-10'-carotenal using *in vitro* cell models.

The key findings of this thesis project are summarized as follows:

1. Ferret Carotene-9',10'-Monooxygenase (CMO2) has a much broader substrate specificity than previously recognized, cleaving lutein, zeaxanthin and β-cryptoxanthin.
2. Ferret CMO2 cleaves carotenoids at both the 9,10 and 9',10 double bond, exhibiting cleavage preference for symmetrically substituted carotenoids, producing a number of volatile C_{13} and non-volatile C_{27} apo-carotenoid products.

3. Ferret CMO2 possesses a higher affinity for zeaxanthin and lutein than the monohydroxy xanthophyll β-cryptoxanthin. There was no difference in affinity between zeaxanthin and lutein. CMO2 cleaved both the β-ionone and α-ionone ring of lutein with similar affinity.
4. 3-OH-β-apo-10'-carotenal is oxidized to 3-OH-β-apo-10'-carotenoic acid in the presence of ferret liver homogenates and NAD^+. Formation of 3-OH-β-apo-10'-carotenal is inhibited in the presence of the retinaldehyde dehydrogenase (RALDH) inhibitor citral, suggesting enzymatic formation.
5. The partially cloned ferret CMO1 gene contains conserved histidine and acidic residues and the carotene oxygenase family signature sequence.
6. Tissue–specific expression of CMO1 displayed a distribution similar to other animal species. We demonstrated for the first time that CMO2 is highly expressed in the visceral adipose. Comparison of CMO2 expression with CMO1 expression displayed tissue-specific expression of both CMO1 and CMO2. Compared to CMO1, CMO2 expression was the dominant transcript in the lung, kidney and adipose tissue.
7. Supplementation of varying doses of β-cryptoxanthin had no effect on CMO1 expression while CMO2 expression was only effected in the lung. While supplementation with β-cryptoxanthin resulted in a dose-dependent increase in tissue accumulation of β-cryptoxanthin, there were no changes in vitamin A concentrations in selected tissues.
8. 3-OH-β-apo-10'-carotenal significantly decreased cell viability in BEAS-2B, A549 and HepG2 cell lines. While a role in cell proliferation cannot be ruled

out, high content analysis indicates that 3-OH-β-apo-10'-carotenal may function thru induction of apoptosis, suggesting the protective role of xanthophylls against cancer may be mediated thru 3-OH-apo-carotenoids.

6.2 Discussion and Future Directions

6.2.1 Potential cleavage of additional substrates by CMO2

Whether additional carotenoids, or carotenoid metabolites, can serve as CMO2 substrates needs to be further clarified. In the case of lutein and zeaxanthin, several *in vivo* metabolites have been identified. In mice, supplementation with lutein esters resulted in the formation and accumulation of keto-carotenoids (1). Lutein esters were oxidized primarily to 3'-hydroxy-ε,ε-caroten-3-one and, to a lesser extent, ε,ε-caroten-3,3'-dione-one. Metabolites were primarily accumulated in the liver and adipose tissue, which are major sites of CMO2 expression. In humans, pharmacokinetic studies of lutein and zeaxanthin demonstrated that both lutein and zeaxanthin can be converted to the all-E-3'-dehydro-lutein product (2, 3). Formation paralleled the plasma accumulation of both lutein and zeaxanthin, suggesting *in vivo* transformation. Several non-dietary lutein and zeaxanthin metabolites have also been identified in the retina (4). Analysis of the retina identified 3'-epilutein, 3-OH-β,ε-caroten-3'-one, 3'-oxolutein, 3-methoxyzeaxanthin and meso-zeaxanthin as major lutein and zeaxanthin metabolites. Formation of these metabolites is most likely via oxidation-reduction and isomerization reactions of lutein and zeaxanthin (4-6), yet their physiologic relevance is unknown. Investigating cleavage activity of CMO2 towards these additional lutein and zeaxanthin

substrates may provide insight into the biological roles of CMO2, especially regarding xanthophylls and the eye.

6.2.2 Biological activity of 3-OH-β-apo-10'-carotenoid cleavage products in vitro and in vivo.

To date there are no studies investigating the potential biological activity of specific 3-OH-α/β-apo-carotenoids. This is an important undertaking considering the importance of lutein and zeaxathin in the eye. Although no apocarotenoids resulting from excentric cleavage by CMO2 have been identified in the RPE (5), 3-OH-β-apo-14'-carotenal and 3-OH-β-ionone have been identified in cadaver retinas (7). Many reports have suggested that apo-carotenoids may possess biological activity. Our preliminary data suggests that that 3-OH-βapo-10'-carotenal has an effect on cell proliferation and apoptosis. However, the specific pathways and mechanism(s) involved need further exploration.

Recent evidence using oxidized lutein and zeaxathin provide evidence for further exploration of 3-OH-apo-carotenoid activity. Using HeLa cervical cancer cells, lutein and lutein oxidation products were shown to possess antioxidant properties and effect cell viability (8). Oxidation products were tentatively identified by LC-MS as a mixture of dehydration products and apo-carotenoids, however the mixture did not contain 3-OH-β-apo-10'-carotenoids. Lutein oxidation products exhibited greater antioxidant capabilities than lutein, decreased cell proliferation and increased apoptosis compared to lutein alone (20 μM). In human retinal pigment epithelial ARPE-19 cells, carotenoid-derived aldehyde (CDA) breakdown products were shown to induce oxidative stress leading to

apoptotic cell death (9). β-carotene, lutein and zeaxanthin CDA metabolites dose-dependently decreased cell viability (0 -100 uM). Additionally, β-carotene CDA products time-dependently decreased cell proliferation and dose-dependently increased reactive oxygen species (ROS), which was inhibited by the addition of the antioxidant *n*-acetylcysteine (NAC). There was also an increase in apoptosis when cells were incubated with β-carotene, lutein and zeaxanthin CDA as measured by DNA-fragmentation. Increases in apoptosis were paralleled by a decrease in mitochondrial potential and an increase in AP-1 and NF-κB protein expression. While there was no attempt made to characterize the oxidation products used, these results indicate a potential role of apo-carotenoid products in oxidative stress and regulation of cell death. Potential 3-OH-apo-carotenals could play a role in cellular toxicity and apoptosis. Our preliminary data suggests that 3-OH-β-apo-10'-carotenal could mediate many of these effects outlined in these studies and deserves further exploration.

6.2.3 Investigate the kinetic mechanisms and kinetic model of carotenoid cleavage by CMO2.

Our kinetic characterization of CMO2 revealed a possible positive cooperativity allosteric model of enzymatic cleavage. Positive cooperativity is a common kinetic model associated with enzymes involved in metabolism (10). Purified recombinant Human CMO1 was shown to be a tetrameric enzyme *in vitro* (11) yet displayed Michaeli-Menten kinetics. Our study, however, utilized crude enzyme fractions to estimate kinetic parameters of carotenoid cleavage. The use of crude enzyme fractions can lead to erroneous kinetic modeling (12). Therefore, to gain a more in-depth understanding of the

kinetics behind excentric cleavage, the use of purified enzyme should be employed. This would allow for the determination of the *in vitro* oligomeric properties of CMO2, especially whether the allosteric mechanism demonstrated herein is in fact an inherent kinetic mechanism of cleavage by CMO2 or simply a by-product of crude enzyme fraction utilization. Additionally, determination of CMO2 kinetic properties could lead to a more in-depth understanding of CMO2 regulation.

6.2.4 Investigate the role of CMO2 in adipose/adipocyte biology.

We identified expression of CMO2 in ferret visceral adipose. There were significantly higher levels of CMO2 expression compared to CMO1, suggesting an important role of CMO2 in adipose tissue. CMO2 expression was also found in mice visceral adipose tissue and found to be more highly expressed compared to CMO1. The significance of this finding needs further investigation. A role for CMO2 in adipocyte biology has only recently been alluded to. Cleavage of β-carotene at the 14',13' double bond results in the formation of β-apo-14'-carotenal and β-13-carotenone. While a specific enzyme has not been identified, formation of these products has been identified both *in vitro* (13) and *in vivo* (14). Both β-apo-14'-carotenal and β-apo-13-carotene have been shown to be antagonists of RARα nuclear receptor activation.

A role for CMO1 in adipocyte biology is just beginning to be understood. In CMO1-KO mice, gross impairments in lipid metabolism were evident independent of vitamin A status (15). There was an increased susceptibility to diet-induced obesity as well as an increase in PPARγ target genes in visceral adipose tissue. CMO2 expression was increased in both liver and visceral adipose tissues. Further studies have revealed

that RA produced via cleavage of β-carotene by CMO1 are directly involved in the regulation of adipocyte fat storage capacity (16). In NIH 3T3-L1 cells, RA derived from CMO1 cleavage of β-carotene decreased expression of PPARγ via a RAR-dependent manner. Using LRAT-KO mice, supplementation with β-carotene but not retinol decreased PPARγ expression and increased CYP26a1 expression. While CMO2 expression was not assessed in either NIH 3T3-L1 or LRAT-KO models, CMO2 expression was increased in both the liver and visceral adipose tissue of CMO1-KO mice (15, 17). There is also an increase in β-apo-carotenoid formation in CMO1-KO mice supplemented with β-carotene (17). Taken together, these results suggest that CMO2 plays a role in adipocyte biology and deserves further investigation

6.2.5 Investigate *in vivo* 3-OH-apo-carotenoid metabolite formation utilizing labeled carotenoid substrates.

We demonstrated the *in vitro* cleavage of lutein, zeaxanthin and β-cryptoxanthin by CMO2, yet to further confirm formation of 3-OH-apo-carotenoid metabolites by CMO2, formation of metabolites must be accomplished *in* vivo. A major barrier to the study and investigation of carotenoid metabolites is the development of both qualitative and quantitative analytical methods for the identification of apo-carotenoid metabolites. The methods developed in this dissertation were developed for the identification of 3-OH-apo-carotenoids and are feasible for use in *in vivo* identification. Recent reports have identified formation of apo-carotenoid and apo-lycopenoid metabolites *in vivo* (17, 18). Apo-lycopenoids identified in human plasma and in mice were also identified in dietary sources (17, 18). Therefore, it is imperative that apo-carotenoids identified *in vivo* are

differentiated from exogenous sources. One potential method is the use of labeled carotenoids. The use of intrinsically labeled carotenoids represents a practical and unambiguous method of carotenoid metabolite identification by CMO2 (19). A potential model that has been used successfully to demonstrate formation of apo-carotenoids *in vivo* is the use of the intestinal perfusion model (20, 21). The use of labeled carotenoids, especially lutein and zeaxanthin, in a perfusion model may provide the necessary means to identify *in vivo* production of 3-OH-apo-caroetnoids.

6.3 References

1. Yonekura L, Kobayashi M, Terasaki M, Nagao A. Keto-Carotenoids Are the Major Metabolites of Dietary Lutein and Fucoxanthin in Mouse Tissues. J Nutr. 2010 Aug 25.

2. Hartmann D, Thurmann PA, Spitzer V, Schalch W, Manner B, Cohn W. Plasma kinetics of zeaxanthin and 3'-dehydro-lutein after multiple oral doses of synthetic zeaxanthin. Am J Clin Nutr. 2004 Mar;79:410-7.

3. Thurmann PA, Schalch W, Aebischer JC, Tenter U, Cohn W. Plasma kinetics of lutein, zeaxanthin, and 3-dehydro-lutein after multiple oral doses of a lutein supplement. Am J Clin Nutr. 2005 Jul;82:88-97.

4. Bernstein PS, Khachik F, Carvalho LS, Muir GJ, Zhao DY, Katz NB. Identification and quantitation of carotenoids and their metabolites in the tissues of the human eye. Experimental eye research. 2001 Mar;72:215-23.

5. Khachik F, de Moura FF, Zhao DY, Aebischer CP, Bernstein PS. Transformations of selected carotenoids in plasma, liver, and ocular tissues of humans and in nonprimate animal models. Investigative ophthalmology & visual science. 2002 Nov;43:3383-92.

6. Khachik F, Spangler CJ, Smith JC, Jr., Canfield LM, Steck A, Pfander H. Identification, quantification, and relative concentrations of carotenoids and their metabolites in human milk and serum. Analytical chemistry. 1997 May 15;69:1873-81.

7. Prasain JK, Moore R, Hurst JS, Barnes S, van Kuijk FJ. Electrospray tandem mass spectrometric analysis of zeaxanthin and its oxidation products. J Mass Spectrom. 2005 Jul;40:916-23.

8. Lakshminarayana R, Sathish UV, Dharmesh SM, Baskaran V. Antioxidant and cytotoxic effect of oxidized lutein in human cervical carcinoma cells (HeLa). Food Chem Toxicol. 2010 Apr 13.

9. Kalariya NM, Ramana KV, Srivastava SK, van Kuijk FJ. Carotenoid derived aldehydes-induced oxidative stress causes apoptotic cell death in human retinal pigment epithelial cells. Experimental eye research. 2008 Jan;86:70-80.

10. Hill F. Xanthophyll pigmentation in sheep fat. Nature. 1962 Jun 2;194:865-6.

11. Lindqvist A, Andersson S. Biochemical properties of purified recombinant human beta-carotene 15,15'-monooxygenase. The Journal of biological chemistry. 2002 Jun 28;277:23942-8.

12. Rogers AaG, Y. Enzyme Kinetics: Theory and Practice. In: Schwender J, editor. Plant Metabolic Networks. New York: Springer; 2009. p. 98-100.

13. Tang GW, Wang XD, Russell RM, Krinsky NI. Characterization of beta-apo-13-carotenone and beta-apo-14'-carotenal as enzymatic products of the excentric cleavage of beta-carotene. Biochemistry. 1991 Oct 15;30:9829-34.

14. Ziouzenkova O, Orasanu G, Sukhova G, Lau E, Berger JP, Tang G, Krinsky NI, Dolnikowski GG, Plutzky J. Asymmetric cleavage of beta-carotene yields a transcriptional repressor of retinoid X receptor and peroxisome proliferator-activated receptor responses. Molecular endocrinology (Baltimore, Md. 2007 Jan;21:77-88.

15. Hessel S, Eichinger A, Isken A, Amengual J, Hunzelmann S, Hoeller U, Elste V, Hunziker W, Goralczyk R, et al. CMO1 deficiency abolishes vitamin A production from beta-carotene and alters lipid metabolism in mice. The Journal of biological chemistry. 2007 Nov 16;282:33553-61.

16. Lobo GP, Amengual J, Li HN, Golczak M, Bonet ML, Palczewski K, von Lintig J. {beta},{beta}-carotene decreases peroxisome proliferator receptor {gamma} activity and reduces lipid storage capacity of adipocytes in a {beta},{beta}-carotene-oxygenase 1-dependent manner. The Journal of biological chemistry. 2010 Jun 23.

17. Shmarakov I, Fleshman MK, D'Ambrosio DN, Piantedosi R, Riedl KM, Schwartz SJ, Curley RW, Jr., von Lintig J, Rubin LP, et al. Hepatic stellate cells are an important cellular site for beta-carotene conversion to retinoid. Arch Biochem Biophys. 2010 May 12.

18. Kopec RE, Riedl KM, Harrison EH, Curley RW, Hruszkewycz DP, Clinton SK, Schwartz SJ. Identification and Quantification of Apo-lycopenals in Fruits, Vegetables, and Human Plasma. J Agric Food Chem. 2010 Mar 24;58:3290-6.

19. Putzbach K, Krucker M, Albert K, Grusak MA, Tang G, Dolnikowski GG. Structure determination of partially deuterated carotenoids from intrinsically labeled vegetables by HPLC-MS and 1H NMR. J Agric Food Chem. 2005 Feb 9;53:671-7.

20. Wang XD, Russell RM, Liu C, Stickel F, Smith DE, Krinsky NI. Beta-oxidation in rabbit liver in vitro and in the perfused ferret liver contributes to retinoic acid biosynthesis from beta-apocarotenoic acids. The Journal of biological chemistry. 1996 Oct 25;271:26490-8.

21. Wang XD, Russell RM, Marini RP, Tang G, Dolnikowski GG, Fox JG, Krinsky NI. Intestinal perfusion of beta-carotene in the ferret raises retinoic acid level in portal blood. Biochim Biophys Acta. 1993 Apr 7;1167:159-64.

Chapter 7.

Preliminary Data –

Cytotoxic and Apoptotic Effects of the Excentric Cleavage Product 3-OH-β-apo-10'-carotenal *in vitro*

INTRODUCTION

Carotenoids represent a class of lipophilic compounds, consisting of a polyisoprenoid structure, found in various fruits and vegetables. Approximately 730 carotenoids have been characterized in nature. Among the diverse array of carotenoids found in nature, around 50 are found within the human diet with six major carotenoids being routinely found in human plasma and tissues, including β-carotene, β-cryptoxanthin, α-carotene, lutein, zeaxanthin and lycopene (1, 2). Carotenoids typically containing a series of conjugated double bonds in the central chain of the molecule, making them susceptible to oxidative cleavage. Although any of the conjugated double bonds within the carotenoid molecule can be cleaved, many biologically active apocarotenoids are formed via site-specific cleavage (3, 4).

Two major metabolic pathways have been characterized in carotenoid metabolism. For provitamin A carotenoids, such as β-carotene, central cleavage represents the major metabolic pathway, cleaving β-carotene at the 15,15' double bond forming retinal (5-8). For non-provitamin A carotenoids, such as lycopene, lutein and zeaxanthin, excentric cleavage via β-carotene-9',10'-monooxygenase (CMO2) at the 9',10' (9,10) double bond represents the major metabolic pathway and results in the formation of 3-OH-apo-carotenoid, apo-carotenoid, and apo-lycopenoid products (9, 10).

Apo-carotenoid metabolites may have important biological roles different than their parent compound. The biological significance of carotenoid metabolite generation, especially the differential effects of small and large quantities of oxidative metabolites, has been recently reviewed (11, 12). The *in vivo* production of apo-carotenoids and apo-lycopenals has recently been demonstrated in several studies (9, 13-16). Additionally,

several identified apo-carotenoid and apo-lycopenoid cleavage products have demonstrated biological activity *in vitro* and *in vivo* (4, 9, 17-19). Recent reports have suggested that unidentified oxidized lutein and zeaxathin products affect cell viability and apoptosis (20, 21). The recent demonstration of xanthophyll cleavage by CMO2 identified a new class of 3-OH-apo-carotenoids (Mein et al., submitted), yet no studies have investigated the potential biological activity of specific 3-OH-apo-carotenoid products.

The current study was aimed to investigate the potential biological activity of 3-OH-β-apo-10'-carotenal using *in vitro* cell models. Cell viability was assessed using both lung and liver cell lines. Additionally, the effect of 3-OH-β-apo-10'-carotenal on several markers of cell health were investigated using high content screening cellular imaging to gain mechanistic insight into potential biological actions.

MATERIALS AND METHODS

Chemicals

A stock solution (10 mM) of 3-OH-β-apo-10'-carotenal (synthesized and provided by BASF, Germany) was prepared in DMSO and stored at -80°C until use. Upon treatment, aliquots from the stock solution of 3-OH-β-apo-10'-carotenal were added to the cell culture medium to the desired working concentration and mixed thoroughly. The final DMSO concentration in the culture medium was 1%. All procedures were performed under red light.

Cell Culture

HepG2 (hepatocellular carcinoma cell line), A549 (non-small cell lung cancer cell line) and BEAS-2B (adenovirus-12 SV40 hybrid virus transformed, immortalized human bronchial epithelial cell line) cells were purchased from American Type Culture Collection (Manassas, VA). HepG2 cells were grown in EMEM media (Invitrogen, Carlsbad, CA) supplemented with 10% fetal bovine serum, 2mM pyruvate, 2 mM L-glutamine, 1X non-essential amino acids, and 100 units/ml penicillin and 100 μg/ml streptomycin. A549 cells were grown in F12K medium (Invitrogen, Carlsbad, CA) supplemented with 10% fetal bovine serum, 4 mM L-glutamine and 100 units/ml penicillin and 100 μg/ml streptomycin. BEAS-2B cells were grown in serum-free Lechner and LaVeck (LHC-9) bronchial epithelial growth medium (Invitrogen, Carlsbad, CA)) containing all-*trans* retinoic acid and epinephrine, as indicated. Culture flasks and multi-well plates were coated with LHC-basal media containing BSA (10 μg/ml), bovine fibronectin (10 μg/ml), and bovine collagen type I (30 μg/ml) for at least 30 min at 37°C (22). All cells were maintained in 75 cm^2 flasks in a humidified atmosphere at 37°C and 5% CO_2. Media was replaced every 2 – 3 days and were passaged when ~80% confluent.

Cell Viability

A549 or BEAS-2B cells were seeded at $5x10^3$ cells per well in 96 well plates or $1x10^5$ cells per well in 12-well plates. Cells were incubated for 24 to 48 hours prior to treatment to allow cells to achieve approximately 50% confluence. Cells were treated with 3-OH-β-apo-10'-carotenal for 24 or 48 hours without changing the media. Cell viability was estimated using the neutral red uptake assay (23). The neutral red assay determines the accumulation of the vital dye neutral red in the lysosomes of viable, uninjured cells, thus, providing an estimation of cell viability. Following exposure to 3-

OH-β-apo-10'-carotenal, cells were incubated for 3 hours at 37 °C with neutral red dye (50 μg/ml) dissolved in complete media. After incubation, cells were washed with PBS and neutral red was extracted with 100 μl neutral red extractant (Ethanol, Glacial Acetic Acid; 50%:1%) per well and shaken for approximately 10 minutes to obtain a homogenous solution. Absorbance was read at 540 nm using a microplate spectrophotometer. Cell viability is expressed as a percentage of the negative control (1% DMSO). All measurements were performed in triplate.

High Content Screening Cellular Imaging

HepG2 cells were plated at a density of 2000 cells/well in complete growth medium on BD BioCoat black-walled 96-well plate coated with collagen type I. Cells were incubated overnight to allow for attachment. On the second day, cells were treated with 3-OH-β-apo-10'-carotenal, valinomycin (10 μM) or vehicle (1% DMSO). All compounds were solubilized in 100% DMSO and diluted in complete EMEM media to 5X the final concentration, which was added to each well to achieve the final desired concentration. After 72 hours of incubation (37 °C, 5% CO_2, 100% humidity), the cells were stained using the Cellomics® ToxInsight™ Organelle Health Cartidge (ThermoFisher Scientific, Pittsburgh, PA) according to the manufacturers procedures. The cartridge contains a Hoechst DNA dye (Hoechst 33342), cell permeability dye (YOPRO-1), mitochondrial potential dye (Mito-Tracker Orange), and a mouse monoclonal antibody against Cytochrome C, which is stained with a goat anti-mouse DyLight 649-conjugated secondary antibody. Plates were read on the ToxInsight™ (Cellomics, Pittsburgh, PA) instrument. The fluorescent images were captured according to the appropriate absorption and emission spectra of the probes: Hoechst - 350/461 nm;

Permeability – 491/509 nm; Mitochondrial Potential – 551/576; and DyLight 649 conjugate – 646/674 nm. Three image fields were captured per well and analyzed. The ToxInsight software (version 1.6.1.5) and provided Excel worksheet were used for analysis.

Statistical Analysis

Results are expressed as means ± SEM unless otherwise indicated. GraphPad (version 5.02) was used for all non-linear regression curve fitting and estimation of IC_{50} values. High content image analysis was performed using the ToxInsight™ software (version 1.6.1.5).

RESULTS

Cell Viability

3-OH-β-apo-10'-carotenal had a significant effect on both BEAS-2B and A549 cell viability. In BEAS-2B cells (Figure 1), 3-OH-β-apo-10'-carotenal decreased cell viability in a dose-dependent and time-dependent manner. At 24 hours, 3-OH-β-apo-carotenal demonstrated an IC_{50} = 0.603 ± .67 μM at 24 hours and at 48 hours an estimated IC_{50} = 0.478 ± .05 μM was observed. In A549 cells, 3-OH-β-apo-10'-carotenal dose-dependently and time-dependently decreased A549 viability. At 24 hours 3-OH-β-apo-10'-caroteneal (10 μM) decreased A549 cell viability by ~25% (Figure 2) and at 48 hours viability was decreased ~50%.

High Content Cellular Imaging Analysis

To measure a panel of signals that are directly related to key mechanisms of cell viability simultaneously, we applied a multispectral live-cell imaging of HepG2 cells

after treatment with 3-OH-β-apo-carotenal by staining with multiple fluorescent probes (Figure 3). By examining these high content imaging outputs and applying automated imaging analysis algorithms, information regarding potential mechanisms can be extracted (Figure 4). The multi-channel outputs are further quantified using standardized image analysis procedures measuring the intensity and area or size of any object of interest. One advantage of high content imaging is the ability to analyze individual cell populations. Thus, for specific parameters the response is given as a percent of low or high responders. These populations correspond to the percent of individual cells in the well that are significantly higher or lower statistically in the specified response compared to the vehicle control.

To gain mechanistic insight into the action of 3-OH-β-apo-10'-carotenal, a number of cellular parameters were investigated including: cell loss, nuclear morphology, DNA content, cell membrane permeability, mitochondrial membrane potential changes, and Cytochrome C localization and release from the mitochondria (Figure 5). After 72 hrs, 3-OH-β-apo-10'-carotenal dose-dependently decreased HepG2 cell number with an estimated $IC_{50} = 0.378 \pm 0.05$ μM. Among all parameters measured, Cytochrome C release and nuclear swelling showed most significant effects. In low responders, all 3-OH-β-apo-10'-carotenal concentrations used resulted in a significant increase in Cytochrome C release compared to control cells. Similarly, among high responders 3-OH-β-apo-carotenal treatment significantly increased nuclear swelling compared to controls. Among low responders, there was a significant increase in nuclear shrinking at concentrations > 1.2 μM. There was little effect on cell permeability at concentrations < 1.2 μM. At concentrations ≥1.2 μM, there was a decrease in mitochondrial membrane

potential in low responders. These results indicate that sub-lethal concentrations of 3-OH-β-apo-10'-carotenal have an effect both on necrotic and apoptotic pathways of cell death.

DISCUSSION

Apocarotenoids are important bioactive mediators in plants and animals. In plants, they play key roles in reproduction, defense, and architecture (24). In animals, the most important apocarotenoid is retinal and its derivatives, retinol and retinoic acid, playing important roles in immune function (25), in development (26), and in cancer (27). We recently demonstrated cleavage of lutein, zeaxathin and β-cryptoxanthin by ferret CMO2, forming 3-OH-apo-carotenoids (Mein et al., submitted). The present study provides new evidence that 3-OH-β-apo-10'-carotenal possess potential biological activity, especially via effects on cell viability. Furthermore, the growth inhibitory effects may be mediated through induction of apoptosis, decreased mitochondrial potential and induction of necrotic pathways. Our results suggest that the beneficial effects of xanthophyll carotenoids, especially against cancer development (28), may be mediated through production of bioactive 3-OH-apo-carotenoid metabolites.

Previous studies demonstrated that β-cryptoxanthin dose- and time-dependently inhibited cell growth in both premalignant and malignant lung cell lines (29). The BEAS-2B cell line is a non-tumorigenic premalignant cell line derived from normal human bronchial epithelial cells, retaining many features of human bronchial epithelial cells (22). The A549 non-small cell lung cancer cells, however, were less responsive to β-cryptoxanthin treatment than BEAS-2B cells. It was hypothesized that some of the

growth inhibitory effects may be mediated by 3-OH-apo-carotenoids, yet no 3-OH-apo-carotenoids were identified in cells treated with β-cryptoxanthin. Our data demonstrate a dose- and time-dependent inhibition of cell viability in BEAS-2B and A549 cells treated with 3-OH-β-apo-10'-carotenal. Similar to β-cryptoxanthin treatment, A549 cells were less response to 3-OH-β-apo-10'-carotenal, suggesting that the growth inhibitory effects of β-cryptoxanthin may be mediated via 3-OH-apo-carotenoids. This supports previous studies demonstrating that A549 cells are resistant to retinoic acid-induced growth inhibition and differentiation (30). Thus, while not investigated with 3-OH-β-apo-10'-carotenal, β-cryptoxanthin dose-dependently increased RARE-dependent promoter activity in cells co-transfected with RAR expression vector (29) and was shown to bind and activate RAR receptors using a yeast two-hybrid system (31). Considering the oxidation of 3-OHβ-apo-10'-carotenal to 3-OH-β-apo-10'-carotenoic acid (Mein et al., submitted), the effect of 3-OH-apo-carotenoids on RAR activation needs to be investigated.

High content screening cellular imaging analysis revealed potential insights into the mechanisms of 3-OH-β-apo-10'-carotenal action. In HepG2 liver cancer cells, 3-OH-β-apo-carotenal dose-dependently inhibited cell viability and increased markers of both apoptosis and necrosis. Specifically, there was a decrease in mitochondrial membrane potential and an increase in cytochrome C release, which are both associated with apoptosis (32-34). In human retinal pigment epithelial ARPE-19 cells, β-carotene, lutein and zeaxanthin-derived aldehyde (carotenoid-derived aldehydes; CDA) breakdown products were shown to decrease cell viability and induce oxidative stress, leading to apoptotic cell death (20). Oxidized β-carotene, lutein and zeaxanthin CDA oxidation

products dose-dependently decreased cell viability with LC_{50} values of approximately 40 μM, 60 μM and 25 μM, respectively. Additionally, β-carotene CDA products time-dependently decreased cell proliferation and dose-dependently increased reactive oxygen species (ROS). In addition there was an increase in apoptosis when cells were incubated with β-carotene, lutein and zeaxanthin oxidation products as measured by DNA-fragmentation. Increases in apoptosis were paralleled by a decrease in mitochondrial potential. Oxidation products also increased protein expression of AP-1 and NF-κB. Many of the oxidative effects of carotenoid oxidation products were inhibited by the addition of the antioxidant *n*-acetylcysteine (NAC). These results indicate a potential role of apo-carotenoid products in oxidative stress and regulation of cell death. While the products used in this study were not determined, the first products formed from enzymatic cleavage contain aldehyde function groups. Thus, potential 3-OH-apo-carotenals could play a role in cellular toxicity and apoptosis.

Using HeLa cervical cancer cells, lutein and lutein oxidation products were shown to possess antioxidant properties and effect cell viability (21). Lutein oxidation products were prepared by photooxidation of lutein liposomes (exposure to direct sunlight) and were tentatively identified by LC-MS as a mixture of dehydration products and apo-carotenoids. The mixture, however, did not contain 3-OH-β-apo-10'-carotenoids. Lutein oxidation products exhibited greater antioxidant capabilities than lutein, demonstrated by increased radical scavenging activity, decreased glutathione and decreased malondialdehyde (MDA) levels. Oxidized lutein products also decreased cell proliferation and increased apoptosis compared to lutein alone (20 μM). While lutein oxidation products were shown to have a significant effect on antioxidant status and cell

viability, the use of a mixture of oxidation products does not allow the isolation of particular lutein oxidation compounds. While the antioxidant activity of 3-OH-β-apo-10'-carotenal was not assessed in the current study, previous studies using apo-lycopenoids demonstrated an antioxidant effect thru induction of phase II enzymes (35). Interestingly apo-10'-lycopenal showed the strongest effect on heme-oxygenase-1 induction. It was suggested that the reactive aldehyde group could explain this observation (36). Thus, further studies utilizing 3-OH-β-apo-10'-carotenal should investigate potential antioxidant roles, especially induction of phase II enzymes.

Aldehydes are highly reactive function groups, possessing the ability to react with amino acid residues, nucleic acids and lipids. Aldehyde compounds, such as retinal, have been shown to induce uncoupling of mitochondria through induction of uncoupling proteins and adenine nucleotide translocase and decreases in oxidative phosphorylation (37, 38). Breakdown products of β-carotene, especially aldehyde derivatives, have been shown to affect mitochondrial function (39, 40). In the present study, we demonstrated a decrease in mitochondrial potential after treatment with 3-OH-β-apo-10'-carotenal. Whether this is due to the 3-OH-β-apo-10'-aldehyde product is a distinct possibility. We have previously demonstrated oxidation of 3-OH-β-apo10'-carotenal to 3-OH-β-apo-10'-carotenoic acid in the presence on ferret liver homogenate and NAD^+ (Mein et al., 2010). Thus, further studies must evaluate the activity of the acid derivative to eliminate the possibility that changes in cell death are not due to the presence of the reactive aldehyde. However, procurement of sufficient acid compound remains a challenge.

Cleavage of xanthophylls by CMO2 produces both 3-OH-apo-carotenoids and 3-OH-ionone products. While not assessed in this study, the formation of volatile ionone

products must be taken into account, especially when considering the biological activity of 3-OH-apo-carotenoid formation *in vivo*. Volatile apo-carotenoids have been shown to possess biological activity *in vitro* and *in vivo*. The volatile apo-carotenoid β-ionone has also been shown to inhibit cell proliferation and induce apoptosis both *in vitro* (41-44) and *in vivo* (45) and induce expression of phase I and phase II enzymes in rats and mice (46-48). Further studies should investigate the potential activity of 3-OH-ionone products to fully characterize the potential biological functions of excentric cleavage of xanthophylls carotenoids.

The data produced in the current study is significant due to the potential importance of xanthophylls cleavage in the eye. Several carotenoids, including lutein, zeaxanthin, β-carotene, α-carotene, and lycopene, have been identified in the human RPE (49). Both CMO1 and CMO2 are strongly expressed in the RPE (50, 51), and CMO1 actively converts β-carotene (and presumably β-cryptoxanthin) into all-*trans*-retinal (52, 53), which is isomerized to the visual pigment chromophore 11-*cis*-retinal by RPE65 (54). Although 3-OH-β-apo-14'-carotenal and 3-OH-β-ionone have been identified in cadaver retinas (55), no apo-carotenoids resulting from excentric cleavage by CMO2 have been identified (56). In addition, several non-dietary lutein and zeaxanthin metabolites, including 3'-epilutein, 3-OH-β,ε-caroten-3'-one and meso-zeaxanthin, have also been identified in these regions (49). Thus, the potential for 3-OH-β-apo-carotenoid formation is significant. Studies investigating the potential biological activities of 3-OH-apo-carotenoids may have significant impact on eye research.

In summary, our preliminary data indicate that 3-OH-β-apo-10'-carotenal has a significant effect on *in vitro* cell viability. While a role in cellular proliferation cannot be

ruled out, high content analysis indicates that 3-OH-β-apo-10'-carotenal may function thru induction of apoptosis. The exact mechanisms on cellular death need to be further explored. Additionally, as evidenced with apo-lycopoids and oxidized lutein products, the potential impact of antioxidant activity of 3-OH-β-apo-10'-carotenoids needs to be evaluated. The potential impact on eye research is significant. We are continuing to elucidate the role of 3-OH-β-apo-10'-carotenal in biological systems.

REFERENCES

1. Bendich A. Symposium conclusions: biological actions of carotenoids. J Nutr. 1989 Jan;119:135-6.

2. Khachik F, Spangler CJ, Smith JC, Jr., Canfield LM, Steck A, Pfander H. Identification, quantification, and relative concentrations of carotenoids and their metabolites in human milk and serum. Analytical chemistry. 1997 May 15;69:1873-81.

3. Tang GW, Wang XD, Russell RM, Krinsky NI. Characterization of beta-apo-13-carotenone and beta-apo-14'-carotenal as enzymatic products of the excentric cleavage of beta-carotene. Biochemistry. 1991 Oct 15;30:9829-34.

4. Wang XD, Tang GW, Fox JG, Krinsky NI, Russell RM. Enzymatic conversion of beta-carotene into beta-apo-carotenals and retinoids by human, monkey, ferret, and rat tissues. Arch Biochem Biophys. 1991 Feb 15;285:8-16.

5. Lindqvist A, Andersson S. Biochemical properties of purified recombinant human beta-carotene 15,15'-monooxygenase. The Journal of biological chemistry. 2002 Jun 28;277:23942-8.

6. Paik J, During A, Harrison EH, Mendelsohn CL, Lai K, Blaner WS. Expression and characterization of a murine enzyme able to cleave beta-carotene. The formation of retinoids. The Journal of biological chemistry. 2001 Aug 24;276:32160-8.

7. Redmond TM, Gentleman S, Duncan T, Yu S, Wiggert B, Gantt E, Cunningham FX, Jr. Identification, expression, and substrate specificity of a mammalian beta-carotene 15,15'-dioxygenase. The Journal of biological chemistry. 2001 Mar 2;276:6560-5.

8. Wyss A, Wirtz G, Woggon W, Brugger R, Wyss M, Friedlein A, Bachmann H, Hunziker W. Cloning and expression of beta,beta-carotene 15,15'-dioxygenase. Biochem Biophys Res Commun. 2000 May 10;271:334-6.

9. Hu KQ, Liu C, Ernst H, Krinsky NI, Russell RM, Wang XD. The biochemical characterization of ferret carotene-9',10'-monooxygenase catalyzing cleavage of carotenoids in vitro and in vivo. The Journal of biological chemistry. 2006 Jul 14;281:19327-38.

10. Kiefer C, Hessel S, Lampert JM, Vogt K, Lederer MO, Breithaupt DE, von Lintig J. Identification and characterization of a mammalian enzyme catalyzing the asymmetric oxidative cleavage of provitamin A. The Journal of biological chemistry. 2001 Apr 27;276:14110-6.

11. Mein JR, Lian F, Wang XD. Biological activity of lycopene metabolites: implications for cancer prevention. Nutr Rev. 2008 Dec;66:667-83.

12. Wang XD. Carotenoid Oxidative/Degradative Products and Their Biological Activities. In: Krinsky NI, Mayne, S.T., Sies, H., editor. Carotenoids in Health and Disease. New York: Marcel Dekker; 2004. p. 313-35.

13. Eroglu A, Hruszkewycz DP, Curley RW, Jr., Harrison EH. The eccentric cleavage product of beta-carotene, beta-apo-13-carotenone, functions as an antagonist of RXRalpha. Arch Biochem Biophys. 2010 Aug 1.

14. Ho CC, de Moura FF, Kim SH, Clifford AJ. Excentral cleavage of beta-carotene in vivo in a healthy man. Am J Clin Nutr. 2007 Mar;85:770-7.

15. Kopec RE, Riedl KM, Harrison EH, Curley RW, Hruszkewycz DP, Clinton SK, Schwartz SJ. Identification and Quantification of Apo-lycopenals in Fruits, Vegetables, and Human Plasma. J Agric Food Chem. 2010 Mar 24;58:3290-6.

16. Shmarakov I, Fleshman MK, D'Ambrosio DN, Piantedosi R, Riedl KM, Schwartz SJ, Curley RW, Jr., von Lintig J, Rubin LP, et al. Hepatic stellate cells are an important cellular site for beta-carotene conversion to retinoid. Arch Biochem Biophys. 2010 May 12.

17. al-Hasani SM, Parrish DB. Forms of vitamin A and of carotenoids in tissues, blood serum and yolk of eggs from Cotournix coturnix japonica fed -apo-carotenals. J Nutr. 1972 Nov;102:1437-40.

18. Sharma RV, Mathur SN, Dmitrovskii AA, Das RC, Ganguly J. Studies on the metabolism of beta-carotene and apo-beta-carotenoids in rats and chickens. Biochim Biophys Acta. 1976 Jan 18;486:183-94.

19. Zaripheh S, Boileau TW, Lila MA, Erdman JW, Jr. [14C]-lycopene and [14C]-labeled polar products are differentially distributed in tissues of F344 rats prefed lycopene. J Nutr. 2003 Dec;133:4189-95.

20. Kalariya NM, Ramana KV, Srivastava SK, van Kuijk FJ. Carotenoid derived aldehydes-induced oxidative stress causes apoptotic cell death in human retinal pigment epithelial cells. Experimental eye research. 2008 Jan;86:70-80.

21. Lakshminarayana R, Sathish UV, Dharmesh SM, Baskaran V. Antioxidant and cytotoxic effect of oxidized lutein in human cervical carcinoma cells (HeLa). Food Chem Toxicol. 2010 Apr 13.

22. Reddel RR, Ke Y, Gerwin BI, McMenamin MG, Lechner JF, Su RT, Brash DE, Park JB, Rhim JS, Harris CC. Transformation of human bronchial epithelial cells by infection with SV40 or adenovirus-12 SV40 hybrid virus, or transfection via strontium phosphate coprecipitation with a plasmid containing SV40 early region genes. Cancer Res. 1988 Apr 1;48:1904-9.

23. Repetto G, del Peso A, Zurita JL. Neutral red uptake assay for the estimation of cell viability/cytotoxicity. Nat Protoc. 2008;3:1125-31.

24. Bouvier F, Isner JC, Dogbo O, Camara B. Oxidative tailoring of carotenoids: a prospect towards novel functions in plants. Trends in plant science. 2005 Apr;10:187-94.

25. Spilianakis CG, Lee GR, Flavell RA. Twisting the Th1/Th2 immune response via the retinoid X receptor: lessons from a genetic approach. European journal of immunology. 2005 Dec;35:3400-4.

26. Lampert JM, Holzschuh J, Hessel S, Driever W, Vogt K, von Lintig J. Provitamin A conversion to retinal via the beta,beta-carotene-15,15'-oxygenase (bcox) is essential for pattern formation and differentiation during zebrafish embryogenesis. Development (Cambridge, England). 2003 May;130:2173-86.

27. Abu J, Batuwangala M, Herbert K, Symonds P. Retinoic acid and retinoid receptors: potential chemopreventive and therapeutic role in cervical cancer. The lancet oncology. 2005 Sep;6:712-20.

28. Mannisto S, Smith-Warner SA, Spiegelman D, Albanes D, Anderson K, van den Brandt PA, Cerhan JR, Colditz G, Feskanich D, et al. Dietary carotenoids and risk of lung cancer in a pooled analysis of seven cohort studies. Cancer epidemiology, biomarkers & prevention : a publication of the American Association for Cancer Research, cosponsored by the American Society of Preventive Oncology. 2004 Jan;13:40-8.

29. Lian F, Hu KQ, Russell RM, Wang XD. Beta-cryptoxanthin suppresses the growth of immortalized human bronchial epithelial cells and non-small-cell lung cancer cells and up-regulates retinoic acid receptor beta expression. International journal of cancer. 2006 Nov 1;119:2084-9.

30. van der Leede BM, van den Brink CE, van der Saag PT. Retinoic acid receptor and retinoid X receptor expression in retinoic acid-resistant human tumor cell lines. Molecular carcinogenesis. 1993;8:112-22.

31. Matsumoto A, Mizukami H, Mizuno S, Umegaki K, Nishikawa J, Shudo K, Kagechika H, Inoue M. beta-Cryptoxanthin, a novel natural RAR ligand, induces ATP-binding cassette transporters in macrophages. Biochemical pharmacology. 2007 Jul 15;74:256-64.

32. Green DR, Reed JC. Mitochondria and apoptosis. Science (New York, NY. 1998 Aug 28;281:1309-12.

33. Li P, Nijhawan D, Budihardjo I, Srinivasula SM, Ahmad M, Alnemri ES, Wang X. Cytochrome c and dATP-dependent formation of Apaf-1/caspase-9 complex initiates an apoptotic protease cascade. Cell. 1997 Nov 14;91:479-89.

34. Liu X, Kim CN, Yang J, Jemmerson R, Wang X. Induction of apoptotic program in cell-free extracts: requirement for dATP and cytochrome c. Cell. 1996 Jul 12;86:147-57.

35. Lian F, Wang XD. Enzymatic metabolites of lycopene induce Nrf2-mediated expression of phase II detoxifying/antioxidant enzymes in human bronchial epithelial cells. International journal of cancer. 2008 Jun 19;123:1262-8.

36. Esterbauer H, Schaur RJ, Zollner H. Chemistry and biochemistry of 4-hydroxynonenal, malonaldehyde and related aldehydes. Free Radic Biol Med. 1991;11:81-128.

37. Stillwell W, Nahmias S. Effect of retinol and retinoic acid on P/O ratios of coupled mitochondria. Biochem Int. 1983 Mar;6:385-92.

38. Echtay KS, Esteves TC, Pakay JL, Jekabsons MB, Lambert AJ, Portero-Otin M, Pamplona R, Vidal-Puig AJ, Wang S, et al. A signalling role for 4-hydroxy-2-nonenal in regulation of mitochondrial uncoupling. EMBO J. 2003 Aug 15;22:4103-10.

39. Siems W, Wiswedel I, Salerno C, Crifo C, Augustin W, Schild L, Langhans CD, Sommerburg O. Beta-carotene breakdown products may impair mitochondrial functions--potential side effects of high-dose beta-carotene supplementation. The Journal of Nutritional Biochemistry. 2005 Jul;16:385-97.

40. Siems WG, Sommerburg O, Hurst JS, van Kuijk FJ. Carotenoid oxidative degradation products inhibit Na+-K+-ATPase. Free Radic Res. 2000 Oct;33:427-35.

41. Duncan RE, Lau D, El-Sohemy A, Archer MC. Geraniol and beta-ionone inhibit proliferation, cell cycle progression, and cyclin-dependent kinase 2 activity in MCF-7 breast cancer cells independent of effects on HMG-CoA reductase activity. Biochemical pharmacology. 2004 Nov 1;68:1739-47.

42. Liu J, Li B, Ma R, Chen B. [Inhibitory effect on mammary carcinoma cells induced by beta-ionone]. Wei sheng yan jiu = Journal of hygiene research. 2004 Mar;33:151-3, 7.

43. Liu JR, Chen BQ, Yang BF, Dong HW, Sun CH, Wang Q, Song G, Song YQ. Apoptosis of human gastric adenocarcinoma cells induced by beta-ionone. World J Gastroenterol. 2004 Feb 1;10:348-51.

44. Mo H, Elson CE. Apoptosis and cell-cycle arrest in human and murine tumor cells are initiated by isoprenoids. J Nutr. 1999 Apr;129:804-13.

45. Liu JR, Sun XR, Dong HW, Sun CH, Sun WG, Chen BQ, Song YQ, Yang BF. beta-Ionone suppresses mammary carcinogenesis, proliferative activity and induces apoptosis in the mammary gland of the Sprague-Dawley rat. International journal of cancer. 2008 Jun 15;122:2689-98.

46. Aoki K, Takimoto M, Ota H, Yoshida T. Participation of CYP2A in cocaine-induced hepatotoxicity in female mice. Pharmacology & toxicology. 2000 Jul;87:26-32.

47. Jeong TC, Kim HJ, Yun CH, Lee SS, Yang KH, Han SS, Roh JK. Induction of liver cytochrome P450 2B1 by beta-ionone in Sprague Dawley rats. Biochem Biophys Res Commun. 1995 Nov 2;216:198-202.

48. Liu JR, Dong HW, Sun XR, Wang Q, Sun WG, Parry JW, Liu Q, Han XH, Sun CH, et al. Effects of beta-ionone on mammary carcinogenesis and antioxidant status in rats treated with DMBA. Nutr Cancer. 2010;62:58-65.

49. Bernstein PS, Khachik F, Carvalho LS, Muir GJ, Zhao DY, Katz NB. Identification and quantitation of carotenoids and their metabolites in the tissues of the human eye. Experimental eye research. 2001 Mar;72:215-23.

50. Lindqvist A, Andersson S. Cell type-specific expression of beta-carotene 15,15'-mono-oxygenase in human tissues. J Histochem Cytochem. 2004 Apr;52:491-9.

51. Lindqvist A, He YG, Andersson S. Cell type-specific expression of beta-carotene 9',10'-monooxygenase in human tissues. J Histochem Cytochem. 2005 Nov;53:1403-12.

52. Bhatti RA, Yu S, Boulanger A, Fariss RN, Guo Y, Bernstein SL, Gentleman S, Redmond TM. Expression of beta-carotene 15,15' monooxygenase in retina and RPE-choroid. Investigative ophthalmology & visual science. 2003 Jan;44:44-9.

53. Chichili GR, Nohr D, Schaffer M, von Lintig J, Biesalski HK. beta-Carotene conversion into vitamin A in human retinal pigment epithelial cells. Investigative ophthalmology & visual science. 2005 Oct;46:3562-9.

54. Moiseyev G, Takahashi Y, Chen Y, Gentleman S, Redmond TM, Crouch RK, Ma JX. RPE65 is an iron(II)-dependent isomerohydrolase in the retinoid visual cycle. The Journal of biological chemistry. 2006 Feb 3;281:2835-40.

55. Prasain JK, Moore R, Hurst JS, Barnes S, van Kuijk FJ. Electrospray tandem mass spectrometric analysis of zeaxanthin and its oxidation products. J Mass Spectrom. 2005 Jul;40:916-23.

56. Khachik F, de Moura FF, Zhao DY, Aebischer CP, Bernstein PS. Transformations of selected carotenoids in plasma, liver, and ocular tissues of humans and in nonprimate animal models. Investigative ophthalmology & visual science. 2002 Nov;43:3383-92.

FIGURE LEGENDS

Figure 1. Effect of 3-OH-β-apo-10'-carotenal on BEAS-2B cell viability. BEAS-2B cells ($5x10^3$) were treated with 3-OH-β-apo-10'-carotenal (50 μM; 3X dilutions) for 24 (A) and 48 (B) hours. Cell viability was assessed by Neutral Red Uptake, as described in the "Materials and Methods". All concentrations were performed in triplicate and viability was measured as the percent of the vehicle-treated (1% DMSO) control wells. Values represent the mean ± SD of triplicate experiments.

Figure 2. Effect of 3-OH-β-apo-10'-carotenal on A549 cell viability. A549 cells ($5x10^3$) were treated with 3-OH-β-apo-10'-carotenal (10 μM; 2X dilutions) for 24 (A) and 48 (B) hours. Cell viability was assessed by Neutral Red Uptake, as described in the "Experimental Procedures". All concentrations were performed in triplicate and viability was measured as the percent of the vehicle-treated (1% DMSO) control wells. Values represent the mean ± SD of triplicate experiments.

Figure 3. Representative images from the high content image profile of HepG2 cells treated with 3-OH-β-apo-10'-carotenal. HepG2 cells ($2x10^3$) were treated with 3-OH-β-apo-10'-carotenal (100 μM; 3X dilutions) for 72 hours. A vehicle control (1% DSMO) and positive control (valinomycin) are included for comparison. Each set of images was

obtained from the same image field yielding mechanistic information of 3-OH-β-apo-10'-carotenal activity.

Figure 4. Representative images from the high content cellular imaging analysis of HepG2 cells treated with 3-OH-β-apo-10'-carotenal. HepG2 cells ($2x10^3$) were treated with 3-OH-β-apo-10'-carotenal (100 μM; 3X dilutions) for 72 hours. A vehicle control (1% DSMO) and positive control (valinomycin) are included for comparison. Each set of images was obtained from the same image field.

Figure 5. Effect of 3-OH-β-apo-10'-carotenal on markers of cell health. Plots are shown for parameters of cellular toxicity and apoptosis. The vehicle control is indicated by the blue marker (located at 0.002 μM). The X-axis has been log-transformed. Dashed lines represent a significance factor of 2X the vehicle control. For specific parameters the response is given as percent of low or high responders, which corresponds to the percent of individual cells in the well that are statistically significantly lower or higher in response compared to the vehicle control.

Figure 1.

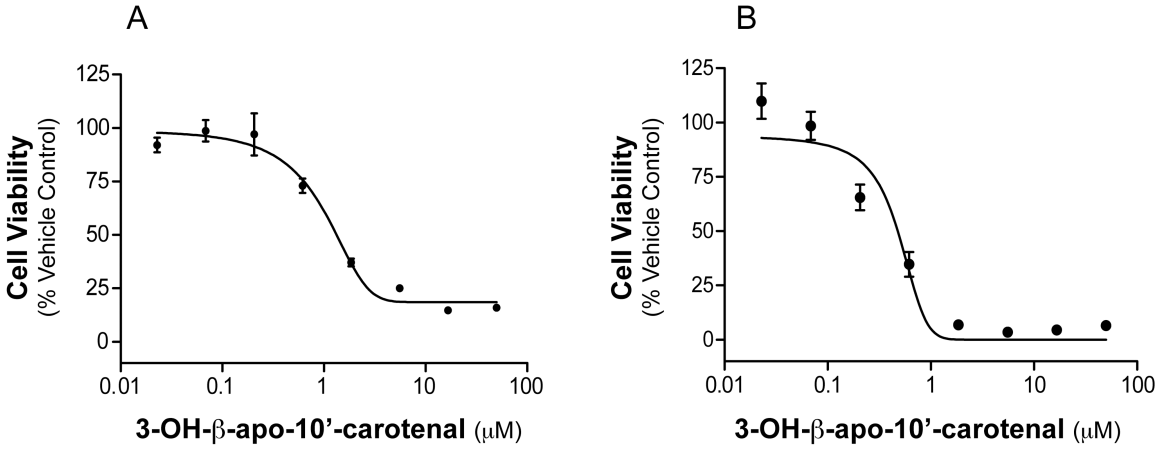
A
B
Cell Viability
(% Vehicle Control)
125
100
75
50
25
0
0.01
0.1
1
10
100
3-OH-β-apo-10'-carotenal (μM)

Figure 2.

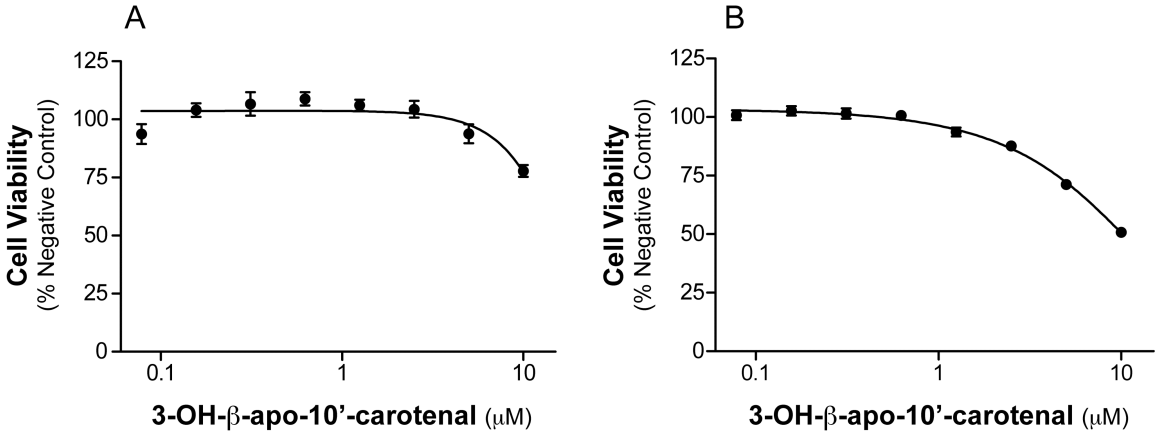
A
B
Cell Viability
(% Negative Control)
125
100
75
50
25
0
0.1
1
10
3-OH-β-apo-10'-carotenal (μM)

Figure 3.

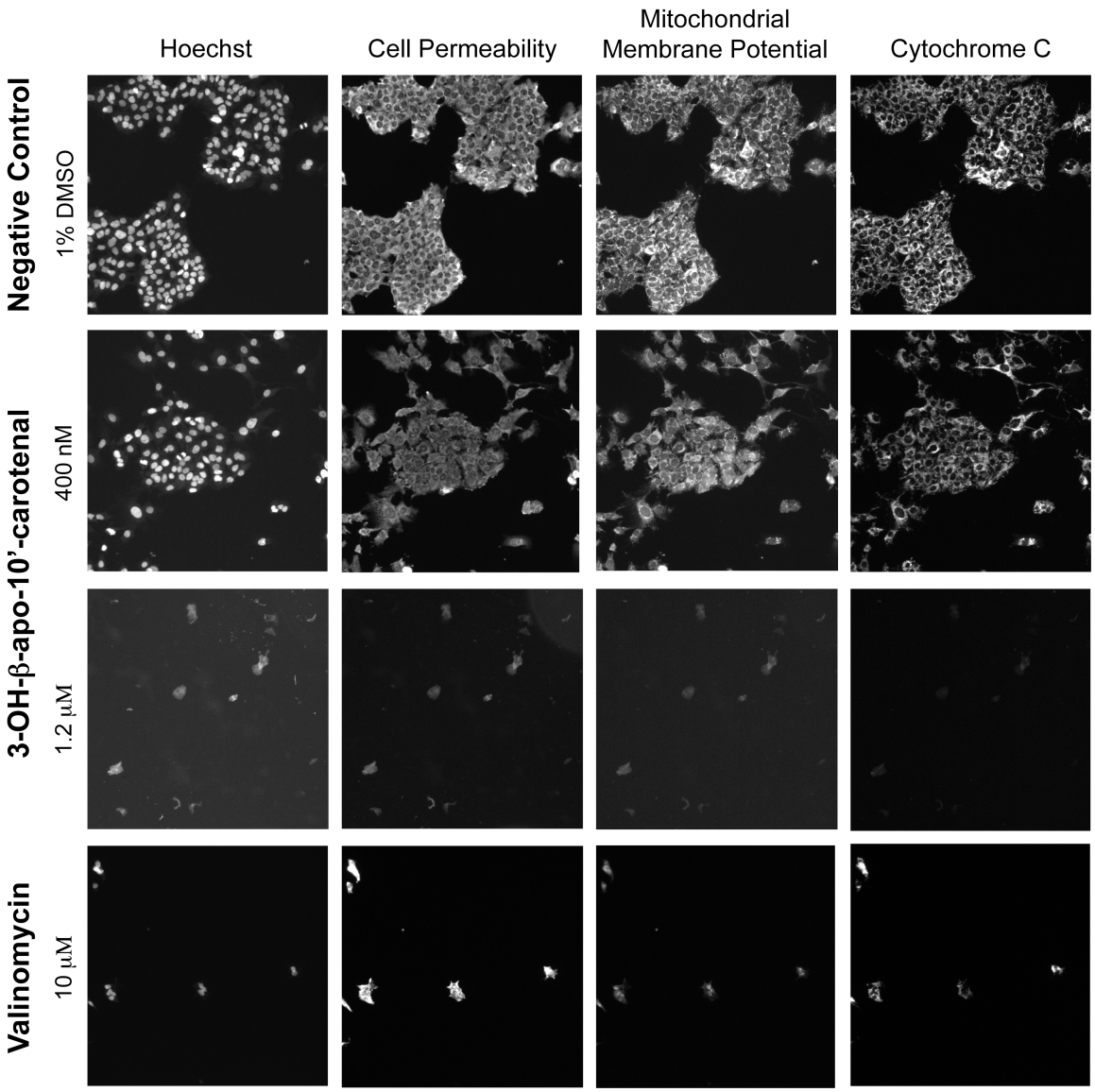
Hoechst
Cell Permeability
Mitochondrial Membrane Potential
Cytochrome C
Negative Control
1% DMSO
3-OH-β-apo-10'-carotenal
400 nM
1.2 μM
Valinomycin
10 μM

Figure 4.

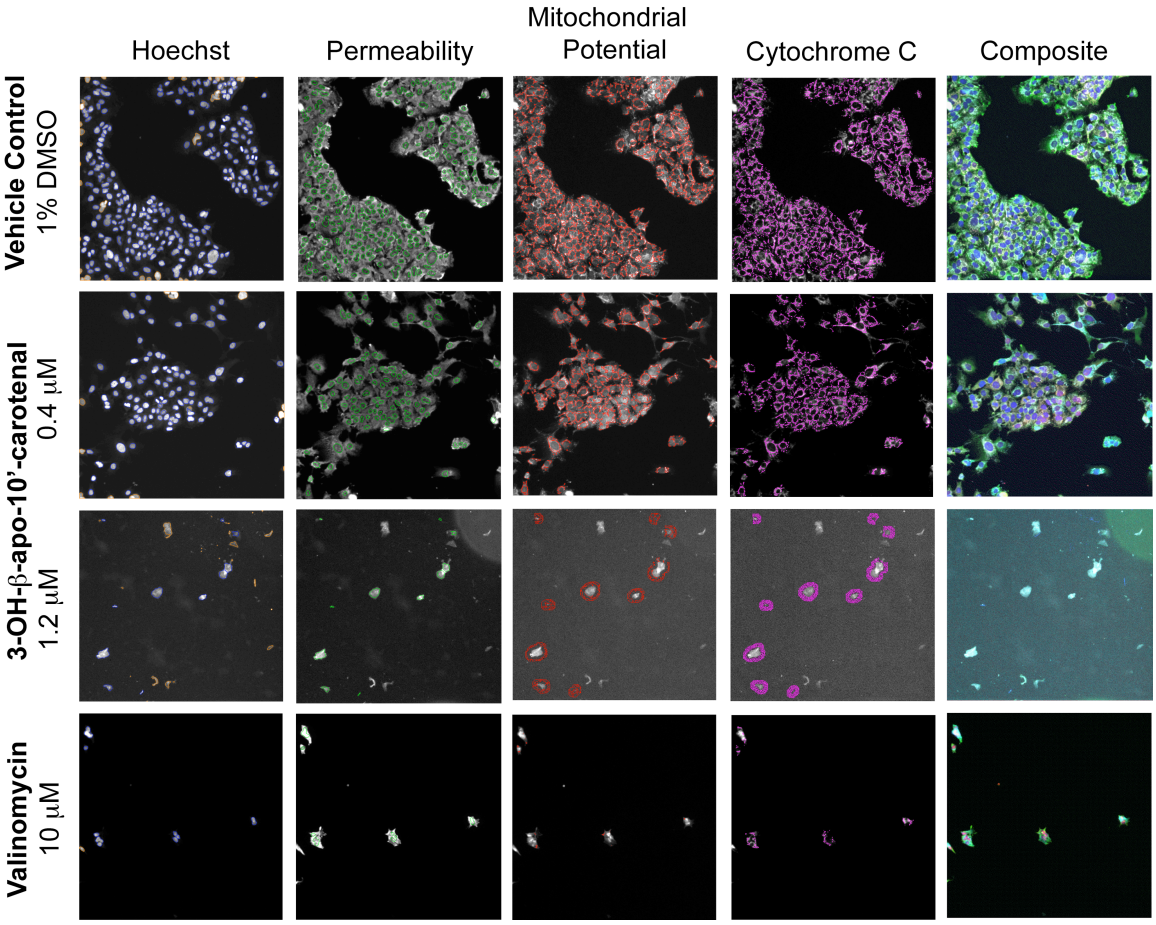
Hoechst
Permeability
Mitochondrial Potential
Cytochrome C
Composite
Vehicle Control
1% DMSO
3-OH-β-apo-10'-carotenal
0.4 μM
1.2 μM
Valinomycin
10 μM

Figure 5.

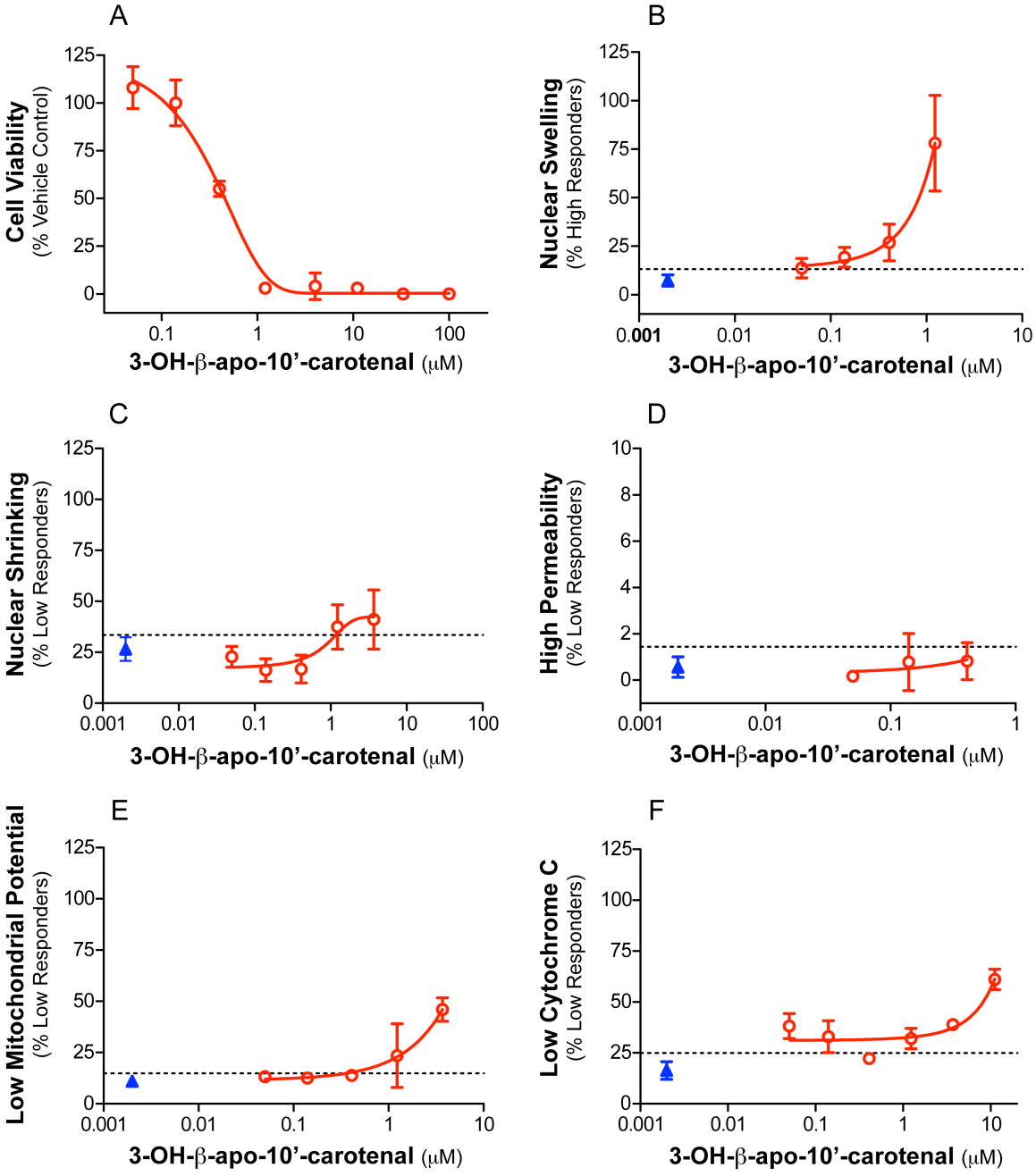
A
Cell Viability
(% Vehicle Control)
125
100
75
50
25
0
0.1
1
10
100
3-OH-β-apo-10'-carotenal (μM)
B
Nuclear Swelling
(% High Responders)
125
100
75
50
25
0
0.001
0.01
0.1
1
10
3-OH-β-apo-10'-carotenal (μM)
C
Nuclear Shrinking
(% Low Responders)
125
100
75
50
25
0
0.001
0.01
0.1
1
10
100
3-OH-β-apo-10'-carotenal (μM)
D
High Permeability
(% Low Responders)
10
8
6
4
2
0
0.001
0.01
0.1
1
3-OH-β-apo-10'-carotenal (μM)
E
Low Mitochondrial Potential
(% Low Responders)
125
100
75
50
25
0
0.001
0.01
0.1
1
10
3-OH-β-apo-10'-carotenal (μM)
F
Low Cytochrome C
(% Low Responders)
125
100
75
50
25
0
0.001
0.01
0.1
1
10
3-OH-β-apo-10'-carotenal (μM)